การศึกษาเบื้องต้นเกี่ยวกับพฤติกรรมการกระเจิงแสงและลักษณะโครงสร้าง ของพอลิเมอร์ผสมระหว่าง พอลิเอทธิลีนชนิดความหนาแน่นสูงและพอลิเอทธิลีนเชิงเส้นชนิดความหนาแน่นต่ำ

นางสาว ปวีณา มีทรัพย์

วิทยานิพนธ์นี้เป็นส่วนหนึ่งของการศึกษาตามหลักสูตรปริญญาวิศวกรรมศาสตรมหาบัณฑิต
สาขาวิศวกรรมเคมี ภาควิชาวิศวกรรมเคมี
คณะวิศวกรรมศาสตร์ จุฬาลงกรณ์มหาวิทยาลัย
ปีการศึกษา 2545

ISBN 974-17-1031-3

PRELIMINARY STUDY OF STATIC LIGHT SCATTERING BEHAVIORS AND MORPHOLOGIES OF POLYMER BLEND BETWEEN HIGH – DENSITY POLYETHYLENE AND LINEAR LOW – DENSITY POLYETHYLENE

Miss Paveena Meesap

A Thesis Submitted in Partial Fulfillment of the Requirements
for the Degree of Master of Engineering in Chemical Engineering

Department of Chemical Engineering
Faculty of Engineering
Chulalongkorn University

Academic Year 2002

ISBN 974-17-1031-3

Thesis Title	Preliminary Study of Static Light Scattering Behaviors and Morphologies of Polymer Blends between High – Density Polyethylene and Linear Low – Density Polyethylene
By	Miss Paveena Meesap
Field of Study	Chemical Engineering
Thesis Advisor	Assistant. Professor ML. Supakanok Thongyai, Ph.D.

Accepted by the Faculty of Engineering, Chulalongkorn University in Partial Fulfillment of the Requirements for the Master's Degree.

..... Dean of Faculty of Engineering
(Professor Somsak Panyakeow, D. Eng.)

THESIS COMMITTEE

..... Chairman
(Associate Professor Chirakarn Muangnapoh, Dr. Ing.)

..... Thesis Advisor
(Assistant Professor ML. Supakanok Thongyai, Ph.D.)

..... Member
(Assistant Professor Siriporn Damrongsakkul, Ph.D.)

..... Member
(Assistant Professor Seeroong Prichanont, Ph.D.)

ปวีณา มีทรัพย์ : การศึกษาเบื้องต้นเกี่ยวกับพฤติกรรมการกระเจิงแสงและลักษณะโครงสร้างของพอลิเมอร์ผสมระหว่างพอลิเอทธิลีนชนิดความหนาแน่นสูง และพอลิ-เอทธิลีนเชิงเส้นชนิดความหนาแน่นต่ำ (PRELIMINARY STUDY OF STATIC LIGHT SCATTERING BEHAVIORS AND MORPHOLOGIES OF POLYMER BLENDS BETWEEN HIGH - DENSITY POLYETHYLENE AND LINEAR LOW - DENSITY POLYETHYLENE). อาจารย์ที่ปรึกษา : ผศ.ดร.มล. ศุภกนก ทองใหญ่, 144 หน้า. ISBN 974-17-1031-3.

งานวิจัยนี้มุ่งเน้นที่จะศึกษาเกี่ยวกับพฤติกรรมการกระเจิงแสงและลักษณะโครงสร้างของพอลิเมอร์ผสมระหว่างพอลิเอทธิลีนชนิดความหนาแน่นสูง และพอลิเอทธิลีนเชิงเส้นชนิดความหนาแน่นต่ำที่อัตราส่วนผสมต่างๆ โดยใช้กล้องจุลทรรศน์อิเลคตรอนแบบส่องกราด (scanning electron microscope) ในการศึกษาลักษณะโครงสร้าง และ ใช้เทคนิค small angle light scattering (SALS) ในการศึกษาพฤติกรรมการกระเจิงแสง ซึ่งได้มีการปรับปรุงประสิทธิภาพของกล้องดิจิตอล (CCD camera), วิธีการวิเคราะห์เชิงตัวเลขของภาพการกระเจิงแสงในลักษณะ 2 มิติ และโปรแกรมคอมพิวเตอร์ ทำให้สามารถแสดงความสัมพันธ์ระหว่างลักษณะโครงสร้างและภาพการกระเจิงแสงได้ โดยโปรแกรมคอมพิวเตอร์ที่ใช้ในการวิเคราะห์ภาพการกระเจิงแสง สามารถประมวลผลได้ภายในเวลา 10 นาที หลังจากที่ได้ทำการเก็บภาพการกระเจิงแสงและค่ารัศมีของสเฟียรูไลท์ (the radius of spherulite), Rs และจากการแก้ไขปรับปรุงสมการทางคณิตศาสตร์ที่เหมาะสมสำหรับใช้อธิบายการพฤติกรรมการกระเจิงแสงของระบบพอลิเมอร์ผสมนี้ รวมทั้งวิธีการวิเคราะห์เชิงสถิติ ทำให้สามารถเชื่อมโยงค่า Rs กับการทำนายภาพการกระเจิงแสงที่เหมาะสมที่สุดของอัตราส่วนผสมต่างๆได้ นอกจากนั้นการใช้เทคนิคการกัดผิว (permanganic etching) และ กล้องจุลทรรศน์อิเลคตรอนแบบส่องกราด สามารถยืนยันได้ว่าพอลิเมอร์ผสมนี้เกิดการตกผลึกร่วมกัน (co-crystallization) สำหรับวิธีการทดสอบพฤติกรรมการกระเจิงแสงและลักษณะโครงสร้าง รวมทั้งระบบของวิธีการวิเคราะห์ของพอลิเมอร์ผสมนี้ สามารถใช้เป็นต้นแบบในการปรับปรุงเพื่อให้เหมาะสมกับการศึกษาโครงสร้างผลึกของระบบพอลิเมอร์ผสมอื่นๆได้

ภาควิชา วิศวกรรมเคมี ลายมือชื่อนิสิต.....

สาขาวิชา วิศวกรรมเคมี ลายมือชื่ออาจารย์ที่ปรึกษา.....

ปีการศึกษา 2545

4270414021: MAJOR CHEMICAL ENGINEERING

KEY WORD: STATIC LIGHT SCATTERING / HIGH – DENSITY POLYETHYLENE / LINEAR LOW – DENSITY POLYETHYLENE / SPHERULITE / PERMANGANIC ETCHING / MORPHOLOGY.

PAVEENA MEESAP: PRELIMINARY STUDY OF STATIC LIGHT SCATTERING BEHAVIORS AND MORPHOLOGIES OF POLYMER BLENDS BETWEEN HIGH – DENSITY POLYETHYLENE AND LINEAR LOW – DENSITY POLYETHYLENE. THESIS ADVISOR: ASSISTANT PROFESSOR ML. SUPAKANOK THONYAI, Ph.D., 144 pp. ISBN 974-17-1031-3.

This research is concerned with studying the static light scattering behaviors and the morphologies of polymer blends between high – density polyethylene (HDPE) and linear low – density polyethylene (LLDPE). The blends were investigated by Small Angle Light Scattering (SALS) and Scanning Electron Microscope (SEM) at various concentration. New modification of SALS by digital camera, new numerical analysis of the 2D image and computer program were used and they can be used to relate the microstructures and the image of SALS. This process can be performed within 10 minutes after getting SALS data and the radius of spherulite, Rs. From the simplified equation of the SALS images and statistical methods, we can link the radius of spherulite , Rs, to predict the most suitable image of various concentrations of these blends. By etching methods, SEM micrographs of the blends confirm the co-crystallization of HDPE and LLDPE. The systematic methods of measurements and the methods of analysis developed in this work can be extended to study other crystalline polymer blends SALS with some minor modifications.

Department	Chemical Engineering	Student's signature.....
Field of study	Chemical Engineering	Advisor's signature.....
Academic year	2002	

Acknowledgement

I would like to express my deeply gratitude to my advisor: Assistant Professor ML. Supakanok Thongyai, Ph.D. to his continuous guidance, enormous number of invaluable discussions, helpful suggestions and warm encouragement. I am grateful to Associate Professor Chirakarn Muangnapoh, Dr.Ing., Assistant Professor Siriporn Damrongsakkul, Ph.D. and Assistant Professor Seeroong Prichanont,Ph.D. for serving as chairman and thesis committees, respectively, whose comments were constructively and especially helpful.

Sincere thanks are made to the Scientific and Technological Research Equipment Center, Chulalongkorn University for using scanning electron microscope and National Metal and Materials Technology Center (MTEC) for supporting single screw extruder used in this study.

Also thanks to Thai Petrochemical Industry Public Co., Ltd. for providing High – density polyethylene and Siam Chemical Trading Co., Ltd. for giving Linear low – density polyethylene.

Sincere thanks to all my friends and all members of the Polymer Engineering Research Laboratory, Department of Chemical Engineering, Chulalongkorn University, for their assistance and friendly encouragement.

Finally, I would like to dedicate this thesis to my parents and my families, who generous supported and encouraged me through the year spent on this study.

Contents

Page

Abstract (in Thai)..... iv

Abstract (in English)..... v

Acknowledgement..... vi

Contents..... vii

List of tables..... x

List of figures..... xi

Chapter

I Introduction..... 1

1.1 General Introduction..... 1

1.2 The objectives of this research..... 3

1.3 The scope of this research..... 3

II Theories..... 4

2.1 Polymer Morphology..... 4

2.1.1 The amorphous state..... 4

2.1.2 Glass transition temperature..... 5

2.1.3 The crystalline polymer..... 6

2.2 Melting Phenomena..... 7

2.3 Thermal Properties..... 8

2.4 Structure of Crystalline Polymer..... 9

2.5 Crystal Structure in Polymers..... 10

2.5.1 Crystallization from dilute solution..... 10

2.5.1.1 Polymer single crystals..... 10

2.5.1.2 The folded chain model..... 12

2.5.1.3 The switchboard model..... 12

2.5.2 Crystallization from the melt..... 13

2.5.2.1 Spherulitic morphology..... 13

2.5.2.2 Mechanism of spherulite formation..... 15

2.5.2.3 Spherulites in polymer blends..... 15

Contents (continued)

Page

2.5.2.4 Effect of crystallinity on Tg..... 16
2.6 Crystallization and Cocrystallization of Polyethylene Blends..... 16
2.7 Light Scattering Theory..... 18
2.8 Polymer Blends..... 23
2.8.1 The blends preparations..... 23
2.8.1.1 Melt mixing..... 24
2.8.1.2 Solvent casting..... 24
2.8.1.3 Freeze drying..... 25
2.8.1.4 Emulsions..... 25
2.8.1.5 Reactive blend..... 25
2.9 Permanganic Etching..... 26
III Literature Reviews..... 27
IV Experiments..... 37
4.1 Materials..... 37
4.1.1 High – density polyethylene (HDPE)..... 37
4.1.2 Linear low – density polyethylene (LLDPE)..... 38
4.2 Sample Preparations..... 39
4.2.1 Sample preparation for light scattering..... 39
4.2.2 Sample preparation for scanning electron microscope..... 39
4.3 Experimental Techniques..... 40
4.3.1 Light Scattering..... 40
4.3.2 Scanning electron microscopy..... 41
V Results and Discussions..... 43
5.1 Light scattering measurement..... 43
5.1.1 Scattered light photographs..... 43
5.1.2 Digital intensity data..... 47
5.1.2.1 Smoothing digital intensity data..... 49
5.1.2.2 Removing the beam stop..... 54
5.2 Intensity Data from Equation..... 56
5.2.1 Example of intensity calculation from equation..... 76

Contents (continued)

Page

5.3 Consistency testing of sample thickness and efficiency of the laser light source 81
5.4 Etching and Scanning Electron Microscope (SEM) 92
5.5 Analysis of unknown composition 97
VI Conclusions and Recommendations 98
6.1 Conclusions 98
6.2 Recommendations 99
References 101
Appendices 105
Vita 144

List of Tables

Page

Table 5-1 Coefficients of each term at the light illumination no.6, area1..... 77

Table 5-2 Coefficients of each term at the light illumination no.6, area2..... 78

Table 5-3 Coefficients of each term at the light illumination no.3, area1..... 78

Table 5-4 Coefficients of each term at the light illumination no.3, area2..... 79

Table 5-5 The radius of spherulite of each composition of blend..... 96

Table C-1 Standard Normal Value at various degree of freedom of n-1..... 108

Table C-2 Critical Values for the F Statistic: $F_{.05}$..... 109

List of Figures

Page

Figure 2-1 Three different configurations of a mono – substituted polyethylene..... 6

Figure 2-2 The fringed micelle model..... 9

Figure 2-3 Electron micrograph of a single crystal of 6 – nylon grown by precipitation from dilute glycerine solution..... 10

Figure 2-4 Optical micrograph showing corrugations in single crystals of linear polyethylene grown from a solution in perchlorethylene..... 11

Figure 2-5 Optical micrograph showing pleats in a crystals of linear polyethylene grown from a solution inperchlorethylene..... 11

Figure 2-6 Schematic view of a polyethylene single crystal exhibiting adjacent reentry..... 12

Figure 2-7 Switchboard model..... 13

Figure 2-8 Different types of light – scattering patterns from spherulitic polyethylene using (a) Vv and (b) Hv polarization..... 14

Figure 2-9 Model of spherulitic structure..... 14

Fiugre 2-10 Phase diagram of the blend system of the LPE with the LDPE..... 17

Figure 2-11 A typical photographic light scattering apparatus..... 19

Figure 2-12 Typical light scattering photographs for (a) unpolarized light, (b) Vv polarization, and (c) Hv polarization..... 20

Figure 2-13 The arrangement of induced dipoles and the expected Vv scattering patterns for spherulites (a) only polarizable tangentially and (b) only polarizable radially..... 21

Figure 2-14 The arrangement of induced dipoles in a tangentially polarizable spherulite which will contribute to Hv scattering..... 22

Figure 3-1 Scattering geometry for the polarized – light scattering experiment..... 28

Figure 3-2 Boundaries of spherulites..... 28

List of Figures (continued)

Page

Figure 3-3 Hv light scattering scans at $\mu = 45^{\circ}$ for the spherulitic system 60.1% growth..... 29

Figure 3-4 Hv light scattering scans at $\mu = 45^{\circ}$ for the spherulitic system 100% growth..... 30

Figure 3-5 Schematic representation of experimental arrangement for LS from polymer films using a laser and an OMA2..... 30

Figure 3-6 Optical microphotographs of the samples crystallized at cooling rate of $2^{\circ}C$ from the melt..... 31

Figure 3-7 Comparison of Hv and Vv SALS patterns from the blend Samples with various compositions crystallized at cooling Rate of $2^{\circ}C$/min from the melt..... 31

Figure 3-8 The changes in spherulitic morphology, Vv and Hv scattering patterns with time during the course of crystallization..... 32

Figure 3-9 SEM images of etched surface of50/50 blend of HDPE/LLDPE, Tc $150^{\circ}C$; (a) after first etch ,(b) after second etch..... 33

Figure 3-10 TEM micrographs of surface replicas of 60% LPE/LDPE blends ; (a) rapidly quenched, (b) cooled at $60^{\circ}C$/min, (c) cooled at $1^{\circ}C$/min..... 34

Figure 3-11 Effect of composition on melting temperatures of HDPE – LLDPE blends..... 34

Figure 3-12 Effect of composition on melting temperatures of LLDPE – LDPE blends..... 35

Figure 3-13 Effect of composition on melting temperatures of HDPE – LDPE blends..... 35

Figure 4-1 The molecular structure of HDPE..... 37

Figure 4-2 The molecular structure of LLDPE..... 38

Figure 4-3 A schematic diagram of static light scattering equipment..... 40

Figure 4-4 A photographic illustration of SEM model JSM – 5410..... 41

List of Figures (continued)

Page

Figure 5-1 Scattered light photographs of pure HDPE, pure LLDPE and all compositions of their blends..... 47

Figure 5-2 Scattered light contour graphs of (a) pure HDPE, (b) 50/50 blended HDPE/LLDPE and (c) pure LLDPE..... 48

Figure 5-3 Schematic diagram of smoothing procedure..... 49

Figure 5-4 Contour graphs of trial and error in smoothing intensity data..... 52

Figure 5-5 Smoothed contour graphs of (a) pure HDPE, (b) 50/50 blended HDPE/LLDPE and (c) pure LLDPE..... 53

Figure 5-6 Contour graphs of (a) pure HDPE, (b) 50/50 blended HDPE/LLDPE and (c) pure LLDPE after improvement at the center..... 55

Figure 5-7 Light scattering contour graphs from the equation of (a) HDPE, (b) 50/50 blended and (c) LLDPE..... 60

Figure 5-8 Modified contour graphs of (a) pure HDPE, (b) 50/50 blended HDPE/LLDPE and (c) pure LLDPE..... 62

Figure 5-9 Comparison of light scattering contour graphs between Experiment and equation of HDPE/LLDPE blends at Gain no.6, area1 and their r^2 values..... 75

Figure 5-10 A pie chart of each term of LLDPE 's equation.....76

Figure 5-11 Coefficient graphs of each term for all blends at (a) gain6, area1 (c) gain6, area2 , (c) gain3, area1 , (d) gain3, area2..... 82

Figure 5-12 Coefficient graphs of each term..... 85

Figure 5-13 Shifted coefficient curves of (a) Term1, (b) Term2, (c) Term3 (d) Term4, (e) Term5, (f) Term B (constant)..... 88

Figure 5-14 Averaged coefficient curve and linear trend – line of (a) Term1, (b) Term2, (c) Term3, (d) Term4, (e) Term5, (e) Term B (constant)..... 91

Figure 5-15 Spherulite morphologies of pure HDPE, pure LLDPE and their blends..... 96

List of Figures (continued)

Page

Figure D-1 Comparison of light scattering contour graphs between experiment and equation of HDPE/LLDPE blends at gain no.6, area2 and their r^2 values..... 121

Figure D-2 Comparison of light scattering contour graphs between experiment and equation of HDPE/LLDPE blends at gain no.3, area1 and their r^2 values..... 132

Figure D-3 Comparison of light scattering contour graphs between experiment and equation of HDPE/LLDPE blends at gain no.3, area2 and their r^2 values..... 143

CHAPTER I

Introduction

1.1 General Introduction

Most ordinary people have been familiar with polymers. Since the first synthetic polymer was made in the beginning of 20th century, their development and commercialization has been spectacular. Regarding where we are or whatever we are doing, the probability of having something made by plastic around us is really high, for example, toys, pipes, many parts of cars and planes, are made by polymeric materials. Their easy processing and cheap price have been the key to their success.

Polyolefins are the most common and at the same time simplest polymer group. The basic polymer of this group is polyethylene. It was synthesized for the first time in 1933 in the laboratories of Imperial Chemical Industries (ICI), England, under high pressure conditions, and its industrial production began 10 years later in the United States. Since then, various processes for its production have been developed. The discovery of production of polyethylene under low pressure, making high density polyethylene in 1953.

The main characteristics of these polymers are their chemical inertia, low density and high crystallinity. All of the good properties happen because their long chains are made only by carbon and hydrogen atoms. Often, there are some regular branchings but they are always consider of the same constituent atoms. This simplicity and regularity allows a good packing of the chains and consequently the formation of crystals. The glass transition temperature of the amorphous fraction is much lower than the crystalline melting temperature, but their high crystallinity gives them good elastic properties at room temperature.

There are several kinds of polyethylene : High Density PE (HDPE), Low Density PE (LDPE), Linear Low Density PE (LLDPE) and Very Low Density PE (VLDPE). They obviously differ in their densities and this is a consequence of their different degrees

of crystallinity. The degrees of crystallinity of each polymer are determined by their chemical structure. Long, flexible and regular chains will give high degrees of crystallinity. The HDPE is produced under low pressure conditions of polymerization and consists of linear molecules without branches. LDPE, also called branched PE, is made under high pressure conditions and consequently inter and intramolecular chain transfers occurred give substantial long chain and short chain branches in the molecules. Typical values of branchings are 10 long chain and 15-30 short chain branches per 1000 carbon atoms. Short branches are essentially due to butyl and ethyl groups. LLDPE is a copolymer of ethylene and other α-olefin, usually butene. The percentage of the second component is often 10% or less in weight. The copolymerization allows the polymers to be linear but still keeping a low density: the branches do not allow such a high degree of packing as in HDPE. The incorporation of the α-olefin in the PE chains is extremely heterogeneous and as a result, LLDPE shows a broad and multimodal short-chain branching distribution. As consequence of it LLDPE shows unique physical properties which have contributed to its big success in the market. Its commercialization has happen over the last 20 years. Finally VLDPE is a terpolymer of ethylene, propylene and butene. It has a rubbery appearance. As indicated by its name it has the lowest density of all.

The two polyethylenes, which are the main interest in this project, are HDPE , LLDPE and their blends. Because both of them are semi-crystalline polymers which is easy to observe their light scattering behaviors. Furthermore, the melting temperature of LLDPE is lower than HDPE so HDPE can melt rapidly when they are mixed together.

The light scattering technique provides information about structure having size of the order of the wavelength of visible light such as fluctuations in density and fluctuations in refractive index of anisotropic regions. For morphology observation, using highly powerful microscopes, it can reveal the internal morphology which is impossible to see with bare eyes. The normal technique is optical microscope. However, as same blends have very tiny components, other more powerful techniques are required such as scanning electron microscope, SEM. It should be noted that in order to see the morphology clearly, preliminary treatments are sometimes necessary, for example, etching.

1.2 The Objectives of this Research

The objectives of this research are to produce light scattering database and to modify the suitable mathematical model for light scattering behavior of polymer blends between high density polyethylene (HDPE) and linear low density polyethylene (LLDPE) by using the new modification of Small – angle light scattering technique, the new numerical analysis of 2 – dimension and the computer program. And this research also studies the morphology and size of crystal structure of HDPE/LLDPE blends by using scanning electron microscope couple with permanganic etching technique and relate the microstructure with light scattering behavior of this system.

1.3 The Scope of this Research

1.3.1 Create light scattering database of polymer blends between high density polyethylene and linear low density polyethylene by using the static light scattering apparatus which is modified to increase the efficiency. This modified apparatus can provide the light scattering photograph and its digital intensity data at every angles of the light scattering photograph.

1.3.2 Modify the suitable mathematical equations for the light scattering behaviors of this system.

1.3.3 Observe the morphology of this system by using scanning electron microscope to find the radius of spherulite which is the required information for light scattering behavior study.

Because this work provides light scattering photograph and digital intensity data. Therefore it can be both qualitative and quantitative preliminary evaluation to identify the composition (weight percent of each component) of this polymer blend.

CHAPTER II

Theories

2.1 Polymer Morphology

Generally, there are two morphologies of polymers ; (a) amorphous and (b) crystalline. The former is a physical state characterized by almost complete lack of order among the molecules. The crystalline refers to the situation where polymer molecules are oriented, or aligned. Because polymers for all practical purposes never achieve 100% crystallinity, it is more practical to categorize their morphologies as amorphous and semi-crystalline.

2.1.1 The Amorphous State

Some polymers do not crystallize at all. Therefore they remain in an amorphous state throughout the solidification. The amorphous state is characteristic of those polymers in the solid state that, for reasons of structure, exhibit no tendency toward crystallinity. In the amorphous state, the polymer resembles as a glass.

We can imagine the amorphous state of polymers like a bowl of cooked spaghetti. The major difference between the solid and liquid amorphous states is that with the former, molecular motion is restricted to very short – range vibrations and rotations, whereas in the molten state there is considerable segmental motion or conformational freedom arising from rotation about chemical bonds. The molten state has been likened on a molecular scale to a can of worms, all intertwined and wriggling about, except that the average worm would be extremely long relative to its cross – sectional area. When an amorphous polymer achieves a certain degree of rotational freedom, it can be deformed. If there is sufficient freedom, the polymer flows then the molecules begin to move past one another. At low temperatures amorphous polymers are glassy, hard and brittle. As the temperature is raised, they go through the glass-rubber transition characterized by the glass transition temperature Tg.

2.1.2 Glass Transition Temperature, Tg

One of the most important characteristics of the amorphous state is the behavior of a polymer during its transition from solid to liquid. If an amorphous glass is heated, the kinetic energy of the molecules increases. Motion is still restricted, however, to short – range vibrations and rotations so long as the polymer retains its glasslike structure. As temperature is increased further, there comes x_o a point where a decided change takes place; the polymer loses its glasslike properties and assumes those more commonly identified with a rubber. The temperature at which this takes place is called *the glass transition temperature, Tg*. If heating is continued, the polymer will eventually lose its elastomeric properties and melt to a flowable liquid. The glass transition temperature is defined as the temperature at which the polymer softens because of the onset of long-range coordinated molecular motion. The amorphous parts of semicrystalline polymers also experience glass transition at a certain temperature Tg.

The importance of the glass transition temperature cannot be overemphasized. It is one of the fundamental characteristics as it relates to polymer properties and processing. The transition is accompanied by more long – range molecular motion, greater rotational freedom and consequently more segmental motion of the chains. It is estimated that between 20 and 50 chain atoms are involved in this segmental movement at the Tg. Clearly for this increased motion to take place, the space between the atoms (the free volume) must increase, which gives rise to an increase in the specific volume. The temperature at which this change in specific volume takes place, usually observed by dilatometry (volume measurement), may be used as a measure of Tg. Other changes of a macroscopic nature occur at the glass transition. There is an enthalpy change, which may be measured by calorimetry. The modulus, or stiffness, decreases appreciably, the decrease readily detected by mechanical measurements. Refractive index and thermal conductivity change.

2.1.3 The Crystalline Polymer

Polymers crystallized in the bulk state are never totally crystalline, a consequence of their long – chain nature and subsequent entanglements. The melting temperature of the polymer, Tm , is always higher than the glass transition temperature, Tg. Thus the polymer may be either hard and rigid or flexible. For example, ordinary polyethylene which has a Tg of about –80 °C and a melting temperature of about +139 °C. At room temperature it forms a leathery product as a result. Factors that control the Tm include polarity, hydrogen bonding and packing capability.

The development of crystallinity in polymers depends on the regularity of structure in the polymer , the tacticity of the polymer. The different possible spatial arrangements are called the tacticity of the polymer. If the R groups on successive pseudochiral carbons all have the same configulation , the polymer is called isotactic. When the pseudochiral centers alternate in configuration from one repeating unit to the next , the polymer is called syndiotactic. If the pseudochiral centers do not have any particular order , but in fact are statistical arrangements , the polymer is said to be atactic.

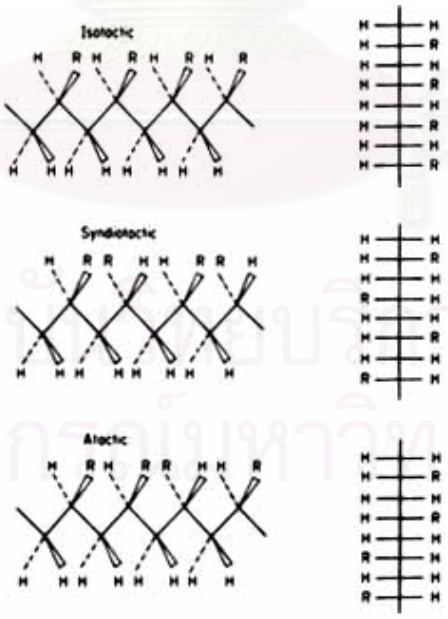

Figure 2-1: Three different configurations of a mono-substituted polyethylene, $(\text{----}CH_2\text{—}CHR\text{---})_n$, The dotted and triangular lines represent bonds to substitutents below and above the plane of the carbon – carbon backbone chain, respectively [Sperling, L.H. 2001]

Thus isotactic and syndiotactic structures are both crystallizable , because of their regularity along the chain but their unit calls and melting temperatures are not the same. On the other hand , atactic polymers are usually completely amorphous unless the side group is so small or so polar as to permit some crystallinity.

Nonregularity of structure first decreases the melting temperature and finally prevents crystallinity. Mers of incorrect tacticity tend to destroy crystallinity. Thus statistical copolymers are generally amorphous. Blends of isotactic and atactic polymers show reduced crystallinity , with only the isotactic portion crystallizing. Furthermore, the long – chain nature and the subsequent entanglements prevent total crystallization.

Crystalline polymers constitute many of the plastics and fibers of commerce. Polyethylene is used in films to cover dry – cleaned cloths , and as water and solvent containers. Polypropylene makes a highly extensible rope , finding particularly important applications in the marine industry. Polyamides and polyesters are used as both plastics and fibers. Their use in clothing is world famous , Cellulose , mentioned above , is used in clothing in both its native state and its regenerated state.

2.2 Melting Phenomena

The melting of polymers may be observed by any of several experiments. For linear or branched polymer , the melting cause the samples to becomes liquid and flows. First of all , simple liquid behavior may not be immediately apparent because of the polymer ‘s high viscosity. If the polymer is cross – linked , it may not flow at all. It must also be noted that amorphous polymers soften at their glass transition temperature , Tg , which is emphatically not a melting temperature. If the sample does not contain colorants , it is usually hazy in the crystalline state because of the difference in refractive index between the amorphous and crystalline portions. On melting , the sample becomes clear , or more transparent.

Ideally , the melting temperature, Tm , should give a discontinuity in the volume , with a concomitant sharp melting point. In fact, because of the very small size of the crystallites in bulk crystallized polymers , most polymers melt over a range of several

degrees. The melting temperature is usually taken as the temperature at which the last trace of crystallinity disappears. This is the temperature at which the largest and / or most perfect crystals are melting.

2.3 Thermal Properties

The existence of a polymeric system as a rigid glassy liquid, a mobile liquid, a microcrystalline solid or a liquid crystalline mesophase depends on the temperature and the chemical structure of the polymer. Changes from a microcrystalline state to a liquid crystalline or isotropic liquid state takes place at the equilibrium melting temperature.

Tm and Tg of crystallizable polymers vary widely with a change in the chemical structure. The presence of amide and of aromatic groups in the chain raise Tm and Tg. The morphology of a thermoplastic crystallizable homopolymer at a particular usage temperature depends on Tm, which is in turn dependent on the intermolecular forces. If the usage temperature is greater than Tm for a crystallizable polymer, only a rubbery liquid morphology will be realized. At temperatures below Tm but above Tg such a material will be partially crystalline, when crystallized quiescently, with rubbery interlayers. Below Tg, the interlayers between crystallites will be glassy.

In various kind of the polymers, the melting points refer to the melting of crystal form with the highest Tm. Changes from one form to another at easily attained temperatures and pressures can be reversible or involve melting of one form and crystallization of the other.

Some polymers with few chain irregularities, although intrinsically crystallizable, can be easily supercooled, without appreciable crystallizable, into a glassy amorphous state upon rapid cooling from the melt to a temperature below Tg. Polymers showing this type of behavior usually contain rings in the main or side chains. Examples are poly(ethylene terephthalate) and various polymers that form liquid crystalline mesophases. These supercooled materials can be crystallized by heating to a temperature where the polymer is below Tm but above Tg. Sufficient time for the various portions of the chains to adopt the conformation necessary for crystallization is then supplied.

2.4 Structure of Crystalline Polymers

Very early studies on bulk materials showed that some polymers were partly crystalline. X – ray line broadening indicated that the crystals were either very imperfect or very small. Because of the known high molecular weight, the polymer chain was calculated to be even longer than the crystallites. Hence it was reasoned that they passed in and out of many crystallites and many unit cells. These findings led to the fringed micelle model.

Figure 2-2: The fringed micelle model. Each chain meanders from crystallite to crystallite, binding the whole mass together. [Sperling, L.H. 2001]

According to the fringed micelle model, the crystallites are about 100 $^{\circ}$A long. The disordered regions separating the crystallites are amorphous. The chains wander from the amorphous region through a crystallite, and back into the amorphous region. The chains are long enough to pass through several crystallites, binding them together.

The fringed micelle model was used with great success to explain a wide range of behaviour in semi-crystalline plastics and also in fibers. The amorphous regions, if glassy, yielded a stiff plastic. However, if they were above Tg, then they were rubbery and were held together by the hard crystallites. This model explains the leathery behaviour of ordinary polyethylene plastics. The greater tensile strength of polyethylene over that of low – molecular – weight hydrocarbon waxes was attributed to amorphous chains wandering from crystallite to crystallite, holding them together by primary bonds. However, the exact stiffness of the plastic was related to the degree of crystallinity, or fraction of the polymer that was crystallized.

2.5 Crystal Structure in polymers

2.5.1 Crystallization from dilute solution

2.5.1.1 Polymer Single Crystals

Although the formation of single crystals of polymers was observed during polymerization many year ago, such crystals could not be produced from polymer solution because of molecular entanglement. In several laboratories, the phenomenon of growth has been reported for so many polymers, including polyethylene, polypropylene and other poly (α - olefins), that it appears to be quite general and universal.

All the structures described as polymer single crystals have the same general appearance, being composed of thin, flat platelets (lamellae) about 100 angstroms thick and often many micrometers in lateral dimensions. They are usually thickened by the spiral growth of additional lamellae from screw dislocations. A typical lamellae crystal is shown in figure 2-3

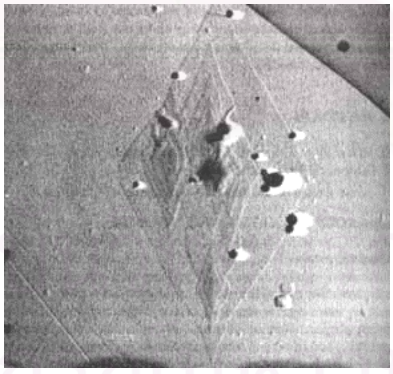

Figure 2-3 : Electron micrograph of a single crystal of 6-nylon grown by precipitation from dilute glycerine solution. The lamellae are about 60 $^{\circ}$A thick. [Sperling, L.H. 2001]

The size, shape, and regularity of the crystals depend on their growth conditions, such as solvent, temperature, and growth rate being important. The thickness of the lamellae depends on crystallization temperature and any subsequent annealing treatment. Electron – diffraction measurements indicated that the polymer chains are oriented very

nearly normal to the plane of the lamellae. Since the molecules in the polymers are at least 1000 angstroms long and the lamellae are only about 100 angstroms thick, the only reasonable description is that the chains are folded, for example, the molecules of polyethylene can fold in such a way that only about five chain carbon atoms are involved in the fold itself.

Many single crystals of essentially linear polyethylene show secondary structural features, including corrugations as shown in Figure 2-4 and pleats as shown in Figure 2-5

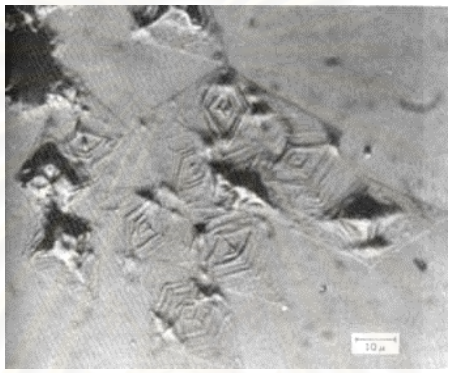

Figure 2-4: Optical micrograph showing corrugations in single crystals of linear polyethylene grown from a solution in perchlorethylene. [Sperling, L.H. 2001]

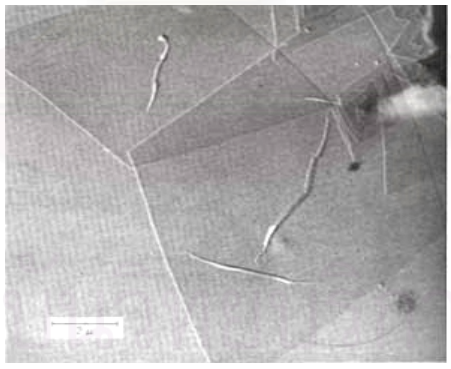

Figure 2-5 : Electron micrograph showing pleats in a crystal of linear polyethylene grown from a solution in perchlorethylene. [Sperling, L.H. 2001]

Both these features result from the fact that many crystals of polyethylene grow in the form of hollow pyramids. When solvent is removed during the preparation of the crystals for microscopy, surface – tension forces cause the pyramids to collapse.

2.5.1.2 The Folded Chain Model

This led to the folded chain model, shown in Figure 2-6

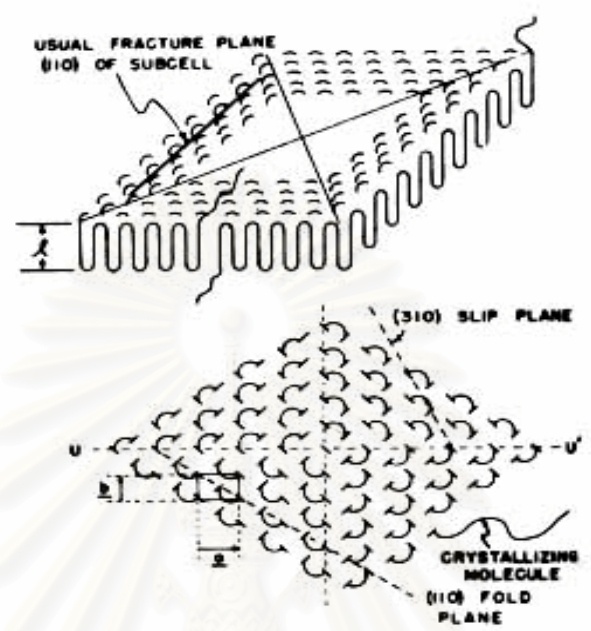

Figure 2-6 : Schematic view of a polyethylene single crystal exhibiting adjacent reentry. [Sperling, L.H. 2001]

Ideally, the molecules fold back and forth with hairpin turns building a lamellar structure by regular folding. The chain folding is perpendicular to the plane of the lamellar. While adjacent reentry has been generally confirmed by small – angle neutron scattering and infrared studies for single crystals. For many polymers, the single crystals are not simple flat structures. The crystals often occur in the form of hollow pyramids, which collapse on drying. If the polymer solution is slightly more concentrated, on if the crystallization rate is increased, the polymers will crystallize in the form of various twins, spirals, and dendritic structures, which are multilayered.

2.5.1.3 The Switchboard Model

In the switchboard model, the chains do not have a reentry into the lamellae by regular folding, but rather reentry more or less randomly. Both the perfectly folded chain and switchboard models represent limiting cases. Real system may combine elements of both.

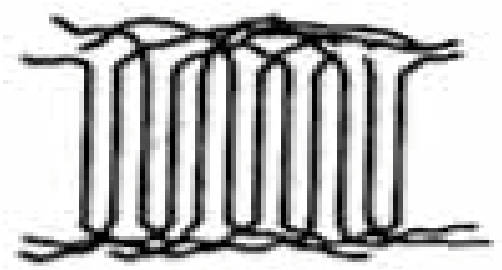

Figure 2-7 : Switchboard Model [Sperling, L.H. 2001]

2.5.2 Crystallization From the Melt

2.5.2.1 Spherulitic Morphology

When polymer samples are crystallized from the bulk of an unstained melt, the most obvious of the observed structures are the spherulites. Spherulites are sphere – shaped crystalline structure that form in the bulk. Usually the spherulites are really spherical in shape only during the initial stages of crystallization. During the latter stages of crystallization, the spherulites impinge on their neighbours. When the spherulites are nucleated simultaneously, the boundaries between them are straight. However, when the spherulites have been nucleated at different times, so that they are different in size when impinging on one another, their boundaries form hyperbolas. Finally, the spherulites form structures that pervade the entire mass of the material.

Electron microscopy examination of the spherulitic structure shows that the spherulites are composed of individual lamellar crystalline plates. The lamellar structures sometimes resemble staircases, being composed of nearly parallel lamellae of equal thickness.

The growth and structure of spherulites may also be studied by small- angle light scattering. The sample is placed between polarizers, a laser light beam is passed through, and the resultant scattered beam is photographed. Two types of scattering patterns are obtained, depending on polarization condition. When the polarization of the incident beam

and that of the analyser are both vertical, it is called a Vv type of pattern. When the incident radiation is vertical in polarization but the type of pattern. When the incident radiation is vertical in polarization but the analyser is horizontal (polarizers crossed), an Hv pattern is obtained.

(a) (b)

Figure2-8 : Different types of light – scattering patterns are obtained from spherulitic polyethylene using (a) Vv and (b) Hv polarization. [Stein, R.S. 1960]

These patterns arise from the spherulitic structure of the polymer, which is optically anisotropic, with the radial and tangential refractive indices being different.

A model of the spherulite structure is illustrated in Figure 2-9

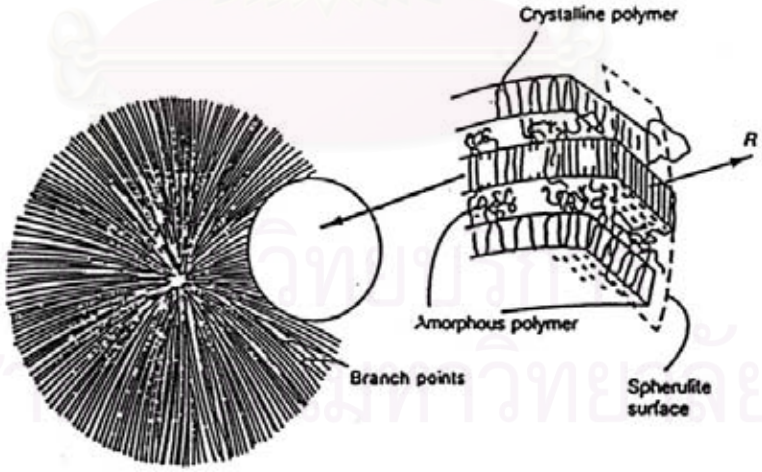

Figure 2-9 : Model of spherulitic structure. [Sperling, L.H. 2001]

The chain direction in the bulk crystallized lamellae is perpendicular to the broad plane of the structure, just like the dilute solution crystallized material. The spherulite lamellae also contain low – angle branch points, where new lamellar structures are initiated.

The new lamellae tend to keep the spacing between the crystallites constant. While the lamellar structures in the spherulites are the analogue of the single crystals. In between the lamellar structures lies amorphous material. This portion is rich in components such as atactic polymers, low – molecular – weight material, or impurities of various kinds.

The individual lamellae in the spherulites are bonded together by tie molecules, which lie partly in one crystallite and partly in another. Sometimes these lies molecules are actually in the form of what are called intercrystalline links, which are long, threadlike crystalline structures. These intercrystalline links are thought to be important in the development of the great toughness characteristic of semi-crystalline polymers. They serve to tie the entire structure together by crystalline regions and / or primary chain bonds.

2.5.2.2 Mechanism of Spherulite Formation

On cooling from the melt, the first structure that forms is the single crystal. These rapidly degenerate into sheaflike structures during the early stages of the growth of polymer spherulites. These sheaflike structures have been variously called axialites or hedrites. These transitional, multilayered structures represent an intermediate stage in the formation of spherulites.

2.5.2.3 Spherulites in Polymer Blends

There are two cases to be considered. Either the two polymers composing the blend may be miscible and form one phase in the melt, or they are immiscible and form two phase. If the glass transition of the noncrystallizing component is lower than that of the crystallizing component (i.e., its melt viscosity will be lower, other things being equal), then the spherulites will actually grow faster, although the system is diluted. The crystallization behavior is quite different if the two polymers are immiscible in the melt. On spherulite formation, the droplets, which are non-crystallizing, become ordered within the growing arms of the crystallizing component.

2.5.2.4 Effect of Crystallinity on Tg

Semi – crystalline polymers such as polyethylene or polypropylene types also exhibit glass transitions, though only in the amorphous portions of these polymers. The Tg is often increased in temperature by the molecular – motion restricting crystallites. Sometimes Tg appears to be masked, especially for high crystalline polymers.

Many semi – crystalline polymers appear to possess two glass temperatures : (a) a lower one, Tg (L) , which refers to the completely amorphous state and which should be used in all corrlations with chemical structure, and (b) an upper value, Tg (U), which occurs in the semi – crystalline material and varies with extent of crystallinity and morphology.

2.6 Crystallization and Cocrystallization of polyethylene blends

Crystallization is the process whereby an ordered structure is produced from a disordered phase, usually a melt or dilute solution, and melting can be thought of as being essentially the opposite of this process. When the temperature of a polymer melt is reduced to the melting temperature there is a tendency for the random tangled molecules in the melt to become aligned and form small ordered regions. This process is known as nucleation and the ordered regions are called nuclei. These nuclei are only stable below the melting temperature of the polymer since they are disrupted by thermal motion above this temperature. The second step in the crystallization process is growth whereby the crystal nuclei grow by the addition of further chains. Crystallization is therefore a process which takes place by two distinct steps, nucleation and growth which may be considered separately.

Nucleation is classified as being either homogeneous or heterogeneous. During homogeneous nucleation in a polymer melt or solution it is envisaged that small nuclei form randomly throughout the melt. Although this process has been analyzed in detail from a theoretical viewpoint it is thought that, in the majority of cases of crystallization from polymer melts and solutions, nucleation takes place heterogeneously on foreign bodies such as dust particles or the walls of the containing vessel. The number of nuclei formed

depends, when all other factors are kept constant, upon the temperature of crystallization. At low undercoolings nucleation tends to be sporadic and during melt crystallization a relatively small number of large spherulites form. On the other hand when the undercooling is increased many more nuclei form and a large number of small spherulites are obtained.

The crystallization behavior of blends of linear polyethylene (LPE) with branched polyethylene (BPE) has been a topic of debate for over 30 years. Recently the phase behavior of these blends in the melt has also attracted interest. The chemical similarity of the components makes it difficult to study this behavior directly. However, there are indirect techniques for studying the crystallization behavior of this system such as differential scanning calorimetry (DSC) and X – ray scattering technique.

The crystalline textures of rapidly quenched blends have been determined using DSC. Blends quenched from the single phase region of the phase diagram in Figure 2-10 [R.L. Morgan, 1999] exhibit a single melting peak and a uniform morphology indicating one crystal population (banded throughout for some compositions and blend system, unbanded throughout for others). Blends quenched from the two phase region of the phase diagram exhibit two melting peaks and a double morphology, indicating two crystal types.

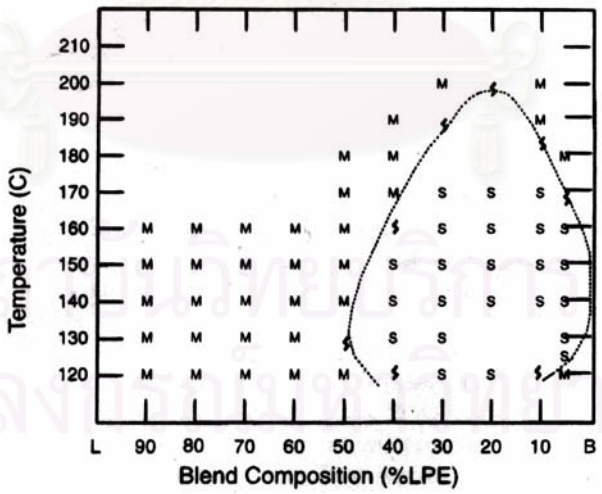

Figure 2-10 : Phase diagram of the blend system of the LPE with the LDPE. "M" indicates that the melt was found to consist of single phase, and "s" that it was found to be separated into two phases. [Point, J.J. 1992]

The degree of cocrystallization in polyethylene blends was first studied in the 1960s, using differential thermal analysis techniques. More recent studies have employed further

techniques: electron microscopy, both small and wide angle X – ray scattering, small angle light scattering, infrared spectroscopy and neutron scattering. In general LPE and BPE have been found to seperate on crystallization, to varying degrees. It is expected that some segregation will occur in all systems at slow enough cooling rates. The more similar the temperature ranges over which the pure components in the blend crystallize, the slower the cooling rate required to observe any segregation has not been detected even after cooling at the slowest rate used (typically 1 $^{\circ}$C/min). Such crystallization behavior can be achieved when a low molecular weight LPE is blended with a BPE of particular branch content or when a medium – high molecular weight LPE is blended with a BPE of very low branch content. In some cases complete cocrystallization has been reported in blends of LPE with linear low density polyethylene (LLDPE), but it should be noted that LLDPEs are very broad in intermolecular branch distribution and so they will contain both material prone to cocrystallization with the LPE and material prone to segregation. When studying the cocrystallization of a LLDPE with a LPE, the LLDPE cannot be treated as a single component. The cocrystallization of this system varies with blend composition such that (i) in the HDPE – rich blend addition of LLDPE slows down nucleation and enhances growth: and (ii) in the LLDPE – rich blend, addition of HDPE increases the overall growth rate while the nucleation rate first decreases and then increases above 20% of HDPE. These variations of nucleation and growth of crystallization produce differences in crystalline morphology in the respective regions of the blend composition. In other systems, for example blends of medium – high molecular weight LPE with low density polyethylene (LDPE) or with hydrogenated polybutadienes, varying degrees of segregation depend on the experimental techniques, the materials used and the cooling rate.

2.7 Light Scattering Theory

The phenomenon of light scattering is encountered widely in everyday life. For example, light scattering by airborne dust particles causes a beam of light coming through a window to be seen as a shaft of light, the poor visibility in a fog results from light scattering by airborne water droplets, and laser beams are visible due to scattering of the radiation by atmospheric particles. Also, light scattering by gas molecules in the atmosphere gives rise to the blue color of the sky and the spectacular colors that can

sometimes be seen at sunrise and sunset. These are all examples of *static light scattering* since the time-averaged intensity of scattered light is observed.

In general, interaction of electromagnetic radiation with a molecule results in scattering of the radiation. Scattering results from interaction of the molecules with the oscillating electric field of the radiation, which forces the electrons to move in one direction and the nuclei to move in the opposite direction. Thus a dipole is induced in the molecules, which for isotropic scatterers is parallel to, and oscillates with, the electric field. Since an oscillating dipole is a source of electromagnetic radiation, the molecules emit light, the *scattered light*, in all directions. Almost all of the scattered radiation has the same wavelength (and frequency) as the incident radiation and results from elastic scattering, that is zero energy change. Additionally, a small amount of the scattered radiation has a higher, or lower, wavelength than the incident radiation and arises from inelastic scattering, that is non-zero energy change. Inelastically scattered light carries information relating to bond vibrations and is the basis of Raman spectroscopy, a technique which increasingly is being used in studies of polymer structure and polymer deformation micromechanics.

The scattering of light from crystalline polymeric films has been studied for long time. This scattering arises principally from orientation fluctuations among aggregates of crystals. The scattering patterns are complex, especially with polarized light and oriented samples. This technique described involved photometric measurement of the scattered intensity as a function of sample and scattering angle. The photographic technique like the photographic X – ray diffraction except that a laser is used as a radiation source as a substitute for an X – ray tube. A typical photographic light scattering apparatus is shown in Figure 2-11.

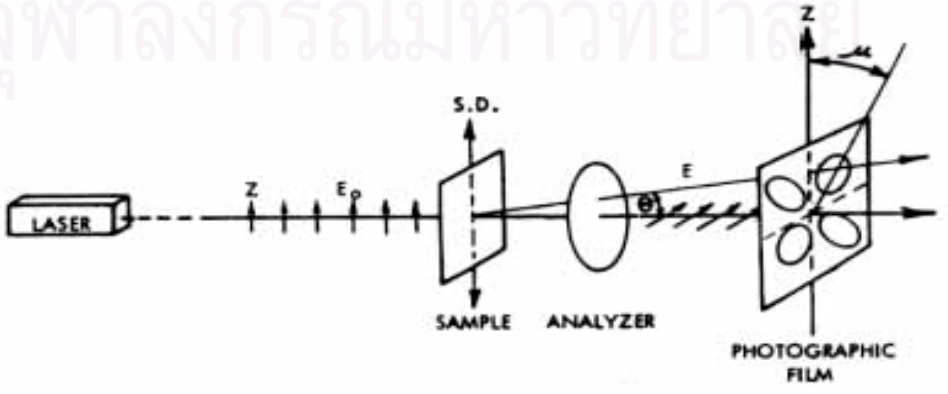

Figure 2-11 : A typical photographic light scattering apparatus. [Stein, R.S. 1964]

The intensity depends upon the scattering angle θ between the incident and scattered ray and the azimuthal angle μ. The range of θ that may be record in a picture depends upon the sample to film distance, d since $\tan\theta = (x/d)$, where x is the distance from the center of the photographic film to the point where the intensity is recorded.

Some typical scattering patterns from an unoriented medium density polyethylene film are presented in Figure 2-12.

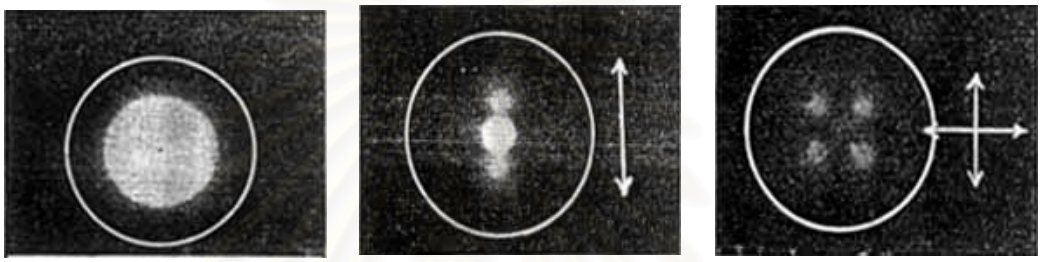

(a) (b) (c)

Figure 2-12 : Typical light scattering photographs for (a) unpolarized light, (b) Vv polarization, and (c) Hv polarization. The arrows represent directions of polarization. [Stein, R.S. 1960]

Two types of polarized patterns are (1) Vv patterns obtained when the polarizer in the incident beam and the polarizer (or known as analyzer) in the scattering beam are both vertical, and (2) Hv patterns where the polarizer is vertical and the analyzer is horizontal. It is observed that the Vv scattering patterns are elongation in the direction of polarization. An anisotropic scattering pattern of this sort is usually interpreted in terms of an oriented scattering object. This cannot be the case with an unoriented polyethylene sample, particularly since the direction of extension of the scattering pattern is dependent upon the direction of polarization. Consequently, the interpretation may be made in terns of an anisotropic but unoriented arrangement of principal polarizability directions.

Polyethylene crystallites are known to be arranged in spherical aggregates called spherulites with differing radial and tangential refractive indexes. This optical anisotropy is a consequence of the arrangement of the anisotropic crystallites within the spherulites.

There are two idealized cases illustrated in Figure 2-13

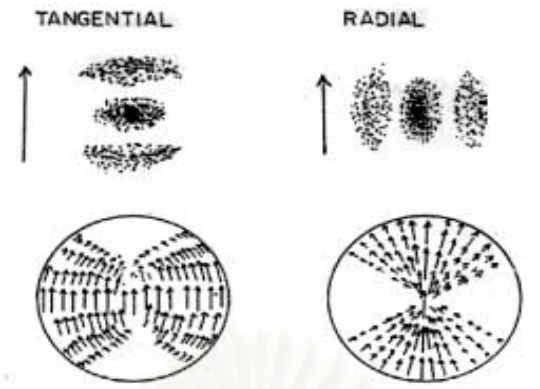

(a) (b)

Figure 2-13 : The arrangement of induced dipoles and the expected Vv scattering patterns for spherulites which are (a) only polarizable tangentially and (b) only polarizable radially. [Stein, R.S. 1960]

For case (a), it is assumed that the electrons within the spherulite may only be displaced in a tangential direction. It is apparent that for vertically polarized light, dipoles are induced in only the equatorial regions of the spherulite. The scattering pattern, which is most elongated in the direction of smallest extension of the spherulite, is extended in the vertical direction. In case (b), where the electrons may move only along the radii of the spherulite, the induced dipoles are principally in the polar regions and the scattering pattern is extended horizontally. For isotropic spherulites, radial and tangential motion of the electrons is equally easy, and induced dipoles are uniformly arranged throughout the spherulite. The scattering pattern will be the sum of those for cases (a) and (b) and will have circular symmetry. The observed extension of the Vv scattering pattern in the polarization direction corresponds to case (a) and indicates that it is the tangential component of polarizability which give rise to scattering. The low intensity of scattering in the direction perpendicular to polarization observed in Vv polarization pattern indicates that the radial polarizability contribution is negligible. This probably arise because of destructive interference among adjacent spherulites.

The cloverleaf type pattern obtained with crossed polaroids may also be understood in terms of spherulite anisotropy. For vertical polarization of the incident light, the induced dipoles are distributed as in case (a). If these are viewed through a horizontally oriented

analyzer, the large dipoles along the equator will be oriented perpendicularly to the analyzer and will not contribute to the scattered light passed by the analyzer. It will be the dipoles in planes of the spherulite oriented at 45 degree to both the polarizer and analyzer that will make the maximum contribution to scattering. The arrangement of these is indicated in Figure 2-14. The cloverleaf arrangement of these is apparent.

Figure 2-14 : The arrangement of induced dipoles in a tangentially polarizable spherulite which will contribute to Hv scattering. [Stein, R.S. 1960]

Figure 2-14 show the arrangement of induced dipoles in a tangentially polarizable spherulite which will contribute to Hv scattering. The dotted arrows represent the strength of the induced dipoles, while the solid arrows represent the component of this passing through a horizontal analyzer.

It is also apparent that in isotropic spherulites, the induced dipole will be oriented in the direction of polarization of the incident light, and no scattered light will be transmitted through an analyzer perpendicular to polarizer. Consequently, the Hv component of scattering for isotropic spherulites will be zero.

The correct form of the three – dimensional small – angle light scattering equations for anisotropic spheres is

$$I_{H_V} = A\rho^2 V^2 \left(\frac{3}{U^3}\right)^2 \left\{(\alpha_r - \alpha_t)\left[\frac{\cos^2(\theta/2)}{\cos\theta}\right]\sin\phi\cos\phi(4\sin U - U\cos U - 3SiU)\right\}^2 \quad (1)$$

where I_{Hv} denote scattered intensities ; V is the volume of the anisotropic sphere ; α_r and α_t are the tangential and radial polarizabilities of the sphere, respectively ; θ and ϕ are the

radial and azimuthal scattering angles, respectively (as shown in Figure 2-10) ; and A is a proportionality constant (assumed A=1). The sine integral *SiU* is defined by

$$SiU = \int_o^u \left(\sin x \ / \ x \right) dx \qquad (2)$$

and is solved as a series of error function. The geometric polarization correction term ρ is defined :

$$\rho = \cos\theta\left(\cos^2\theta + \sin^2\theta\sin^2\phi\right)^{-1/2} \qquad (3)$$

U is the sphere shape – factor :

$$U = \left(\frac{4\pi Rs}{\lambda}\right)\sin\left(\theta/2\right) \qquad (4)$$

where Rs is the radius of the anisotropic sphere, and λ is the wavelength of light in the medium. The Hv SALS equation [see equation (1)] is made up of one term ;

$\left(\alpha_r - \alpha_t\right)\left[\frac{\cos^2(\theta/2)}{\cos\theta}\right]\sin\phi\cos\phi\left(4\sin U - U\cos U - 3SiU\right)$, is the major anisotropy term and is the primary contributor of anisotropy to the system.

2.8 Polymer Blends

Polymer blends are the mixtures of at least two or more polymers. The mixing of two or more existing polymers may obtain the new properties of the blend. By using these techniques the designed properties can be explored without synthesizing the new polymer which have the designed properties. The results of blending polymers have many advantages, for example, lower cost than synthesizing the desired properties of new polymer. The new properties can also be under controlled.

2.8.1 The Blends Preparations

There are many methods to mix each polymer together, such as by using heat (melt mixing), by using solvent (solution casting, freeze drying) or by in situ reaction, etc.

2.8.1.1 Melt Mixing

Melt mixing of thermoplastics polymer is performed by mixing the polymers in the molten state under shear in various mixing equipments. The method is popular in the preparation of polymer blends on the large commercial scale because of its simplicity, speed of mixing and the advantage of being free from foreign components (e.g. solvents) in the resulted blends. A number of are available for laboratory – scale mixing such as internal mixer, electrically – heated two – roll mill, extruder, rotational rheometer.

The advantages of this method are the most similar to the industrial practice. The commercial compounding or adding additives into base polymers are applied by melt mixing. So the investigations of polymer blends by melt mixing method are the most practical methods in industrial applications.

2.8.1.2 Solvent Casting

This method group is performed by dissolving polymers in the some solvent. The solution is then cast on a glass plate into thin films and the removal of solvent from the films is performed by evaporating the solvent out at ambient or elevated temperature. To remove traces of solvents from the casting polymer films, the condition of high temperature is invariably needed, and protection of the polymer in case of degradation is essential. The inert gas or lower down the pressure (vacuums) is typically used. In the vacuum conditions, the vapor pressure can be reduced and thus allows the solvents to evaporate more easily. However, too fast evaporation rate of solvent will result in the bubble in the final films produced.

Solvent casting is the simplest mixing method available and is widely practiced in academic studies, usually when the experiments need a very small quantities of polymers.

2.8.1.3 Freeze Drying

In the freeze drying processes, the solution of the two polymers is quenched down immediately to a very low temperature and the solution is frozen. Solvent is then removed from the frozen solution by sublimation at a very low temperature. Dilute solutions must be used and the solution volume must have as large surface area as possible for good heat transfer.

An advantage of this method is that the resulted blend will be independent of the solvent, if the single phase solution is freezed rapidly enough. However, there are many limitations of this method. Freeze drying method seems to work best with solvents having high symmetry, i.e. benzene, naphthalene, etc. The powdery form of the blend after solvent removal is usually not very useful and further shaping must be performed. While not complex, freeze drying does require a good vacuum system for low – boiling solvents and it is not a fast blending method. After solvent removal, the blend is in the powdery form, which usually needs further shaping. The advantage of this method is the simplicity. However, this method needs a good fume trap, vacuum line for the sublimation solvent and it takes to complete the sublimation process.

2.8.1.4 Emulsions

The advantages of the emulsion polymer mixing are the easy handling and all the other advantages as the solvent casting. The mixing or casting of the film requires neither expensive equipment nor high temperature. However, emulsions of polymers are an advantage technique and not always applicable to all monomers.

2.8.1.5 Reactive Blend

Co –crosslinking and interpenetrating polymer networks (IPN) formations are the special methods for forming blends. The ideas of these methods is to enforce degree of miscibility by reactions between the polymer chains. Other methods involve the polymerization of a monomer in the presence of a polymer and the introduction of interface graft co – polymer onto the polymer chains.

2.9 Permanganic etching

The macroscopic properties of crystalline polymers are controlled in large measure by their physical microstructure. Since there is substantial texture in crystalline polymers below the resolution of the optical microscope and for nearly thirty years attempts have been made by using a wide variety of techniques to relate this texture to presumed lamellar structures whose precise arrangement must strongly affect mechanical and other properties. It is only recently, however, that it has become possible to use transmission electron microscopy and scanning electron microscopy to study actual lamellar organization representative of the interior morphology of melt – crystallized polymers. Permanganic etching of various polyolefins and other polymers offer alternative and complementary means of studying polymer lamellae and their organization within spherulites and other textural entities. This technique confirms not only that crystalline polymer, even when of only moderate crystallinity, are profusely lamellar, but also show that there is a hierarchy of lamellae with a systematic spatial distribution through a sample. Premanganic etching offers additional information on differences between different components of the morphology through differential etching. It has been appreciated from the introduction of this technique that etching could be differential between many regions, revealing various differences, including those of polymeric components in blends, lamellar thickness and related segregation, as well as deformed regions representing differences underlying such differential etching.

CHAPTER III

Literature Reviews

Light scattering of crystalline polymers and their morphologies have been studied in many researches. The reviews cover light scattering behavior and morphologies of linear low – density polyethylene, high – density polyethylene and low – density polyethylene and their blends.

Richard S. Stein, A. Misra, T. Yuasa and F. Khambatta [1977] investigated the crystallization kinetics from quantitative measurements of scattered intensities. Because a quantitative comparison of scattered intensities with the predictions indicate the need for theoretical refinement. Quantitative measurements of the variations of scattered intensity with angle may be made with high resolution photometers or by using an optical multichannel analyzer. Such intensity data must be corrected for refraction at sample interfaces as well as for multiple scattering. They found that a quantitative comparison of the theoretically calculated intensity with the experimentally measured leads to two important differences: (1) The theoretical intensity is zero at the scattering angle, $\theta = 0^{\circ}$ and falls off quite rapidly with increasing θ at angles greater than that of the maximun intensity, whereas the experimental intensity is finite at $\theta = 0^{\circ}$ and is much greater than the theoretical prediction at large θ. (2) The theory predicts that the Hv intensity should be zero at the azimuthal angle, $\mu = 0^{\circ}$ and 90° whereas finite intensities are found experimentally. The differences are ascribed to external and internal disorder. By the external disorder is associated with phenomena related to difference in the configuration of the spherulitic boundary which arise from incomplete spherulite development, spherulite truncation resulting from impingement and distribution of spherulite sizes. For the internal disorder arises from the volume filling spherulites are not spheres but are truncated and meet at boundaries. So they concluded that quantitative comparisons of measured scattered intensities of light scattering technique with theoretically calculated values are useful for providing information about the crystallization process.

Koberstein, J. , Russell, T.P. and Stein, R.S. [1979] studied about technique of small – angle light scattering from spherulites within polymeric solids to compare with theoretically assumption for ideal structure of spherulites.

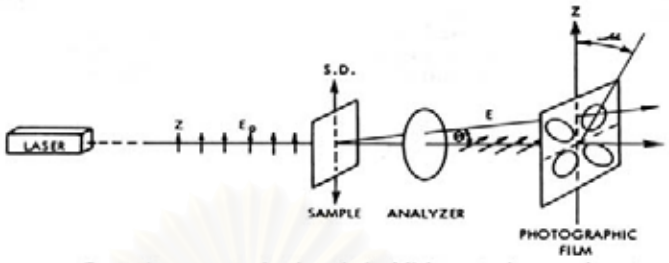

Figure 3-1 : Scattering geometry for the polarized – light scattering experiment [Koberstein, J. 1979]

Ideal spherulites have perfect alignment of optical axes within spherulites and spherical boundaries.

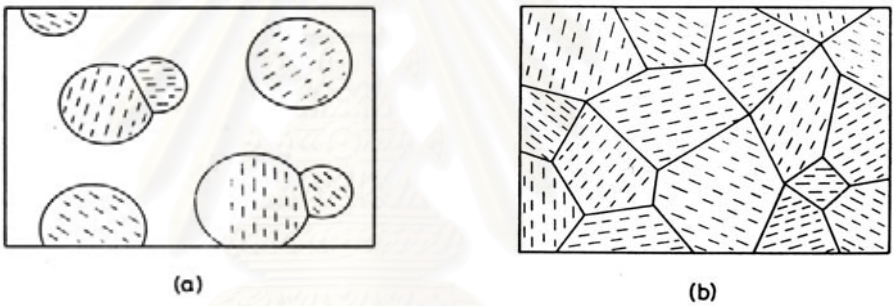

Figure 3-2 : Boundaries of spherulites (a) Anisotropic aggregate having sharp boundaries dispersed in an isotropic matrix , (b) Array of small anisotropic crystals with correlated orientation [Koberstein, J. 1979]

They found that the ideal spherulites differ from their the experimentally observation in four respects:

(a) The theory predicts zero intensity at □□= 0° , □□is the scattering angle between the incident and scattered ray, while experimentally, finite " zero – order " scattering is found.

(b) The scattering maximum is found to be broader and lower than predicted.

(c) Greater intensity is found at large values of □□than are predicted.

(d) Theory predicts zero intensity at □□=0° and 90° , □□is azimuthal angle, while finite intensity is found.

These differences are believed to be due to the disorder of the orientation of optical axes within spherulites and irregular boundaries of spherulites arising from their mutual truncation. And they concluded that this is apparent since spherulite disorder represents a decrease in the degree of nonrandomness of fluctuations.

Tabar, R. J. , Wasiak, A. , Hong, S. D. , Yuasa, T. and Stein, R.S. [1981] studied the effect of the impingement and of growing spherulites on Hv small – angle light scattering patterns. Spherulitic crystallization from the melt usually yields a coherent sample made up of individual structures impinging on and linked to one another by lamellas common to two spherulites. Spherical symmetry is lost when two or more growing spherulites imping on one another or when crystallization of two different crystal forms occur simultaneously. They found that the impingement produces a lowering of the intensity of the scattering maximum and the diminishing of the overall sharpness of the scattering peak. The extent of these effects increases with area fraction of spherulites. From the impecfect shape of the spherulites due to their impingement also produces the truncation effect. They found that while spherulites grow, the extent of truncation effect on the Hv light scattering pattern increase. Both of the impingement effect and the truncation effect are due to the increasing radii of the spherulites. The effect of truncation is to lower the intensity of the scattering maximum and increase the intensity at small and large angles.

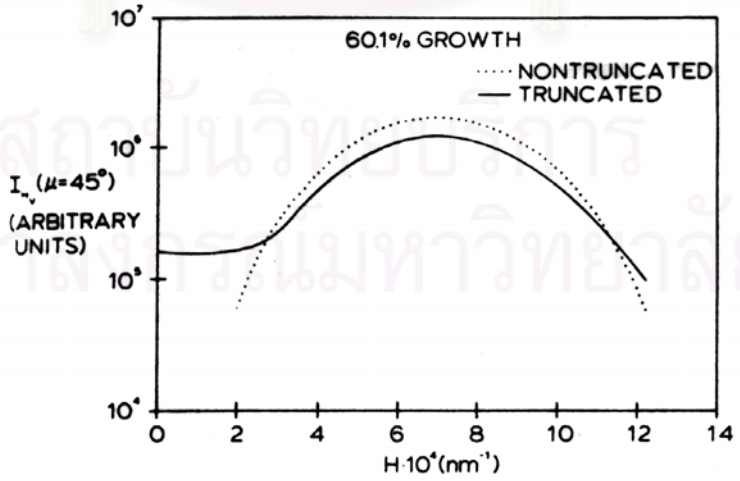

Figure 3-3 : Hv light scattering scans at $\mu = 45^{\circ}$ for the spherulitic system in Figure (___)truncated, 60.1% growth and (.....) nontruncated system with the same angle of maximum intensity and the same total area. [Tabar, R. J. 1981]

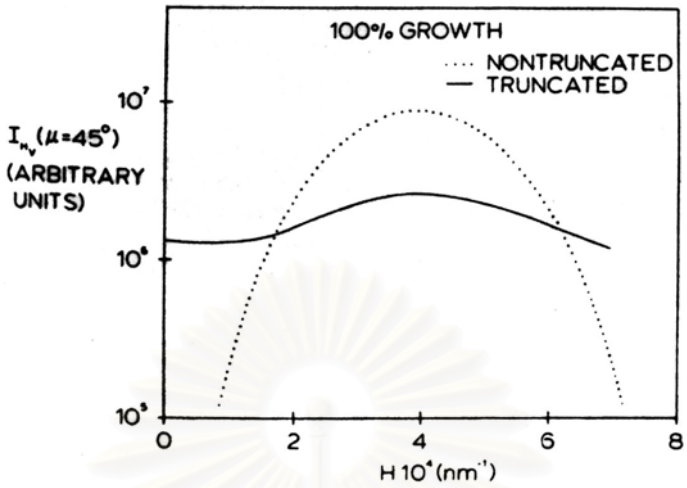

Figure 3-4 : Hv light scattering scans at $\mu = 45^{\circ}$ for the spherulitic system in Figure (——) truncated, 100% growth and (.....) nontruncated system with the same angle of maximum intensity and the same total area. [Tabar, R. J. 1981]

Ree, M. , Kyu, T. and Stein, R.S. [1987] studied the melting and crystallization behavior of blends of linear low – density polyethylene (LLDPE) with conventional low – density polyethylene (LDPE) by using small – angle light scattering technique (SALS).

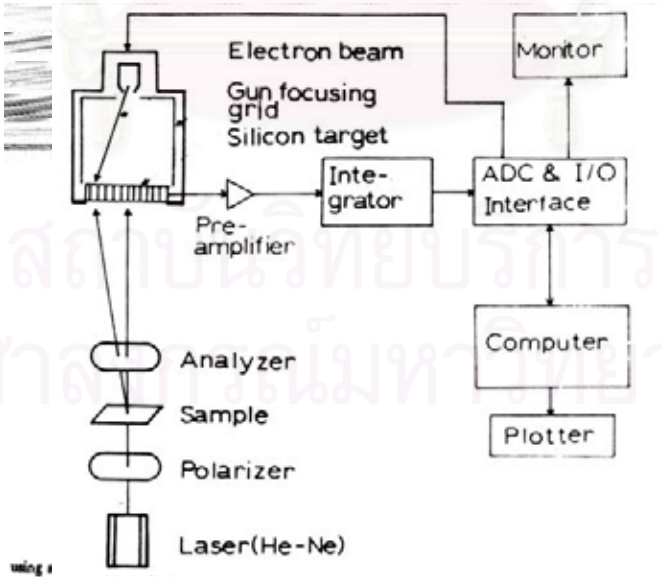

Figure 3-5 : Schematic representation of experimental arrangement for LS from polymer films using a laser and an OMA2. [Ree, M. 1987]

They observed that the LLDPE which is miscible with the LDPE component in the molten state crystallizes first, forming volume – filling spherulites. The LDPE then crystallizes within the performed spherulites. Furthermore the SALS intensity curve changes with composition of the blends that may be interpreted by considering the orientation of crystals within spherulites. It has been observed that the spherulites in the blend have more diffuse boundaries as the LDPE content increases. Moreover, they suggested that the SALS technique is very useful as a complement to DSC for determining crystallization behavior, cocrystallization, or separate crystallization, is this crystallizable blend system.

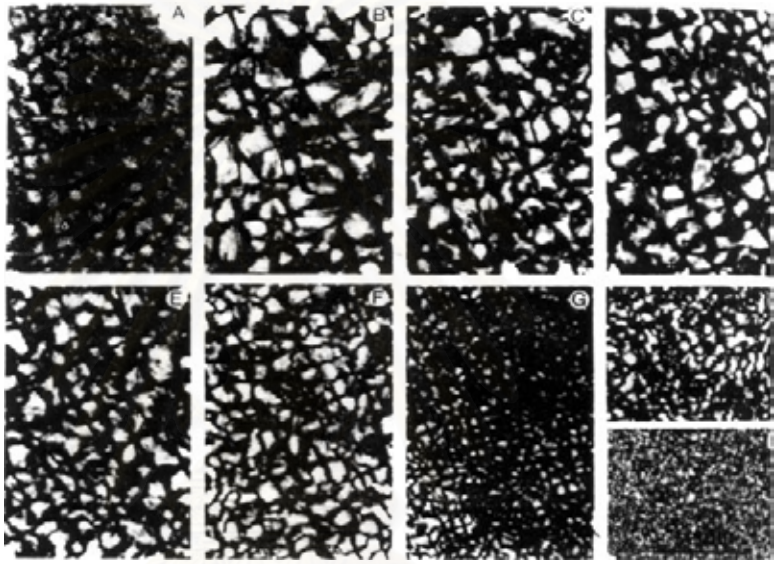

Figure 3-6 : Optical microphotographs of the samples crystallized at cooling rate of 2°C from the melt. (a) Purified LLDPE, (b) LLDPE/LDPE = 90/10 (wt. ratio), (c) 75/25, (d) 50/50, (e) 25/75, (f) 10/90, (g) LDPE, (h) Unpurified LLDPE, (I) Unpurified LDPE. All the micrographs were taken under crossed polars. The original magnification was 200X. [Ree, M. 1987]

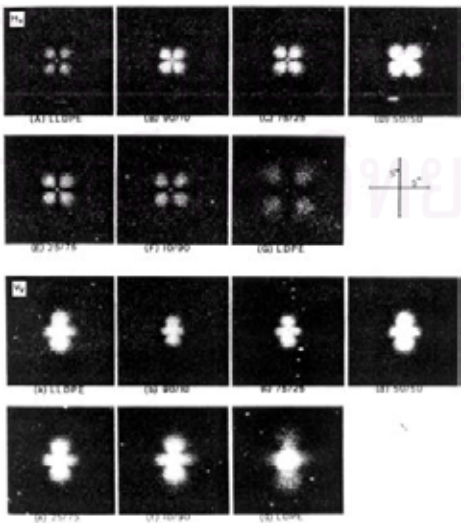

Figure 3-7 : Comparison of Hv and Vv SALS patterns from the blend samples with various compositions crystallized at cooling rate of 2°C/min from the melt. The numbers denote weight ratios of LLDPE and LDPE in the blends. [Ree, M. 1987]

Stien, R.S., Cronauer, J., and Zachmann, H.G. [1996] studied the crystallization of a single polymer component and polymer blends by using the small-angle light scattering technique. They found that this technique can be a conveient method for quantitatively following spherulitic crystallization. Moreover, it provides information about the number and sizes of spherulites as well as their internal crystallinity. From this technique, they observed that most polymers crystallize by a nucleation – and – growth mechanism in which spherulites develop as a consequence of the radial growth of branching crystalline lamellae from heterogeneous nuclei. The amorphous component is included within the spherulites. These grow until they imping and become volume filling. The primary crystallization occurs at the expanding interface of the spherulite with the amorphous polymer. Sometime the secondary crystallization may occur within the spherulite.

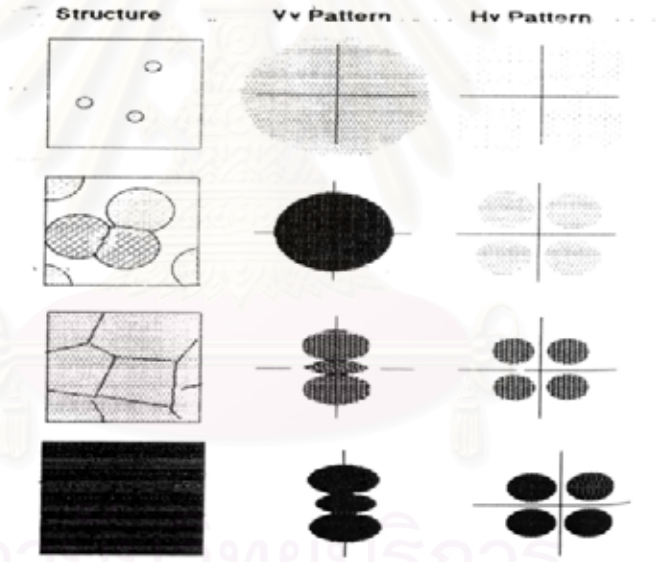

Figure 3-8 : The changs in spherulite morphology, Vv and Hv scattering patterns with time during the course of crystallization [Stein, R.S. 1996]

Marsha S. Bischel, Jerold M. Schulty and Kevin M. Kit [1998] studied etching technique for binary polymer blends of linear low density polyethylene (LLDPE) with high density polyethylene (HDPE). They observed that the optimal etchant for the component neat polymers are different. The etchant attacks the surface, areas of crystal disorder, amorphous regions and damaged regions. The pure LLDPE and HDPE have been etched for 30 min in different chemical formulations of solution of 2wt%, 3wt% of $KMnO_4$

respectively in the solution of phosphoric acid and sulfuric acid. So the blends have been etched using the two step procedure to identify the location of the two component polymers within the blends. The sample is first etched in the standard LLDPE etchant for 30 min. Then it is etched in the standard HDPE etchant for 10 min. The etched surface has been viewed in the SEM. They found that the bands are clearly evident after the first each, but there is little definition of structure in the center of the spherulite. Following the second etch, an axialite is clearly shown in the center of the banded spherulite and the bands are much more detailed.

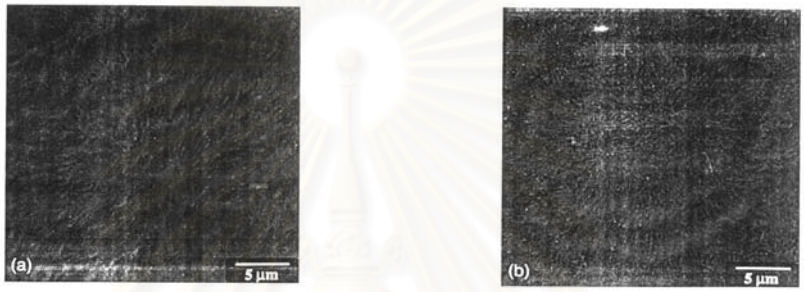

Figure 3-9 : 50/50 blend, Tc 150°C: (a) after first etch; (b) after second etch. SEM images of etched, sputtered surface [Marsha, S.B. 1998]

Morgan, R.J. , Hill, M.J. and Barham, P.J. [1999] investigated the effect of cooling rate on morphology, melting behavior and co – crystallization in a blend of linear polyethylene (LPE) with low density polyethylene (LDPE). The blend compositions, 50-90%wt LPE / LDPE were chosen so that the melt contained a single phase. They explained that the cooling rate has a significant effect on the degree of co – crystallization and segregation between the LPE and LDPE blend systems. The degree of segregation increase with decreasing cooling rate. The factors that affect co – crystallization, changing with cooling rate are likely to be the relative crystallization rates of the two components, the time available for transport of material and the crystal thickness of the LPE rich crystals. Furthermore they observed that a morphology formed in a LDPE rich blend during rapidly quenched from some temperatures in the melt contain two types of tightly packed lamellae, showing a banded texture and thinner lamellae, showing no banding. In addition, they concluded that the double morphologies found in some rapidly quenched blends are best explained in terms of liquid – liquid phase separation, rather than crystallization induces phase segregation.

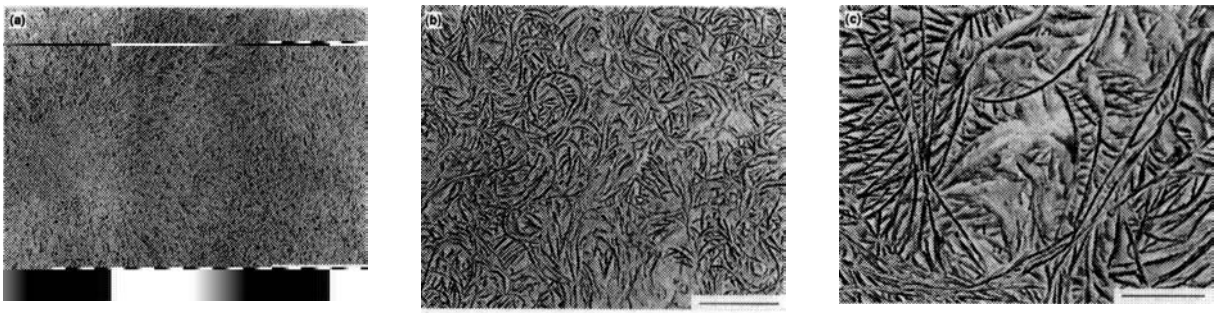

Figure 3-10 : TEM micrographs of surface replicas of 60% LPE/LDPE blends, cooled from the melt at different rates. The scale bars are 1 μm. (a) Rapidly quenched; (b) cooled at 60°C/min; (c) cooled at 1°C/min [Morgan, R.J. 1999]

Heon Sang Lee and Morton M. Denn [2000] studied blends of linear and branched polyethylenes. For example, HDPE/LLDPE blends which show a single melting temperature peak at all compositions because this blends co – crystallize to form a single phase and it is miscible blends.

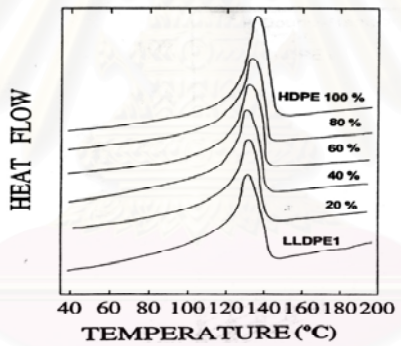

Figure 3-11 : Effect of compositions on melting temperature of HDPE – LLDPE blends [Heon Sang Lee 2000]

In the other hand, LLDPE/LDPE blends show two melting peaks at all composition, indicating crystalline phase separation. The melting peaks of both components are depressed slightly relative to the pure components:

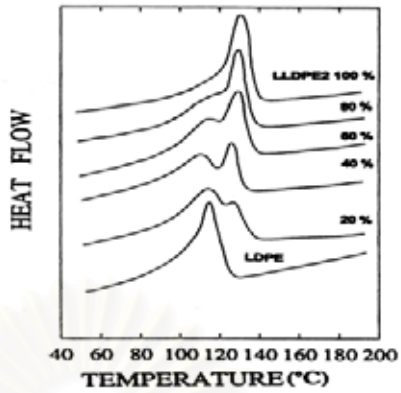

Figure 3-12 . Effect of composition on melting temperatures of LLDPE – LDPE blends. [Heon Sang Lee 2000]

The depression of the higher melting peak (LLDPE) may be due to co – crystallization of LLDPE with the more linear molecules of LDPE. The depression of the lower melting peak (LDPE) may be due to depletion of the more linear (higher – melting) molecules of LDPE.

For HDPE/LDPE blends show two melting peaks for LDPE – rich compositions, but a single peak for HDPE – rich compositions.

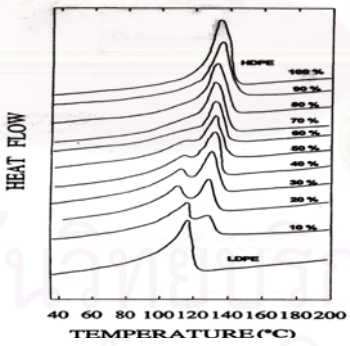

Figure 3-13 : Effect of composition on melting temperatures of HDPE – LDPE blends [Heon Sang Lee 2000]

The results indicated that HDPE/LDPE system is biphasic in the solid state but for HDPE – rich compositions, the crystalline and amorphous of this system is solid – phase miscibility. Furthermore they studied ternary blends of HDPE, LLDPE and LDPE. They found that HDPE is miscible with LLDPE and LDPE in the melt, while LLDPE is partially miscible with LDPE. This observation suggested that HDPE might act as a compatibilizing agent in this ternary blends. As the composition of HDPE is increased for a fixed ratio of the other two

components, the second melting peak disappears and the ternary system shows a single melting peak between those for pure LLDPE and HDPE, indicating that the ternary system forms a single crystalline phase.

Stein, R.S. , Jacob, K. ,et al. [2001] studied light scattering of the crystallization of polymers. They explained that the real time light scattering measurements during polymer crystallization can be interpreted in terms of the number, size and anisotropy of crystallizing species. Such observations have been used to show the lack of ordered regions in amorphous polymers. It is very sensitive for detecting the early stages of crystallization. While the crystals are too small at early stages to affect the angular dependence of scattering, they can appreciably contribute to its intensity, which depends upon their number and size. The subsequent changes in intensity and polarization can be fitted to parameters for a nucleation and growth model. Ultimately, when the dimensions of the growing species become sufficiently large, angularly dependent scattering results, which may be interpreted in terms of their size and state of aggregation. The technique of light scattering may be extended to the study of the crystallization of oriented polymers. It is rapid and may be used to follow the crystallization of films during their processing.

Joo Young Nam, Shigenobu Kadomatsu, Hiromu Saito and Takashi Inoue [2002] investigated the change of the crystalline morphology with temperature and the thermal reversibility in linear low density polyethylene (LLDPE) by Hv and Vv light scattering using CCD camera system in which the time resolved measurement is possible in millisecond order. They found that the morphological change with time after the temperature drop or jump was found to be very fast in several seconds. And the disordering in the heating process is caused by melting of thermally unstable thin lamellae existing between the thick lamellae, which are already developed at high crystallization temperature. So, the thermal reversibility is attribute to the thermally unstable thin lamellae because these thin lamellae are developed fast at wide temperature range in the cooling process and they melt fast in the heating process at narrow temperature range in which they are developed. Because of the crystalline morphology of LLDPE developed at high temperature cannot be frozen by quenching.

CHAPTER IV

Experiments

In this chapter, the materials, sample preparations and experimental techniques will be explained.

4.1 Materials

Polyethylene (PE) is the largest volume plastic. A wide variety of types and grades of polyethylene are available commercially. The basic structure of polyethylene is the chain, $-(CH_2CH_2)_n-$, which has no substitutent groups. Moreover PE is a crystalline solid, somewhat flexible, whose properties are strongly influenced by the relative amounts of crystalline and amorphous phases.

This research studied about light scattering behavior and morphology of polymer blend between two types of polyethylene, high density polyethylene (HDPE) and linear low density polyethylene (LLDPE).

4.1.1 High density polyethylene (HDPE)

HDPE is a highly crystalline, non - polar thermoplastic. Because of the high crystalline and the difference in refractive index between crystalline and amorphous phases, thin HDPE films are translucent, with significantly lower transparency than LLDPE. Additionally, the complex morphological structure of HDPE, such as boundaries between spherulites, further decrease transparency.

Figure 4-1 The molecular structure of HDPE

HDPE has excellent chemical resistance to most household and industrial chemicals. Chemical attack does happen with certain classes of chemicals such as aggressive oxidizing agents, aromatic hydrocarbons (xylene) and halogenated hydrocarbons. This polymer does not absorb moisture and provides good water vapor barrier, which makes it useful in packaging applications.

In this research, HDPE sample (injection molding grade) was provided by THAI PETROCHEMICAL INDUSTRY PUBLIC CO., LTD. The crystalline melting temperature is approximately 200 $^{\circ}$C. The melt flow rate (2.16 kg/190°C) is 3 g/10min and density is 0.957 g/cm^{3}.

4.1.2 Linear low density polyethylene (LLDPE)

LLDPE is characterized by linear molecules without long – chain branches. Short – chain branches in LLDPE are the result of copolymerization of ethylene with other alpha – olefins. The number and length of these short – chain branches are directly related to the concentration and molecular weight of the alpha – olefin comonomer. LLDPE forms a more highly crystalline structure because of the absence of long chain branching. The larger crystallites in LLDPE produce a stiffer product.

Linear low density polyethylene, when compared to conventional low density polyethylene (LDPE) of the same density and melt index in applications, such as films or flexible molded products, is claimed to have better impact, tear, or puncture properties and improved environmental stress – cracking resistance, allowing in a particular downgaging of films. One property where LLDPE suffers relative to LDPE is clarity. The haze and gloss of LLDPE film is poor, mainly because of the effect of its higher crystallinity on film surface roughness.

Figure 4-2 The molecular structure of LLDPE

Structurally, LLDPE differs from HDPE only in the number of short chain branches in the structure. The smaller number of short chain branches in HDPE results in higher density material.

In this research, LLDPE sample (extrusion grade) was provided by SIAM CHEMICAL TRADING CO.,LTD. The crystalline melting temperature is approximately 180°C. The melt flow rate is 0.9 g/10 min. and density is 0.920 g/cm^3.

4.2 Sample Preparations

4.2.1 Sample preparation for light scattering

In this study we use melt mixing method to blend HDPE with LLDPE because this method is the most similar to the industrial practice. The blends of HDPE and LLDPE were prepared at the compositions of 10, 20, 30, ..., 90 % by weight of HDPE by using a HAKKE single screw extruder at MTEC. Both polymers were first mixed as pellets and stirred outside the extruder, then they were put into the single screw extruder, which was operated at temperature between 160-180°C and screw speed of 40 rpm. Samples from the extruder were cut into small pellets by using a pelletiser, the size of pellet can be controlled by the speeds of the pelletiser and the screw. Then the mixed blends were pressed at 190°C and 5000 psi. for 10 minutes to form a thin film with the approximated thickness of 0.065 – 0.07 mm. thickness on a glass cover-slip by using a hydraulic hot press machine at polymer engineering laboratory, the Department of Chemical Engineering, Chulalongkorn University.

4.2.2 Sample preparation for scanning electron microscope

The pellets of each blend from single screw extruder were placed into a perforated plate stainless mould with the diameter of 20 mm. and 1 mm. thickness. The mould was placed between two releasing plates and heated for about 3 minutes until the polymer was almost all melted, then compressed at 200°C and 5000 psi. for 10 minutes by a hydraulic hot

press machine at polymer engineering laboratory, the Department of Chemical Engineering, Chulalongkorn University. After cooled by air about 5 minutes, the pieces of sample were removed from the mould and then etched surfaces by permanganic etching which is a technique of removing material selectively to reveal lamellae in crystalline polymers. In this work, we use a 3.5 % weight by volume solution of potassium premanganate in a concentrated sulfuric acid as the etchant. The samples were immersed and stirred in the etchant for 10 minutes in first etching. After that, samples were washed by water for 5 minutes and then washed by acetone for 5 minutes. Second etching, samples were stirred in the new prepared etchant for 10 minutes. Then the samples were washed by water for 10 minutes and washed by acetone for 10 minutes. Finally, samples were dried at room temperature and taken to investigate morphologies by scanning electron microscope.

4.3 Experimental Techniques

4.3.1 Light Scattering

This experiment was performed using the static light scattering apparatus at the polymer laboratory , the Department of Chemical Engineering, Chulalongkorn University. The equipment is schematically shown in Figure 4.3

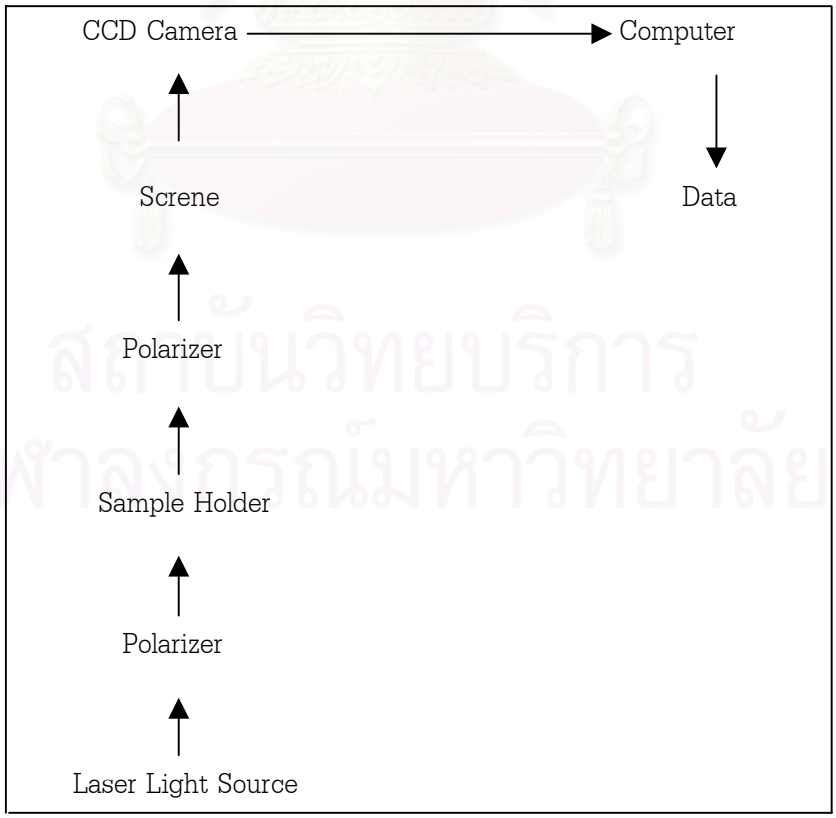

Figure 4.3 A schematic diagram of static light scattering equipment

A He/Ne laser (λ = 632.8 nm) is used as an incident light source. Samples were placed inside a holder, which was mounted between two polarizers where the polarization direction of the polarizer near the incident light was vertical and the other was horizontal. Light scattering photographs were detected by CCD Camera with exposure times 2 minutes, and the illumination of laser light source was set at no.3 (gain3) and no.6 (gain6) by using the computer program which was connected to the apparatus. Then these photographs were transferred to analyze using the computer.

Scanning Electron Microscopy

In scanning electron microscope, a fine beam of electron is first scanned across the surface of an opaque specimen. Once such as electron beam touches the surface, a difference of electron density in the specimen results a variety of scattering electron and photon emission. Those electrons are detected, modified and used to modulate the brightness of the second beam scanned synchronously in cathode ray tube (CRT). A big collected signal produces a bright spot on the CRT while a small signal produces a dimmer spot. Details of this technique can be found elsewhere.

Crystalline morphologies of the etched surfaces of crystalline polymers in this research was observed by using a scanning electron microscope JSM – 5410 at the Scientific and Technological Research Equipment Center, Chulalongkorn University as shown in Figure 4.4

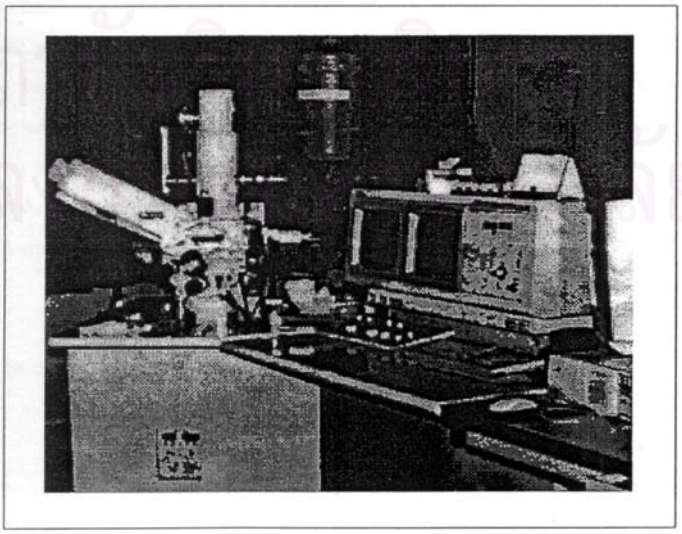

Figure4.4 A photographic illustration of SEM model JSM-5410

Since this technique requires the sample to be good at electron conducting, it is necessary to provide conduction to specimens by coating a thin metal layer. Thin film of gold was coated on specimens and then they were kept in a dry place before experiment. SEM was operated at 15 kV. This is considered to be suitable condition since too high energy can cause burning to samples.

CHAPTER V

Results and Discussions

5.1 Light Scattering Measurement

There are two parts of results from light scattering experiment; scattered light photographs and digital intensity data.

5.1.1 Scattered light photographs

Light scattering behaviors of the system of polymer blends between high density polyethylene (HDPE) and linear low density polyethylene (LLDPE) were investigated by using the modified light scattering apparatus with the illumination of light at no.3 (gain 3) and no.6 (gain 6). This apparatus will show the scattered light photographs which are both the single image and successive images. Furthermore it can provide digital intensity data at every angle of scattering. This modification are different from the original apparatus which use only the photographic light scattering technique and cannot save the light scattering photograph into the computer. Unlike the modified apparatus, the original apparatus can measure intensity at some angle of scattering. Therefore there are many information from the modified apparatus. Figure 5-1 shows scattered light photographs of two pure components and the blends at all compositions from gain3 and gain6. The light scattering photographs of the polymer blends containing small amount of LLDPE (about 10 – 30%) looks similar to that of pure HDPE. Similarly, the light scattering photographs of the polymer blends containing small amount of HDPE look like that of pure LLDPE. For 50/50 blended polymer, the result of light scattering behavior is between two pure components.

Pure HDPE

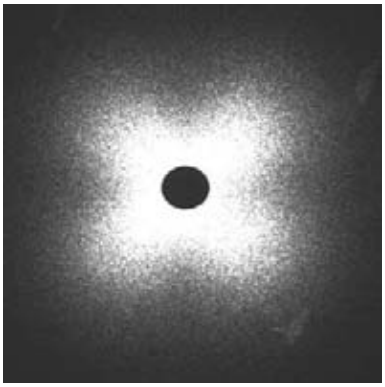

Gain6

(a)

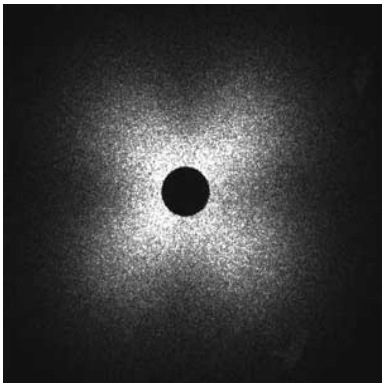

Gain3

HDPE / LLDPE : 90 / 10

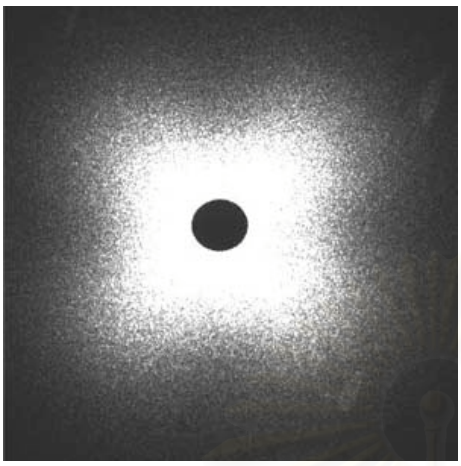

Gain6

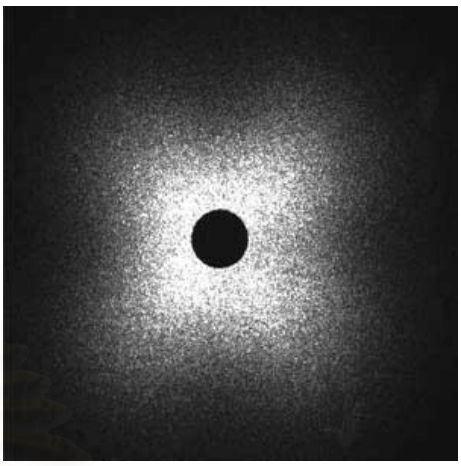

Gain3

(b)

HDPE / LLDPE : 80 /20

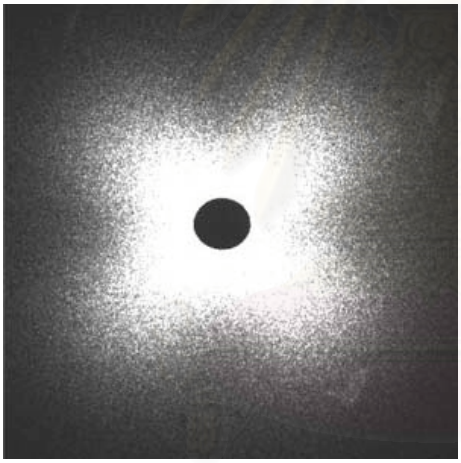

Gain6

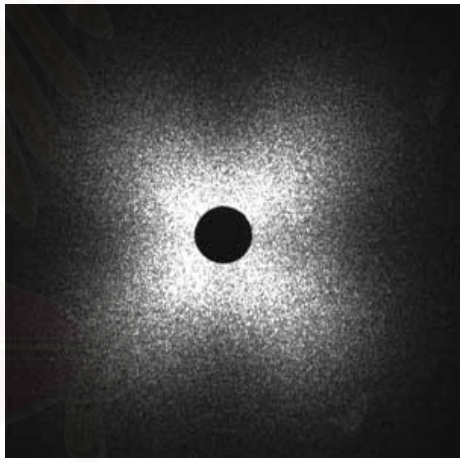

Gain3

(c)

HDPE / LLDPE : 70 / 30

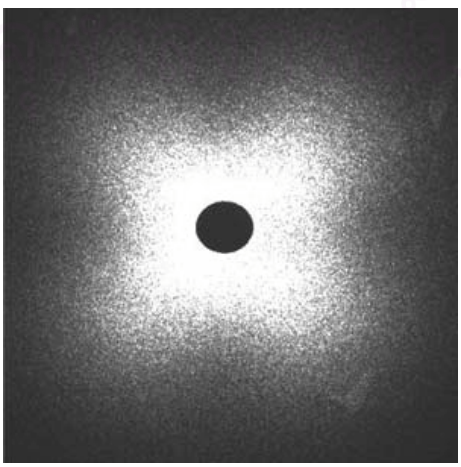

Gain6

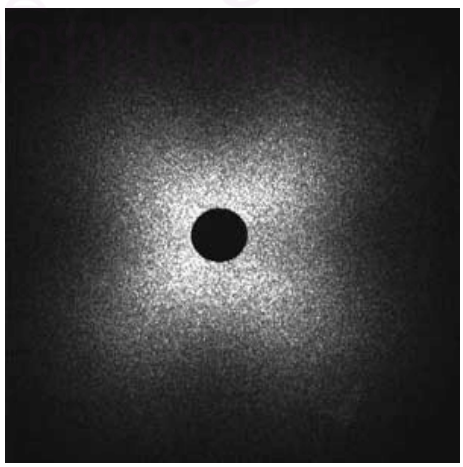

Gain3

(d)

HDPE / LLDPE : 60 /40

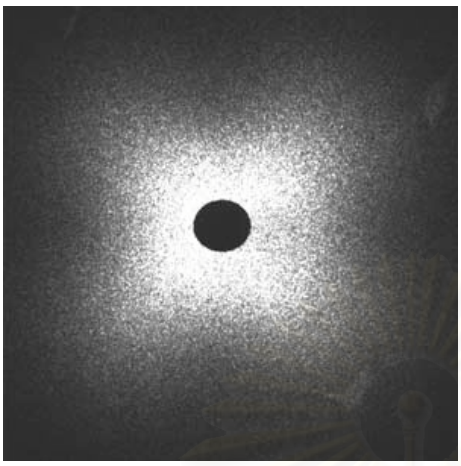

Gain6

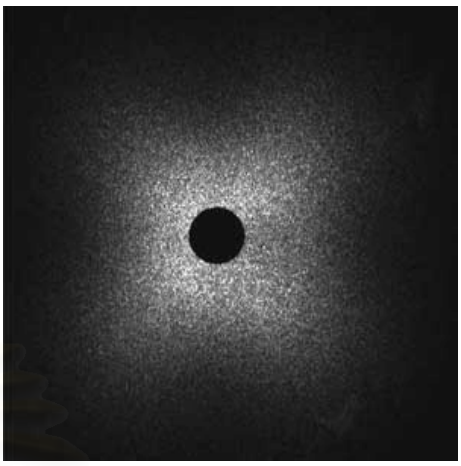

Gain3

(e)

HDPE / LLDPE : 50 / 50

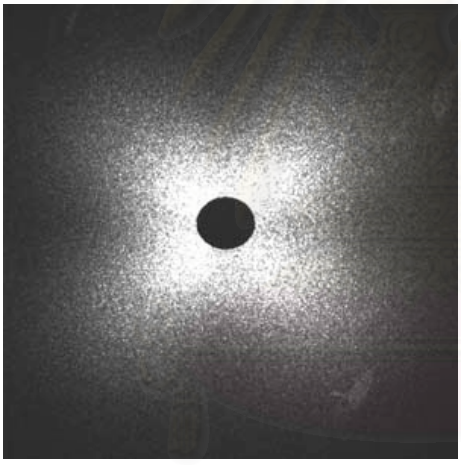

Gain6

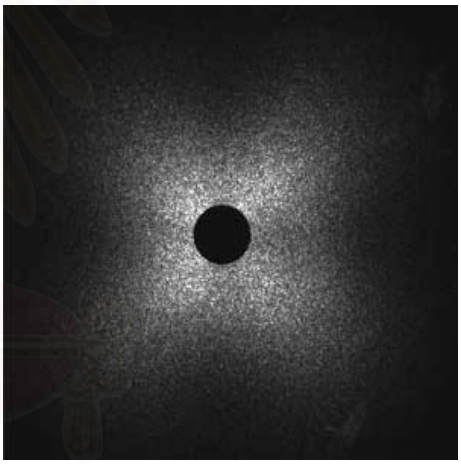

Gain3

(f)

HDPE / LLDPE : 40 /60

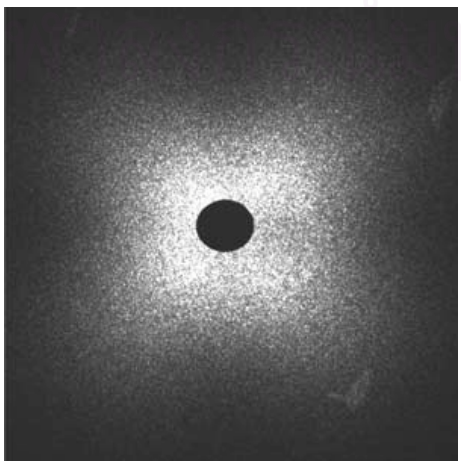

Gain6

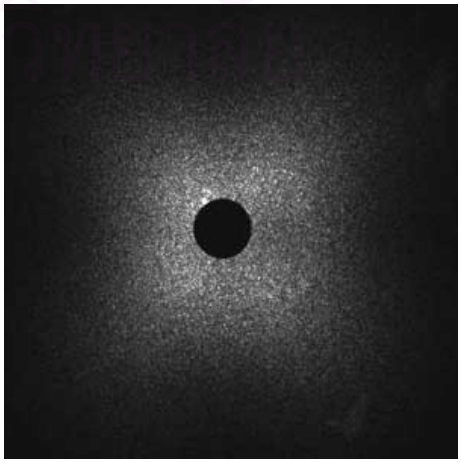

Gain3

(g)

HDPE / LLDPE : 30 / 70

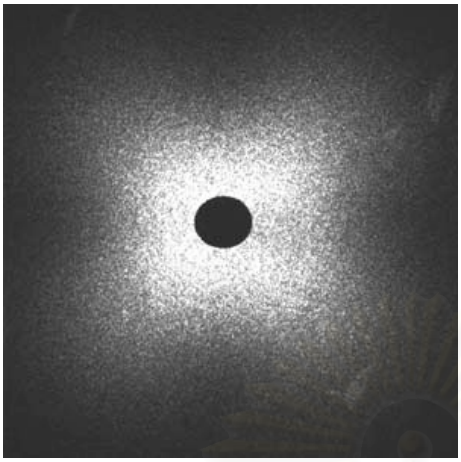

Gain6

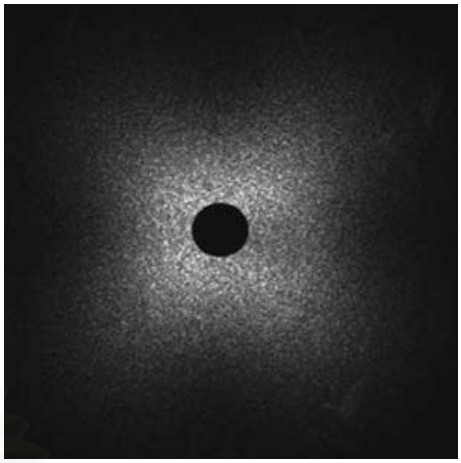

Gain3

(h)

HDPE / LLDPE : 20 / 80

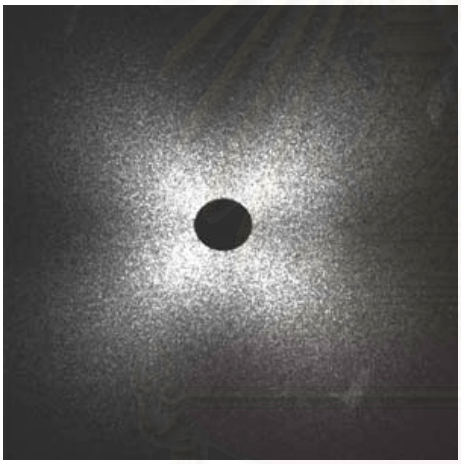

Gain6

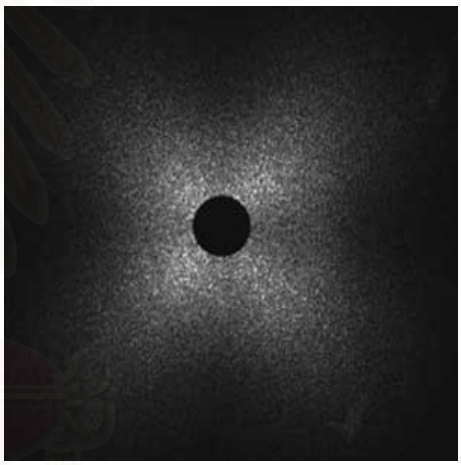

Gain3

(i)

HDPE / LLDPE : 10 / 90

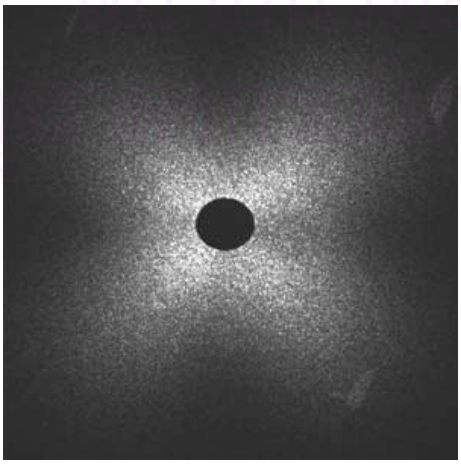

Gain6

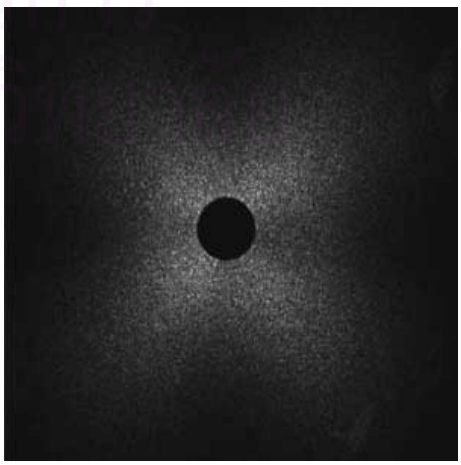

Gain3

(j)

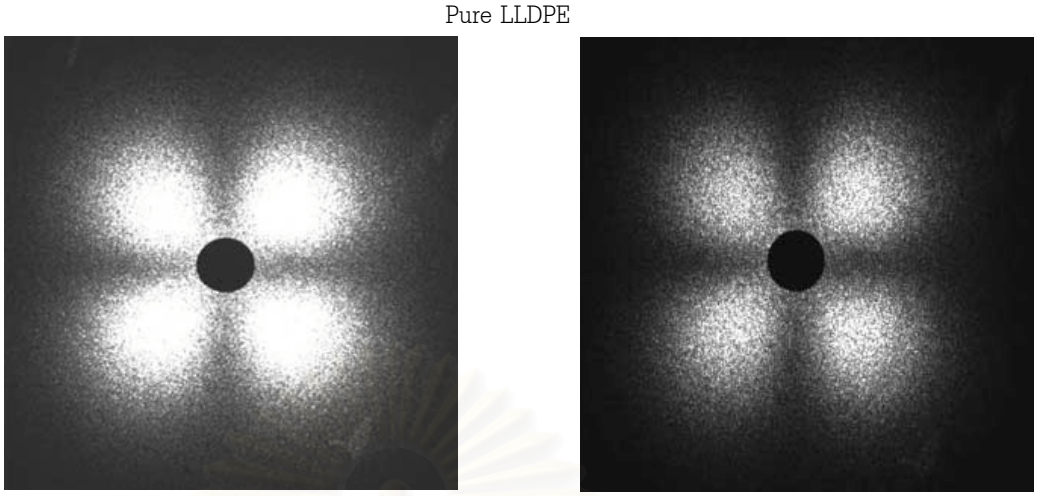

Figure 5-1 : Scattered light photographs of pure HDPE, pure LLDPE and all compositions of their blends

Since HDPE has higher degree of crystallinity than LLDPE therefore it has spherulites in the structure more than LLDPE. So the transparency of HDPE film is less than that of LLDPE film. That is why LLDPE film shows cloverleaf pattern better than HDPE.

5.1.2 Digital intensity data

The static light scattering apparatus can provide digital intensity data for every pixels. For one light scattering photograph, it contain 59049 data points of digital intensity and it can be plot as shown in Figure 5-2.

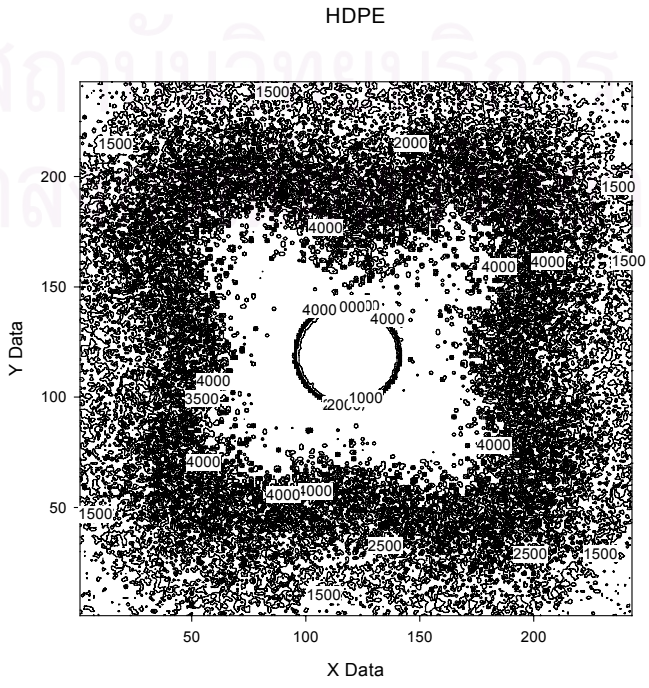

(a)

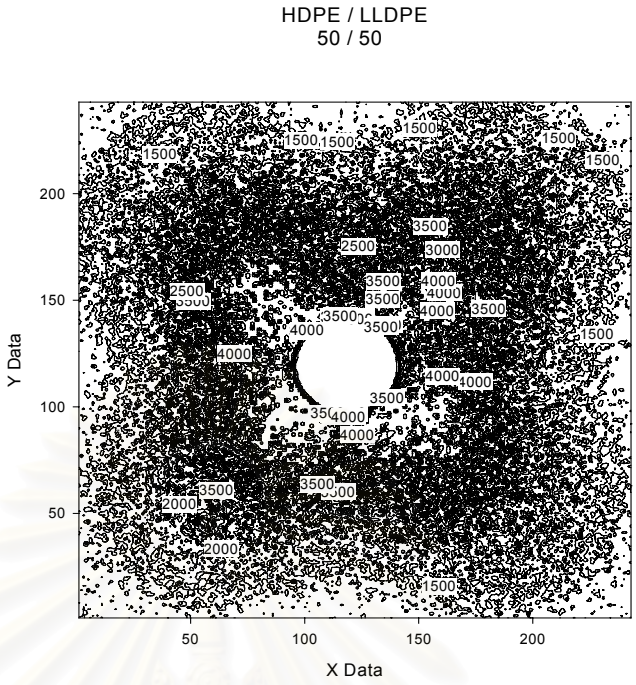

(b)

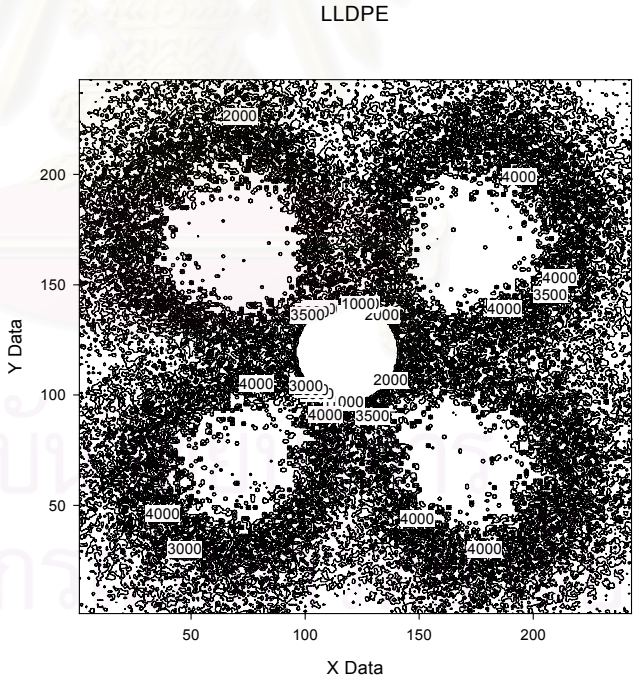

(c)

Figure 5-2 : Scattered light contour graphs of (a) pure HDPE, (b) 50/50 HDPE/LLDPE blends and (c) pure LLDPE

From figure 5-2, the data points are processed as shown in the schematic diagram (Figure 5-3) in order to obtain smooth contour lines.

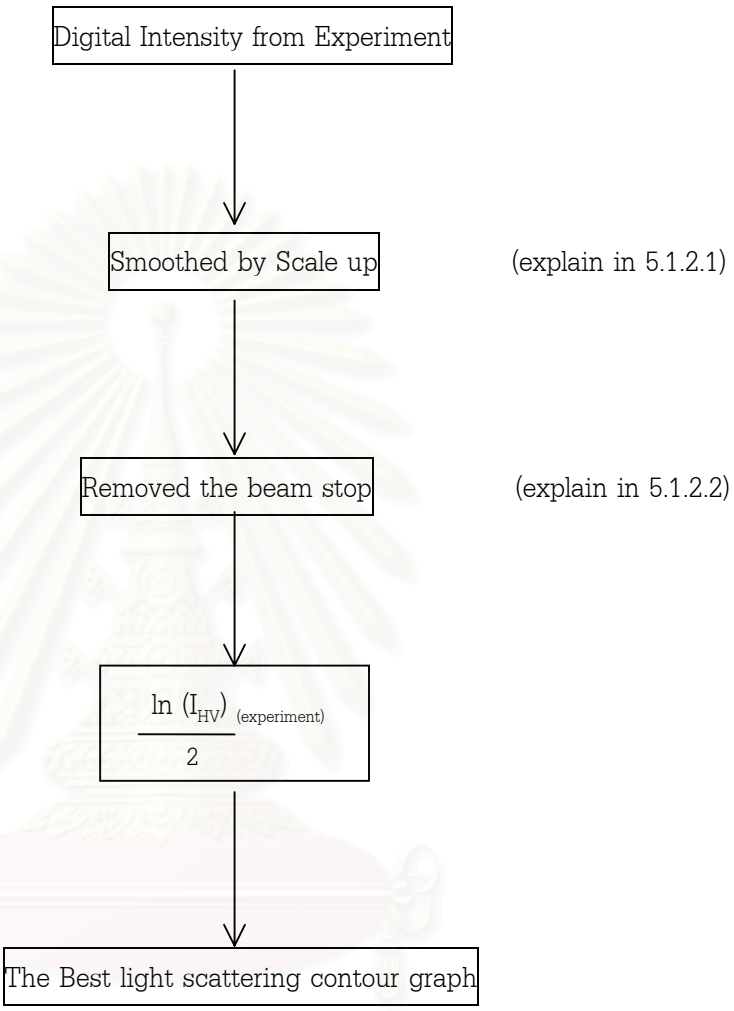

Figure 5-3: Schematic diagram of smoothing procedure

This procedure is auto – running by using sub – programming which can be run within 3 minutes.

5.1.2.1 Smoothing Digital Intensity Data

Digital intensity data are smoothed by using the average of intensity data to get better contour graphs that are clear and the characteristics of their curvatures are the same.

In searching the standard procedure, many trials and errors were done by varying the number of intensity data, which are averaged, and collected in details.

The detail of that trial can be concluded as follow,

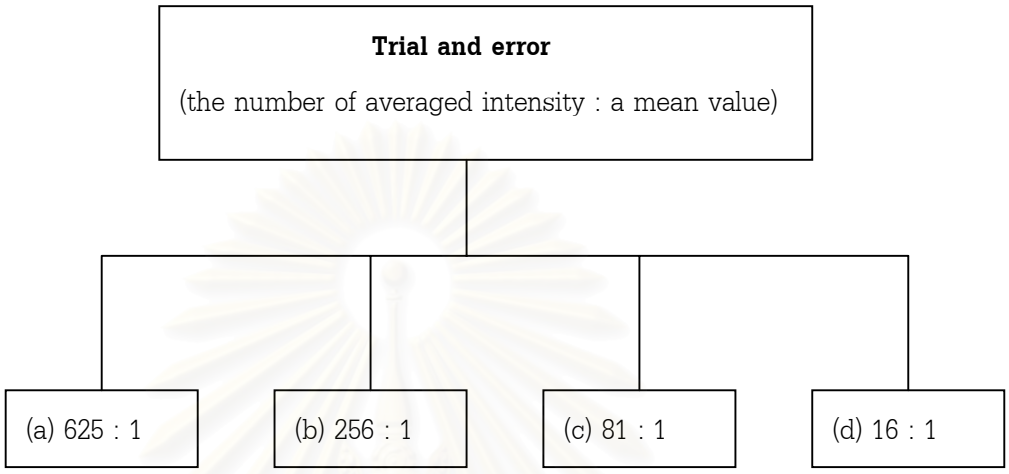

Results from trial and error are shown as contour graphs.

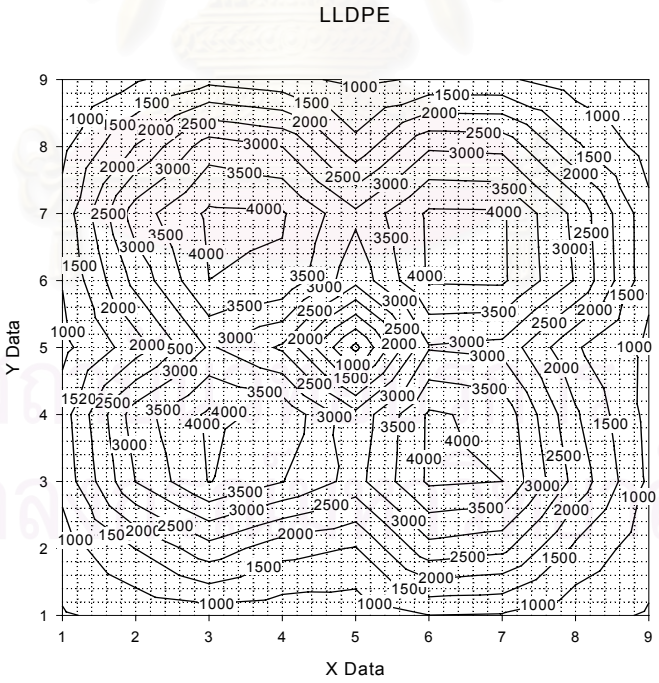

(a) 625 : 1

LLDPE

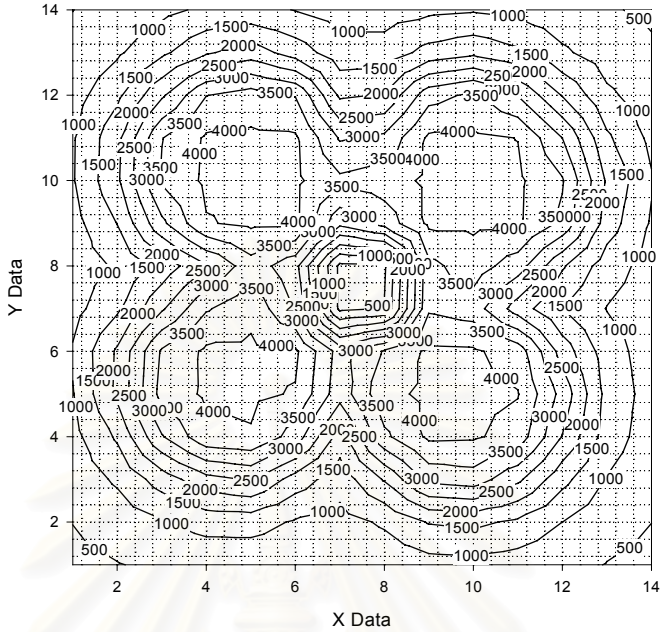

(b) 256 : 1

LLDPE

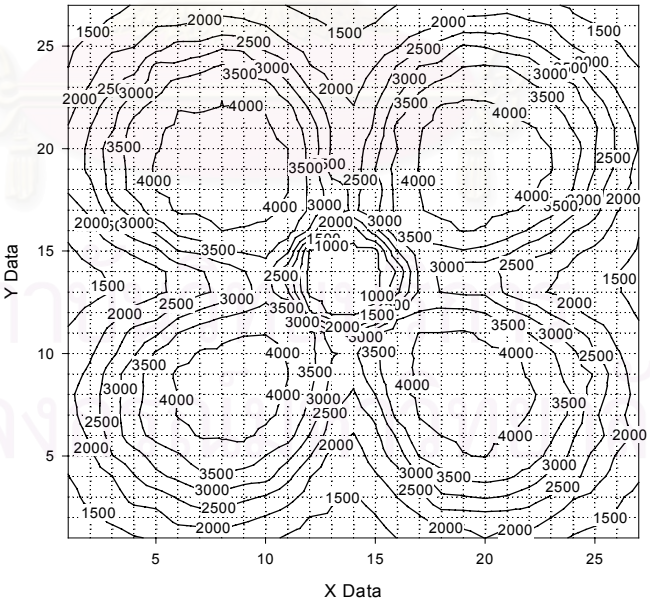

(c) 81 : 1

LLDPE

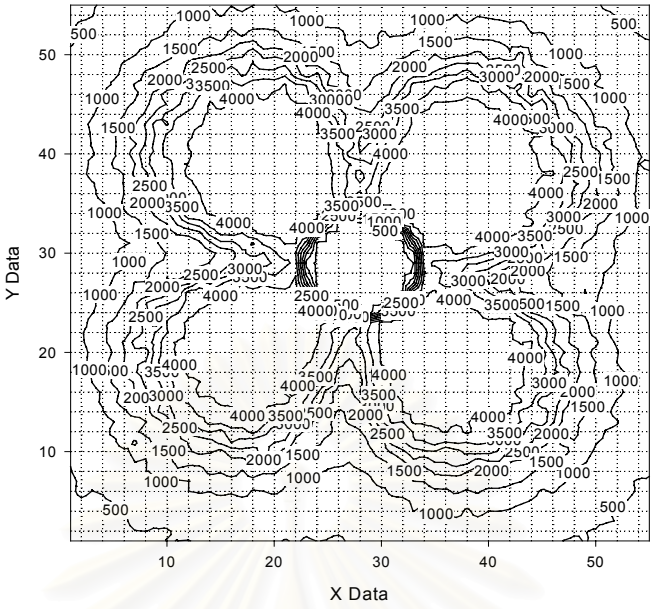

(d) 16 : 1

Figure5-4: Contour graphs of trial and error in smoothing intensity data

From these results, the best result is 81 : 1 because the graph fit with the scale and it is not too small graph as well as its contour line can be distinguishable.

HDPE

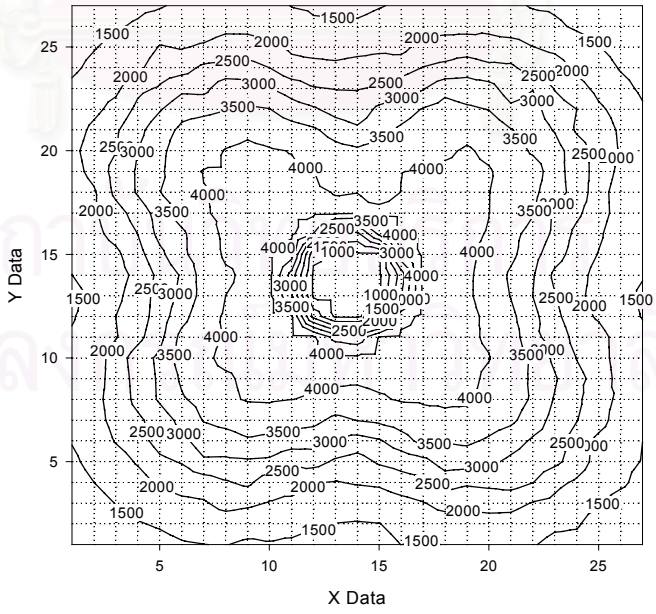

(a)

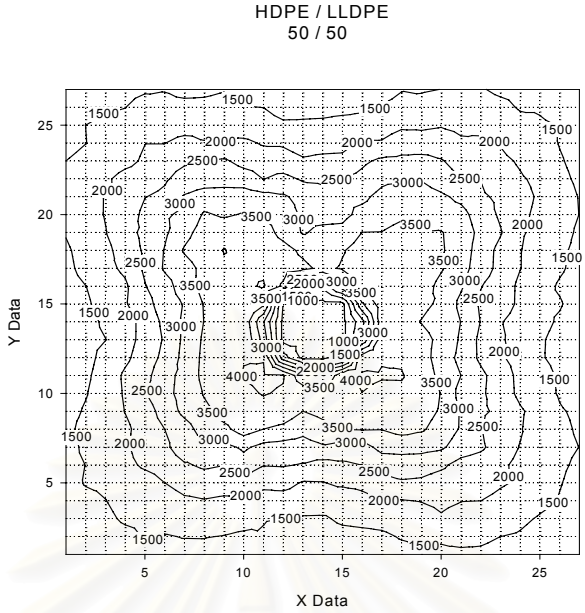

(b)

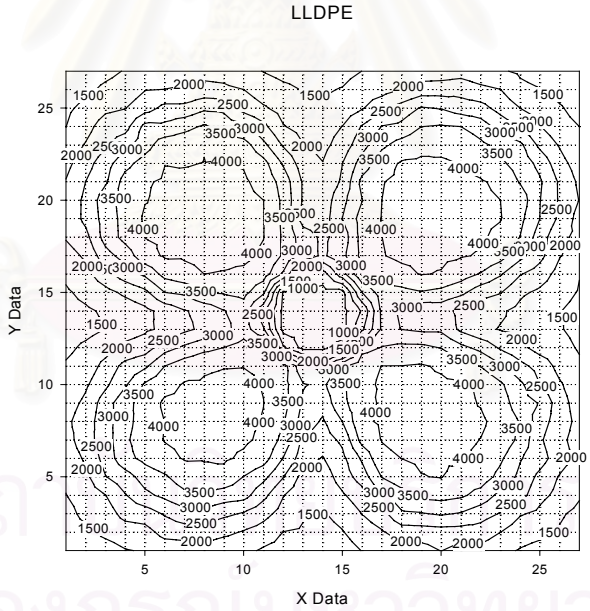

(c)

Figure5-5: Smoothed contour graphs of (a) pure HDPE, (b) 50/50 HDPE/LLDPE blends and (c) pure LLDPE

5.1.2.2 Removing the beam stop

At the center of each contour graph, it shows a small circle of the beam stop which comes from placing a coin at the center of the scene to protect the lens of the CCD Camera from the incident beam. Because the intensity data at this area do not arise from the light scattering of sample so they should be adjusted by using average intensity data from the outermost edge of the circle in this area. Adjusted results are shown in Figure 5-6

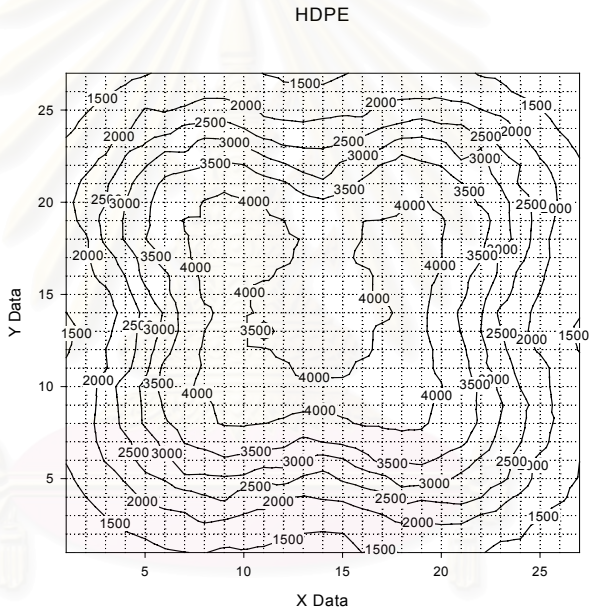

(a)

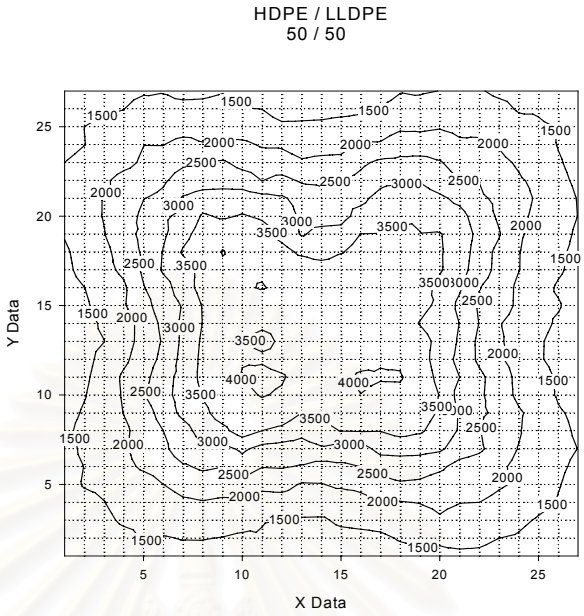

(b)

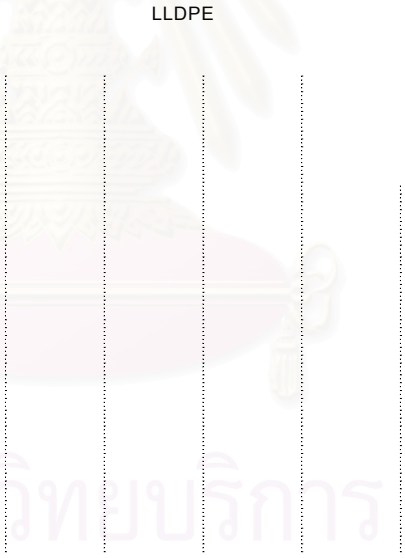

(c)

Figure 5-6: Contour graphs of (a) pure HDPE, (b) 50/50 HDPE/LLDPE blends and (c) pure LLDPE after improvement at the center

5.2 Intensity Data from Equation

In this study, the equation which is used to calculate intensity data is

$$I_{HV} = AV^2\left[\frac{3}{U^3}\frac{\cos^2\theta/2}{\cos\theta}\sin\phi\cos\phi\cos\rho_2\left(4\sin U - U\cos U - 3SiU\right)\right]^2$$

----------(5-1)

, as explained in chapter II. And the sine integral SiU is linearized by using Taylor series in order to simplify this equation.

$$SiU = U - \frac{U^3}{3\cdot 3!} + \frac{U^5}{5\cdot 5!} - \frac{U^7}{7\cdot 7!} + \frac{U^9}{9\cdot 9!}$$

----------(5-2)

when ;

$$U = \frac{4\pi Rs}{\lambda}\sin\theta/2$$

----------(5-3)

$$\cos\rho_2 = \frac{\cos\theta}{\sqrt{\cos^2\theta + \sin^2\theta\sin^2\phi}}$$

----------(5-4)

$$V = \frac{4}{3}\pi Rs^3$$

----------(5-5)

and $A = 1$ ----------(5-6)

Then take ln in two sides of equation ;

$$\frac{\ln(I_{HV})}{2} = \ln\left[AV\frac{3}{U^3}\frac{\cos^2\theta/2}{\cos\theta}\sin\phi\cos\phi\cos\rho_2\left(4\sin U - U\cos U - 3SiU\right)\right]$$

----------(5-7)

substituted (5-5), (5-6), (5-7) ;

$$\frac{\ln(I_{HV})}{2} = \ln\left[\frac{3}{U^3}\frac{\cos^2\theta}{\sqrt{\cos^2\theta+\sin^2\theta\sin^2\phi}}\sin\phi\cos\phi(4\sin U - U\cos U - 3SiU)\frac{4}{3}\pi Rs^3\right]$$

----------(5-9)

then ;

$$\frac{\ln(I_{HV})}{2} = \ln\left[\frac{3}{U^3}\right] + \ln\left[\frac{\cos^2\theta}{\sqrt{\cos^2\theta+\sin^2\theta\sin^2\phi}}\right] + \ln[\sin\phi\cos\phi] + \ln[4\sin U - U\cos U - 3SiU] + \ln\left[\frac{4}{3}\pi Rs^3\right]$$

----------(5-10)

substituted (5-5), (5-6) and separated to 5 terms ;

Term 1 : $\ln\left[\frac{3}{\left(\frac{4\pi Rs}{\lambda}\sin\theta/2\right)^3}\right]$

Term2 : $\ln\left[\frac{\cos^2\theta}{\sqrt{\cos^2\theta+\sin^2\theta\sin^2\phi}}\right]$

Term 3 : $\ln[\sin\phi\cos\phi]$

Term 4 : $\ln\left[\left\{4\sin\left(\frac{4\pi Rs}{\lambda}\sin\theta/2\right)\right\} - \left\{\left(\frac{4\pi Rs}{\lambda}\sin\theta/2\right)\cos\left(\frac{4\pi Rs}{\lambda}\sin\theta/2\right)\right\} - 3\left\{\left(\frac{4\pi Rs}{\lambda}\sin\theta/2\right) - \frac{\left(\frac{4\pi Rs}{\lambda}\sin\theta/2\right)^3}{3\cdot 3!} + \frac{\left(\frac{4\pi Rs}{\lambda}\sin\theta/2\right)^5}{5\cdot 5!} - \frac{\left(\frac{4\pi Rs}{\lambda}\sin\theta/2\right)^7}{7\cdot 7!} + \frac{\left(\frac{4\pi Rs}{\lambda}\sin\theta/2\right)^9}{9\cdot 9!}\right\}\right]$

Term 5 : $\ln\left[\frac{4}{3}\pi Rs^3\right]$

The radius of spherulite, Rs, is obtained from SEM photograph of etched surface of samples. The coefficient of each term is obtained by using the statistical calculation of LINEST function.

This LINEST function can be used to calculate the statistic for a line by using the "least squares" method to calculate a straight line that best fits the data, and returns an array that describes the line. The model of equation for the line and for multiple ranges of x – values is

$$y = m_1x_1 + m_2x_2 + ...+ B$$

where the dependent y – value is a function of the independent x – values. The m – values are coefficients corresponding to each x – value, and B is a constant value. In this work, the equation will be

$$\frac{\ln I_{HV}}{2} = m_1\text{Term1} + m_2\text{Term2} + m_3\text{Term3} + m_4\text{Term4} + m_5\text{Term5} + B$$

The array that obtains from LINEST is { m_n, m_{n-1}, ...,m_5, m_4, m_3, m_2, m_1, B}. LINEST can also provide additional regression statistics as follow;

	A	B	C	D	E	F
1	m_n	m_{n-1}	.....	m_2	m_1	B
2	se_n	se_{n-1}	.....	se_2	se_1	se_B
3	r^2	se_y				
4	F	d_f				
5	ss_{reg}	ss_{resid}				

where; se_1, se_2,....,se_n are the standard error values for the coefficients m_1, m_2,...,m_n.

se_B is the standard error value for the constant B

r^2 is the coefficient of determination. Compares estimated actual y – values, and ranges in value from 0 to 1. If it is 1, there is a perfect correlation in the sample – there is no difference between the estimated y – value and the actual y – value. At the other extreme, if the coefficient of determination is 0, the regression equation is not helpful in predicting a y – value.

se_y is the standard error for the y estimate.

F is the F statistic, or the F – observed value. use the F statistic to determine whether the observed relationship between the dependent and independent variables occurs by chance.

d_f is the degrees of freedom. Use the degrees of freedom to find F – critical values in a statistical table.

ss_{reg} is the regression sum of squares.

ss_{resid} is the residual sum of squares.

Results from this equation is shown as contour graphs in Figure 5-7

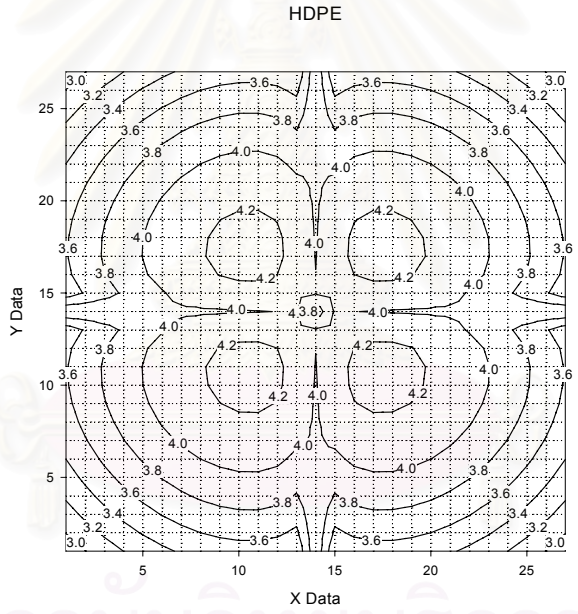

(a)

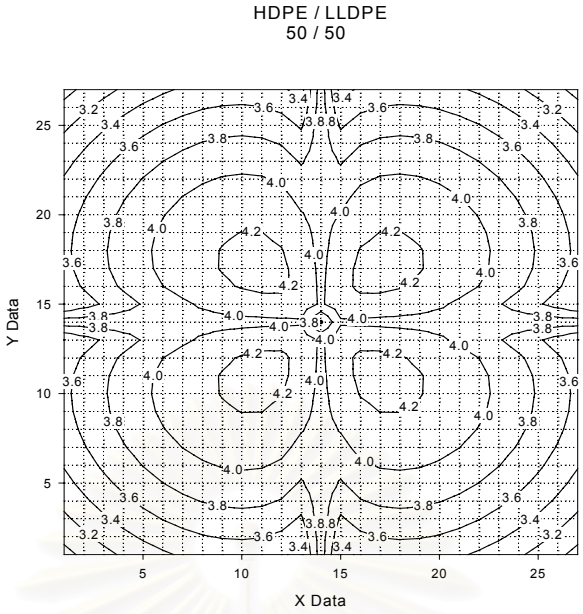

(b)

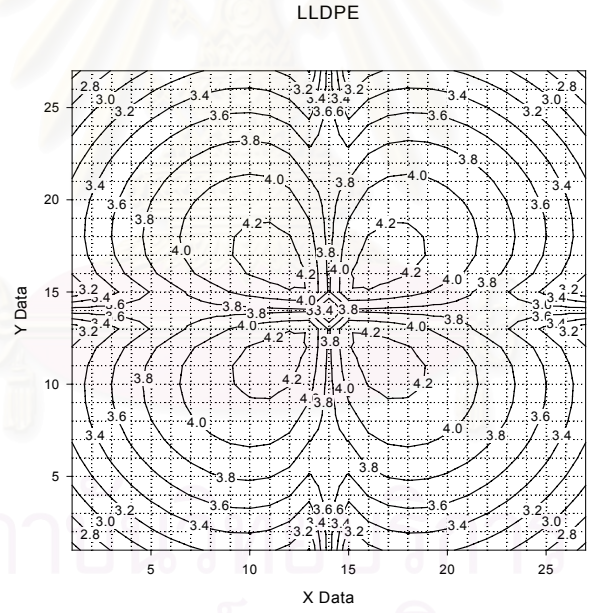

(c)

Figure 5-7 : Light scattering contour graphs from the equation of (a) HDPE, (b) 50/50 HDPE/LLDPE blends and (c) LLDPE

From this Figure, it shows incomplete light scattering I_{HV} pattern at x, y axis, contour lines converge to infinity. These results arise from the effect of the average of intensity data. Furthermore, term2 and term3 in the equation are the functions of sin 0° and sin 180° at x axis which are infinity. Similarly, the values of the function of cos 90° and cos 270° at y axis are infinity. And the r^2 value for curve fitting is 0.6651 which is not in the acceptable range. So the equation is modified at these axis in each term by substitution with average intensity data along the tangent of circle. Modified results as shown in Figure 5-8

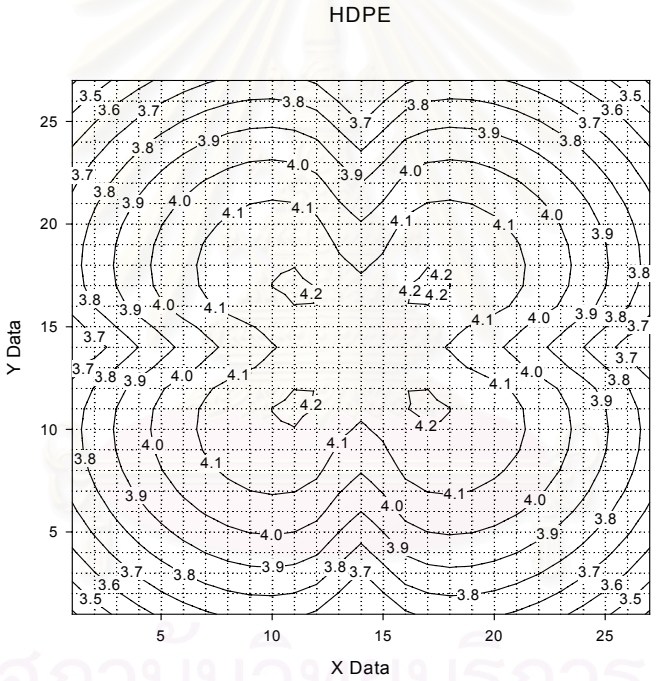

(a)

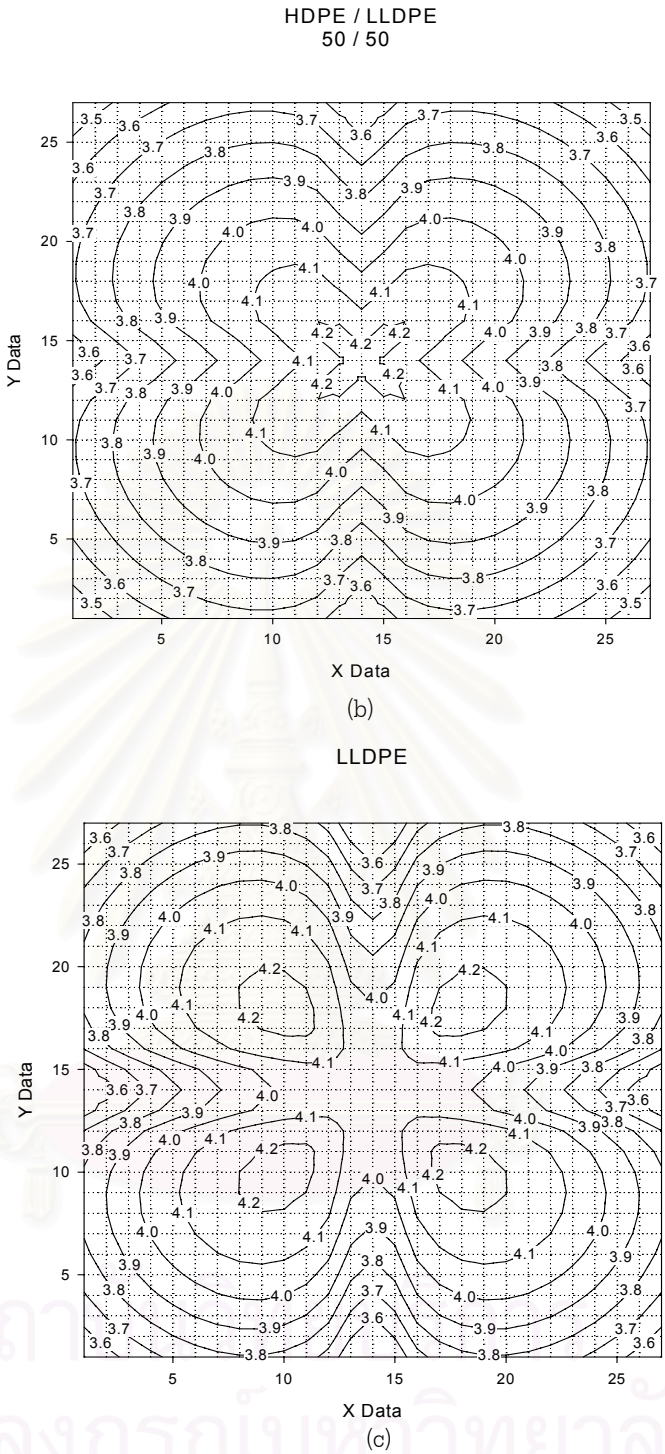

Figure 5-8: Modified contour graphs of (a) pure HDPE, (b) 50/50 HDPE/LLDPE blends and (c) pure LLDPE

The modified contour graphs are much similar to light scattering patterns. And they are confirmed by r^2, the multiple coefficient of determination, which is obtained by fitting the curve of $\frac{\ln I_{HV(\text{experiment})}}{2}$ with the equation (5-10) with the statistical function, LINEST.

Generally, an individual parameter coefficient in the model has particular practical significance and they can be tested by using the t test statistic. The form of the t test for this research can be explained as follows;

Test of the Individual Parameter Coefficient in the Multiple Regression Model

$$y = m_1x_1 + m_2x_2 + ...+ m_kx_k + B$$

Two – Tailed Test

$H_0 : m_i = 0$

$H_a : m_i \neq 0$

Test statistic : $t = \frac{m_i}{se_{mi}}$

Rejection region : $|t| > t_{\alpha/2}$

Where ; n = Number of observations

k = Number of independent variables in the model

and $t_{\alpha/2}$ is based on [n – (k+1)], d_f, the error degrees of freedom.

The calculated t values for testing $H_0 : m_i = 0$ for each coefficient in the model. For this research, there are many intensity data so $d_f = \infty$ and $\alpha/2 = 0.025$ thus ,from Table 1 in Appendix, $t_{\alpha/2} = 1.960$ with using the 95% confidence. If the t values of m_1, m_2,..... fall in the rejection region $|t| > 1.960$, it can be concluded that these terms make an important contribution to the model. These results of the illumination of light from gain no.6, area1 which is the area around the left – hand side of the sample are shown in Figure 5-9. The similar results from gain no.6, area2 which is the area around the right – hand side of the sample, gain no.3, area1 and gain no.3, area2 are shown in Appendix. Testing the overall utility of Multiple Regression Model can be done by using the analysis of variance F test. The form of the F test for this research can be explained as follows;

Hypothesises; Ho : $m_1 = m_2 = ... = m_k = 0$

Ha : At least one of the parameters, m_1, m_2, ..., m_k, differs from 0.

The test is formally used to test the global utility of the model. The test statistic used to test this null hypothesis is

Test statistic :

$$F = \frac{\text{Mean square for model}}{\text{Mean square for error}} = \frac{SS\ (Model) / k}{SSE / [n - (k+1)]}$$

where n is the number of data points, k is the number of parameters in the model (not including m_0), and SS(Model) = SS(Total) − SSE. When Ho is true, this F test statistic will have an F probability distribution with k df in the numerator and [n − (k + 1)] df in the denominator. The upper − tail values of the F distribution are given in Table C-2 of Appendix C. It can be shown that an equivalent form of this test statistic is

$$F = \frac{r^2/k}{(1 - r^2) / [n - (k + 1)]}$$

therefore, the F test statistic becomes large as the coefficient of determination r^2 becomes large.

The rejection region as follows :

$$\text{Rejection region} : F > F_{\alpha}$$

where ν_1 = k df and ν_2 = n − (k + 1) df

For this research, n = 729, k = 5, n − (k + 1) = 723, and α = 0.05. Consequently, it will reject Ho : $m_1 = m_2 = 0$ if $F > F_{.05}$ where $\nu_1 = 5$ and $\nu_2 = \infty$ or F > 2.21. If the F values of m_1, m_2,... fall in the ejection region F > 2.21, it can be concluded that at least one of the model coefficients is nonzero. The model appears to be useful for calculating intensity. These results from the data of gain no.6, area1 are shown in Figure 5-9. And results of gain no.6, area2 , gain no.3, area1 and area2 are shown in Appendix.

pure HDPE (gain6, area1)

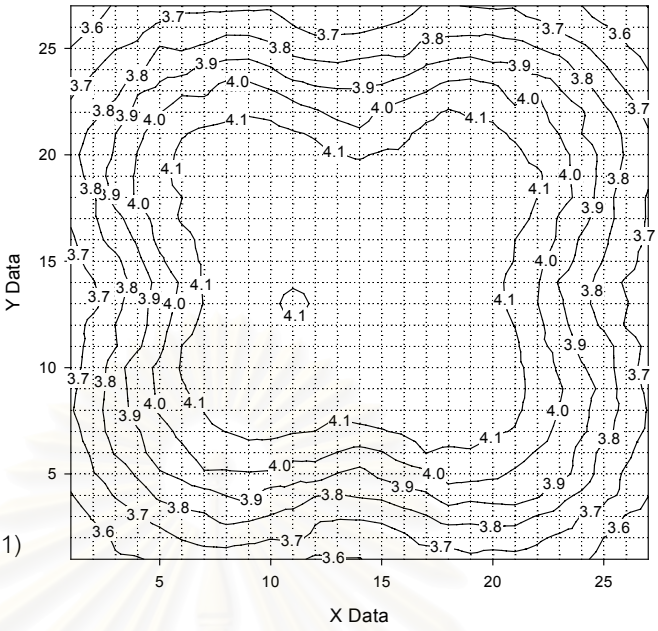

(a-1)

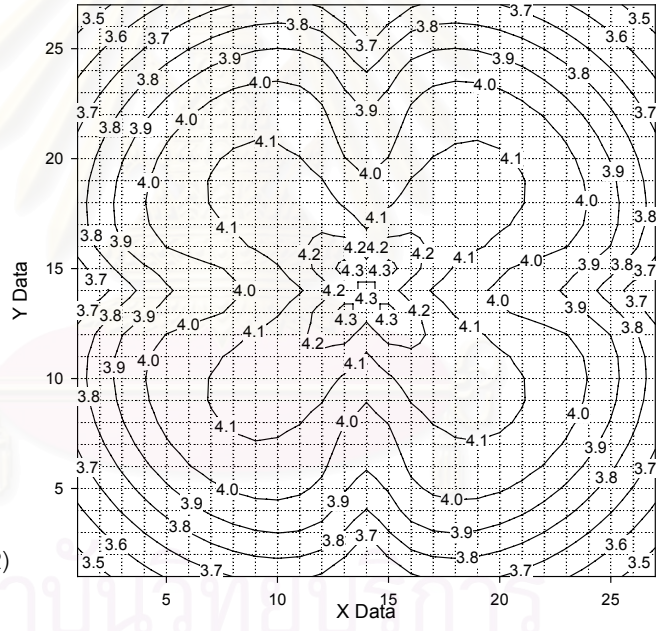

(a-2)

Regression Statistic Values

HDPE	TERM5	TERM4	TERM3	TERM2	TERM1	B
	0.033629	-0.124729	0.1173533	-74.41228	0.0176947	3.4827533
	430.61447	0.0027491	0.0042825	15.312993	0.0025654	13599.521
	0.9104671	0.0583843	#N/A	#N/A	#N/A	#N/A
	1470.4483	723	#N/A	#N/A	#N/A	#N/A
	25.061792	2.4645104	#N/A	#N/A	#N/A	#N/A
	#N/A	#N/A	#N/A	#N/A	#N/A	#N/A
t-test	7.81E-05	-45.37163	27.40286	-4.859421	6.8974852	0.0002561

(a) Pure HDPE from experiment(a-1) and from equation(a-2), r^2 = 0.9104

HDPE/LLDPE : 90 / 10 (gain6, area1)

(b –1)

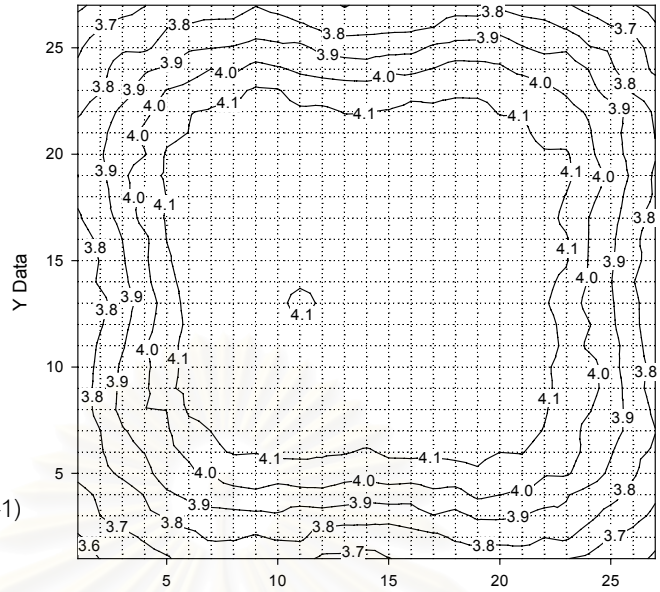

(b –2)

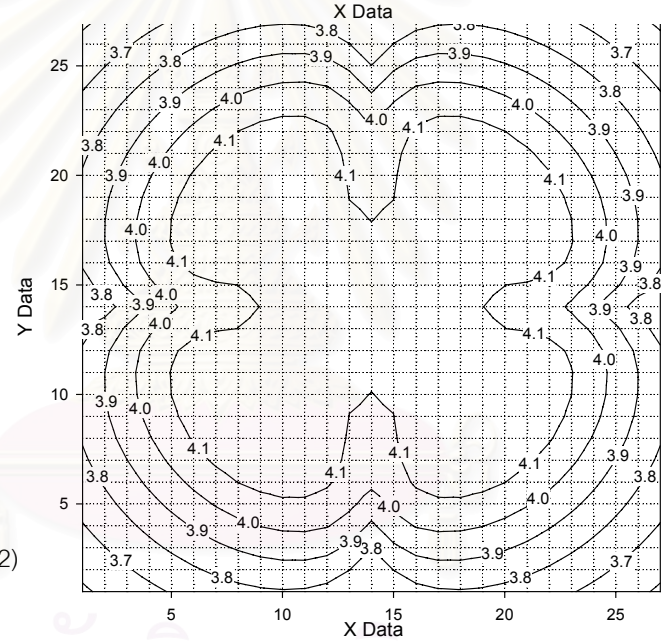

Regression Statistic Values

90-10	TERM5	TERM4	TERM3	TERM2	TERM1	B
	0.088236	-0.09878	0.082633	-69.4042	-0.02196	1.55958
	0	0.001423	0.002849	10.30102	0.001928	0
	0.945566	0.039275	#N/A	#N/A	#N/A	#N/A
	2511.85	723	#N/A	#N/A	#N/A	#N/A
	19.37296	1.115246	#N/A	#N/A	#N/A	#N/A
	#N/A	#N/A	#N/A	#N/A	#N/A	#N/A
t - test	α	-69.4079	29.00575	-6.73761	-11.3937	α

(b) 90 / 10 blended from experiment (b-1)and from equation (b-2), r^2 = 0.9455

HDPE/LLDPE : 80 / 20 (gain6, area1)

(c –1)

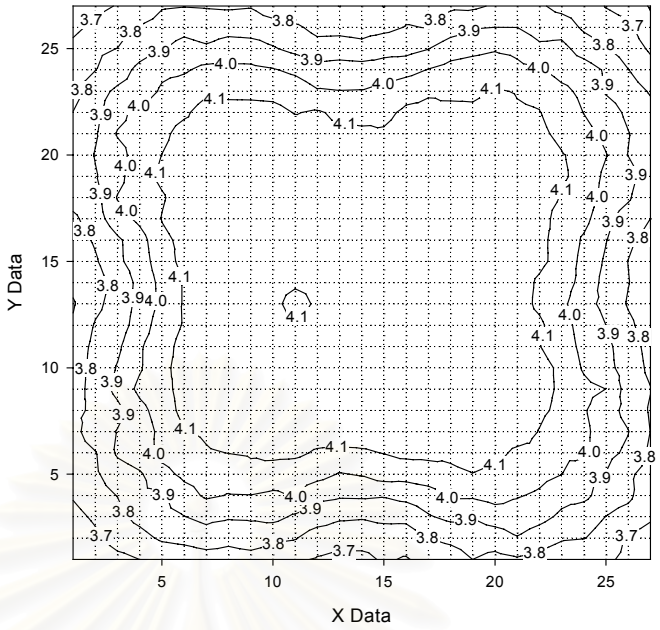

(c –2)

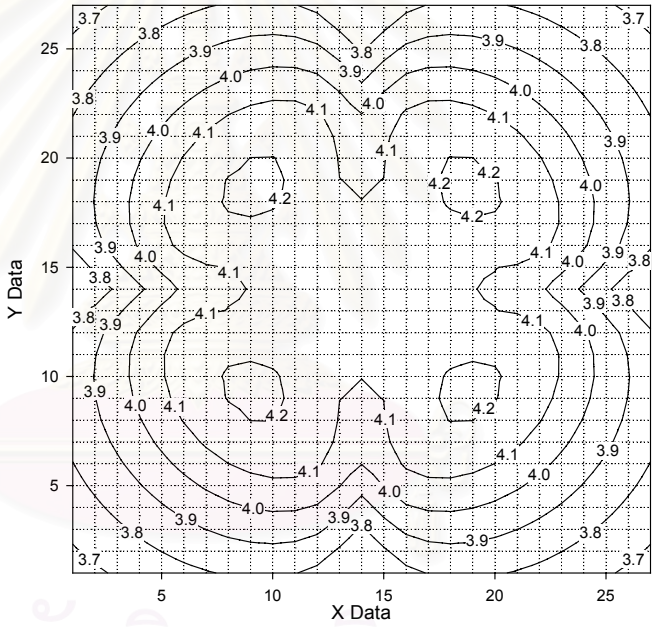

Regression Statistic Values

80-20	TERM5	TERM4	TERM3	TERM2	TERM1	B
	0.039298	-0.08502	0.098026	-55.4498	-0.02959	3.089427
	349.6297	0.001415	0.003022	10.98481	0.002191	11303.93
	0.929975	0.041882	#N/A	#N/A	#N/A	#N/A
	1920.364	723	#N/A	#N/A	#N/A	#N/A
	16.84268	1.268224	#N/A	#N/A	#N/A	#N/A
	#N/A	#N/A	#N/A	#N/A	#N/A	#N/A
t - test	0.000112	-60.1001	32.43623	-5.04786	-13.5042	0.000273

(c) 80 /20 blended from experiment (c-1) and from equation (c-2), r^2 = 0.9299

HDPE/LLDPE : 70 / 30 (gain6, area1)

(d –1)

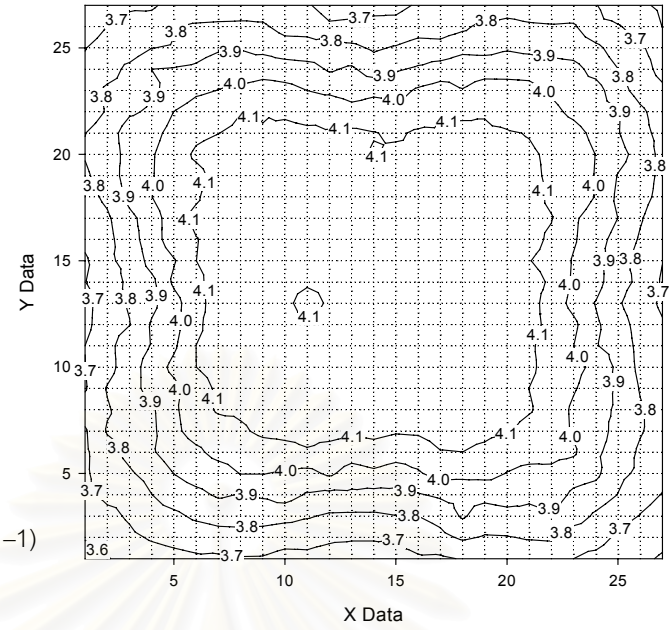

(d –2)

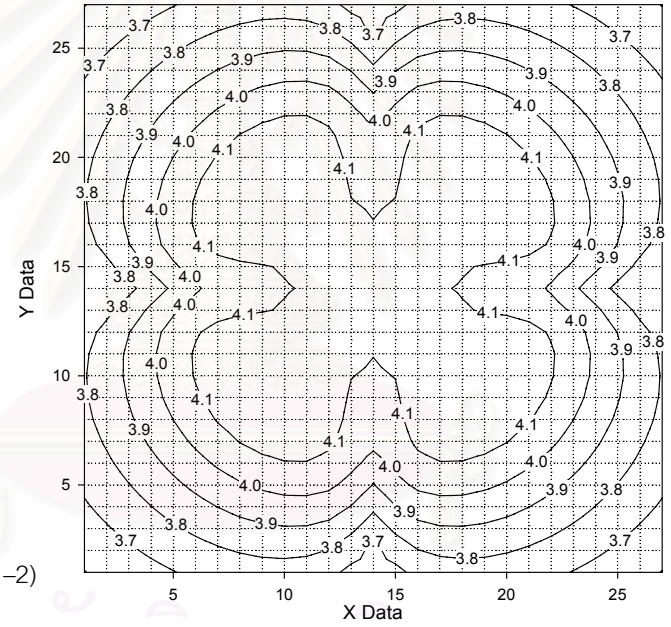

Regression Statistic Values

70-30	TERM5	TERM4	TERM3	TERM2	TERM1	B
	0.041244	-0.0834	0.090772	-62.843	-0.01745	3.035871
	0	0.001337	0.002881	10.4794	0.002115	0
	0.945246	0.039955	#N/A	#N/A	#N/A	#N/A
	2496.298	723	#N/A	#N/A	#N/A	#N/A
	19.92559	1.154205	#N/A	#N/A	#N/A	#N/A
	#N/A	#N/A	#N/A	#N/A	#N/A	#N/A
t - test	α	-62.3642	31.51101	-5.99681	-8.25131	α

(d) 70 /30 blended from experiment (d-1) and from equation (d-2), r^2 = 0.9452

HDPE/LLDPE : 60 / 40 (gain6, area1)

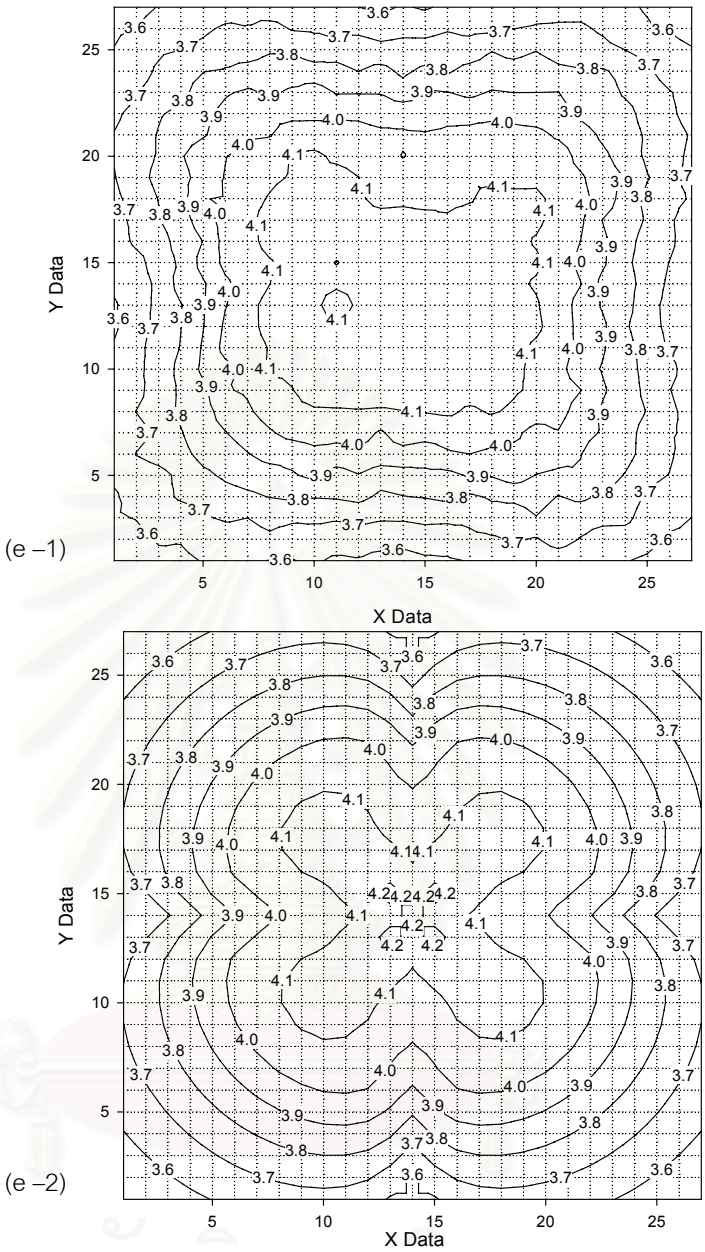

(e –1)

(e –2)

Regression Statistic Values

60-40	TERM5	TERM4	TERM3	TERM2	TERM1	B
	0.084262	-0.07374	0.083048	-65.6009	0.011261	1.656426
	0	0.001332	0.00289	10.52273	0.002148	0
	0.953782	0.04012	#N/A	#N/A	#N/A	#N/A
	2984.02	723	#N/A	#N/A	#N/A	#N/A
	24.01602	1.163771	#N/A	#N/A	#N/A	#N/A
	#N/A	#N/A	#N/A	#N/A	#N/A	#N/A
t - test	α	-55.3588	28.73398	-6.23421	5.243497	α

(e) 60 /40 blended from experiment (e-1) and from equation (e-2), r^2 = 0.9537

HDPE/LLDPE : 50 / 50 (gain6, area1)

(f –1)

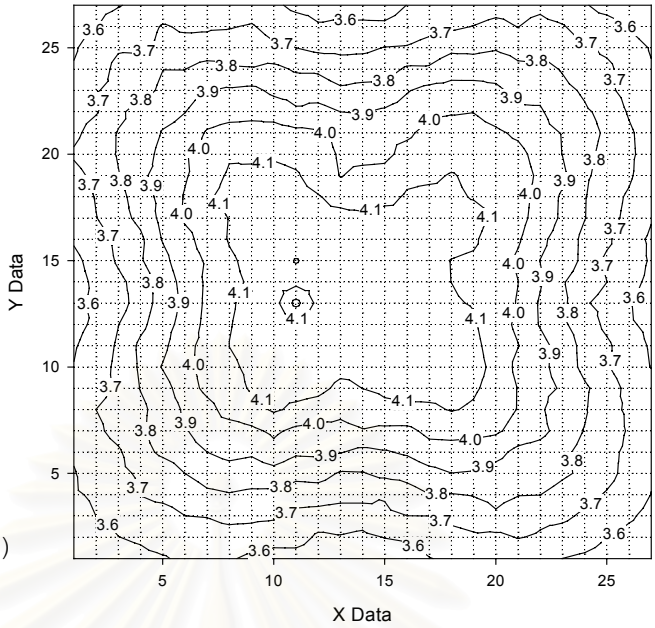

(f –2)

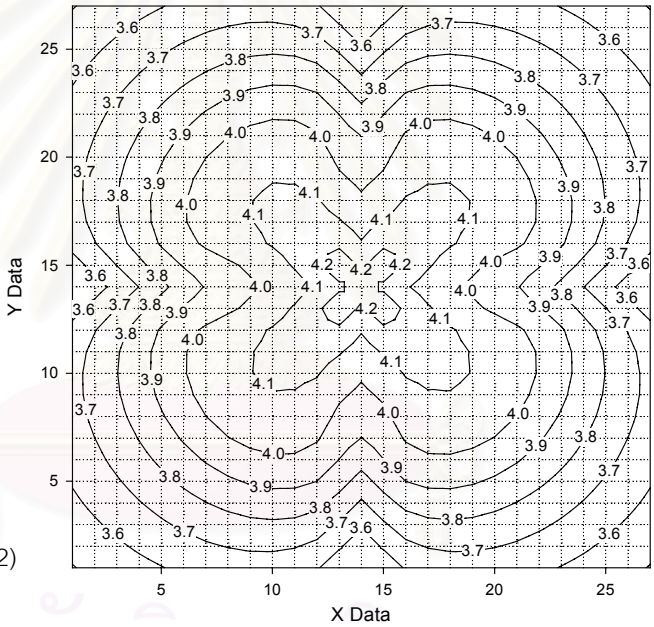

Regression Statistic Values

50-50	TERM5	TERM4	TERM3	TERM2	TERM1	B
	5.49E-05	-0.0704	0.10991	-35.6346	0.023209	4.422172
	458.9808	0.001526	0.003253	11.82074	0.002352	14835.2
	0.943636	0.045069	#N/A	#N/A	#N/A	#N/A
	2420.859	723	#N/A	#N/A	#N/A	#N/A
	24.58676	1.468588	#N/A	#N/A	#N/A	#N/A
	#N/A	#N/A	#N/A	#N/A	#N/A	#N/A
t - test	1.2E-07	-46.1458	33.79013	-3.01459	9.867502	0.000298

(f) 50 /50 blended from experiment (f –1) and from equation (f –2), r^2 = 0.9436

HDPE/LLDPE : 40 / 60 (gain6, area1)

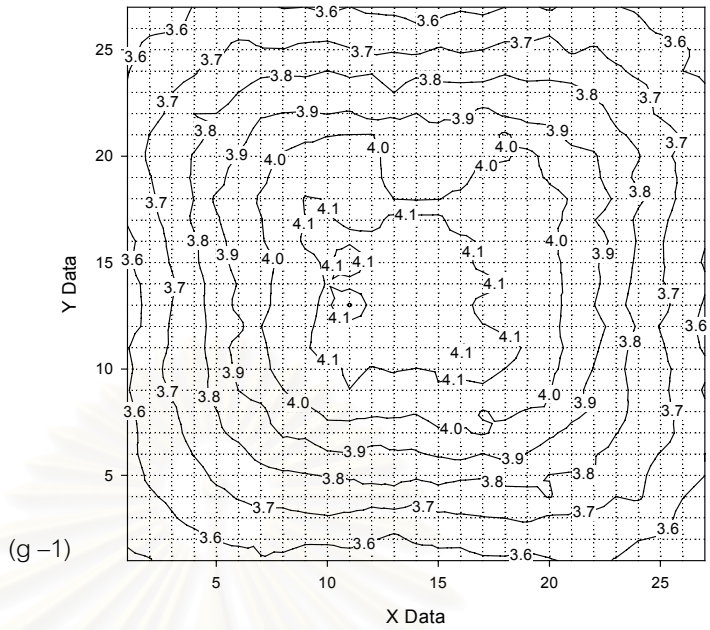

(g –1)

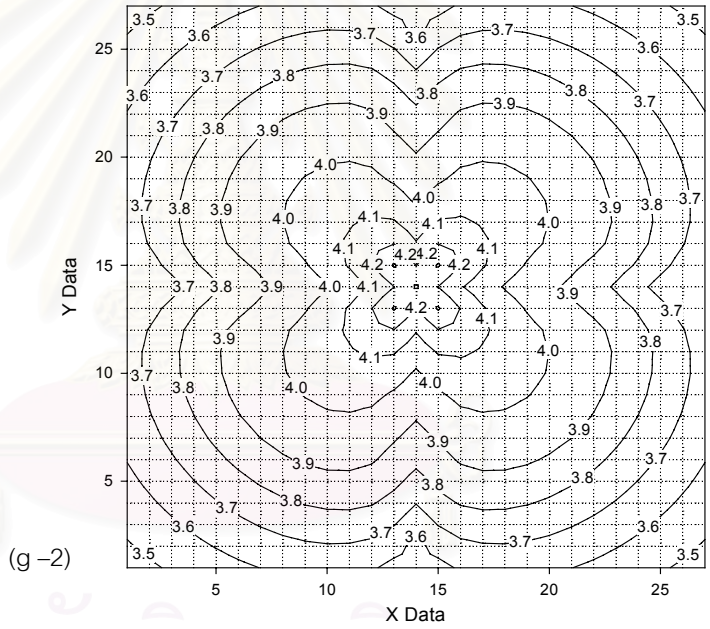

(g –2)

Regression Statistic Values

40-60	TERM5	TERM4	TERM3	TERM2	TERM1	B
	0.069575	-0.06133	0.070942	-55.9552	0.051587	2.158419
	0	0.00176	0.003389	12.22271	0.002228	0
	0.933943	0.046602	#N/A	#N/A	#N/A	#N/A
	2044.417	723	#N/A	#N/A	#N/A	#N/A
	22.19967	1.570165	#N/A	#N/A	#N/A	#N/A
	#N/A	#N/A	#N/A	#N/A	#N/A	#N/A
t - test	α	-34.8525	20.93603	-4.57797	23.15741	α

(g) 40 /60 blended from experiment (g-1) and from equation (g-2), r^2 = 0.9339

HDPE/LLDPE : 30 / 70 (gain6, area1)

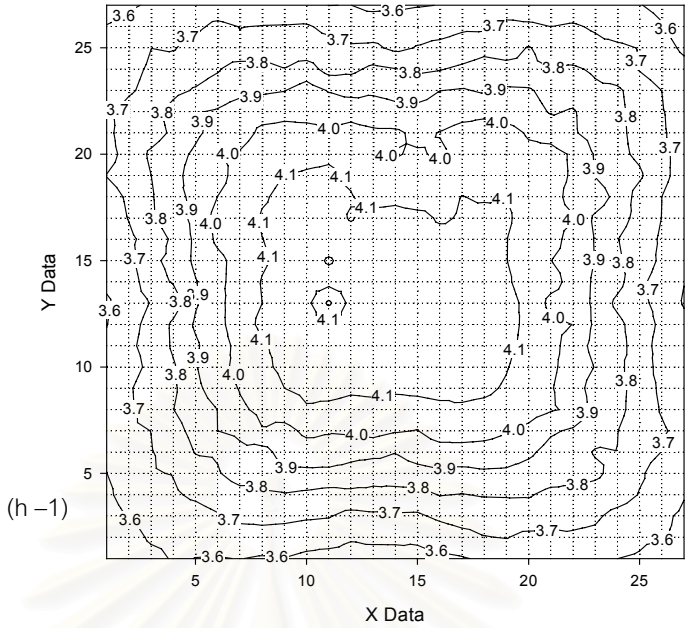

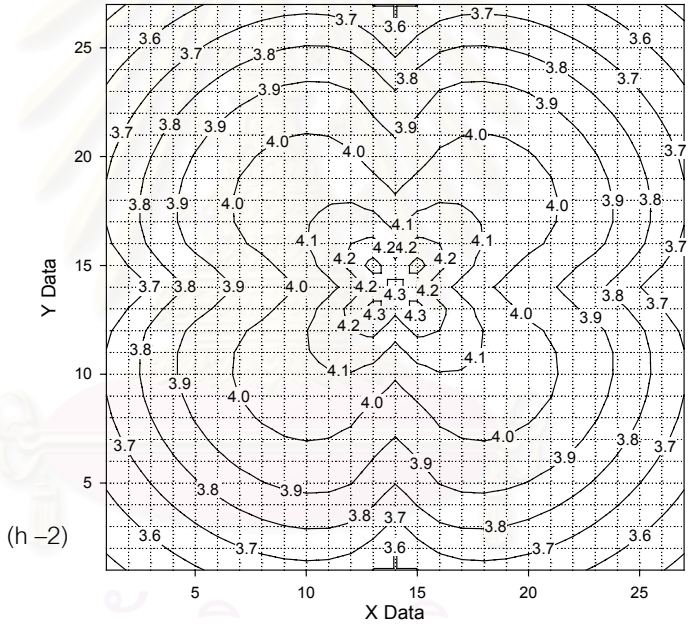

Regression Statistic Values

30-70	TERM5	TERM4	TERM3	TERM2	TERM1	B
	0.069354	-0.07427	0.082444	-63.0184	0.046876	2.226854
	421.5941	0.002296	0.004055	14.56466	0.002542	13403.76
	0.908441	0.055531	#N/A	#N/A	#N/A	#N/A
	1434.716	723	#N/A	#N/A	#N/A	#N/A
	22.1212	2.229518	#N/A	#N/A	#N/A	#N/A
	#N/A	#N/A	#N/A	#N/A	#N/A	#N/A
t - test	0.000165	-32.3437	20.32981	-4.3268	18.43871	0.000166

(h) 30 /70 blended from experiment (h-1) and from equation (h-2), r^2 = 0.9084

HDPE/LLDPE : 20 / 80 (gain6, area1)

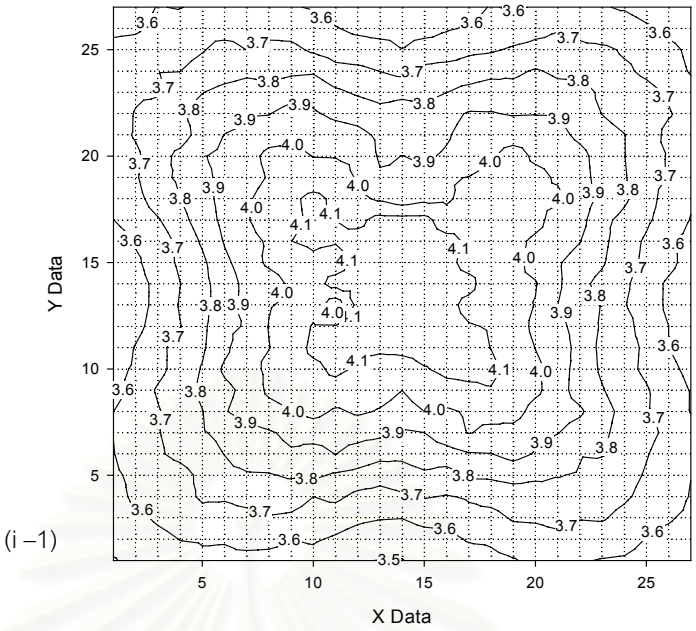

(i –1)

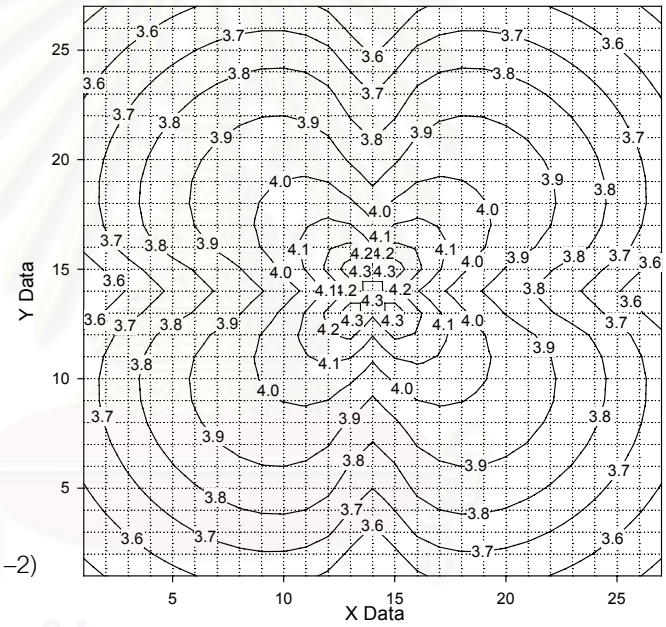

(i –2)

Regression Statistic Values

20-80	TERM5	TERM4	TERM3	TERM2	TERM1	B
	0.093581	-0.05985	0.111275	-53.1778	0.06573	1.457533
	501.5698	0.002472	0.004021	14.39518	0.002441	15873.83
	0.906838	0.054885	#N/A	#N/A	#N/A	#N/A
	1407.543	723	#N/A	#N/A	#N/A	#N/A
	21.20012	2.177935	#N/A	#N/A	#N/A	#N/A
	#N/A	#N/A	#N/A	#N/A	#N/A	#N/A
t - test	0.000187	-24.2139	27.6762	-3.69414	26.92968	9.18E-05

(i) 20 /80 blended from experiment (i-1) and from equation (i-2), r^2 = 0.9068

HDPE/LLDPE : 10 / 90 (gain6, area1)

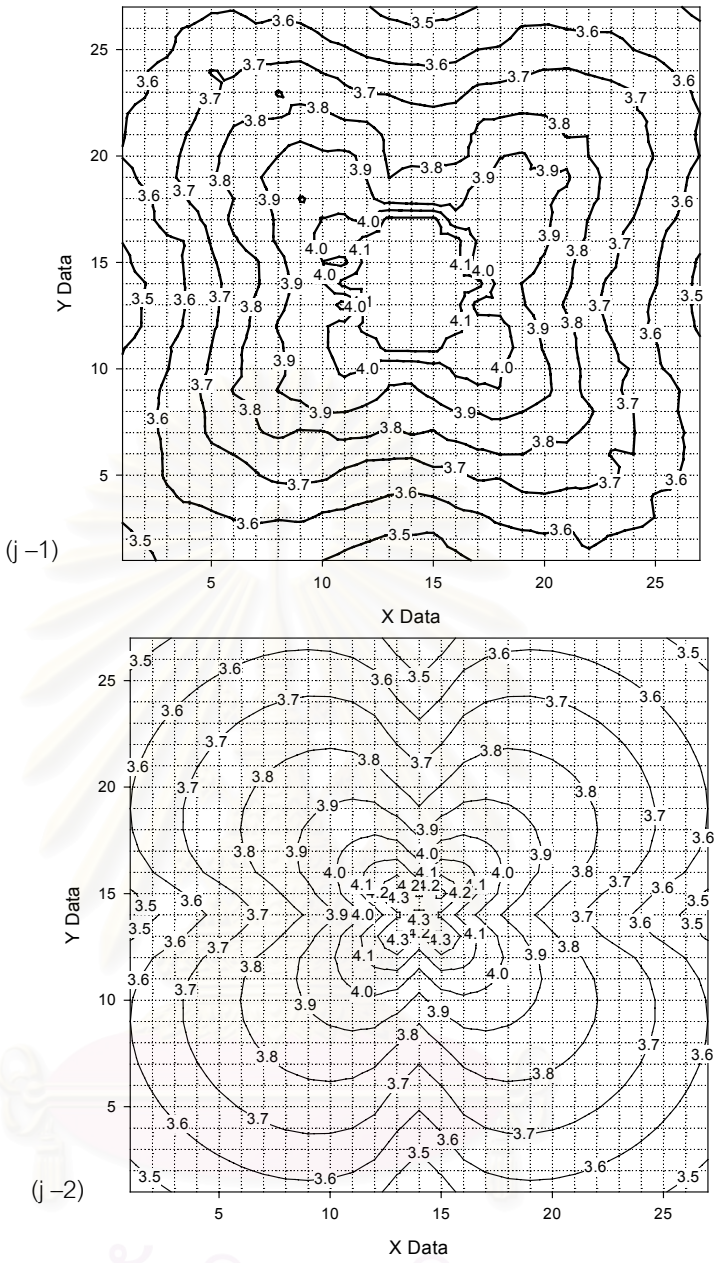

Regression Statistic Values

10.0-90.0	TERM5	TERM4	TERM3	TERM2	TERM1	B
	0.067609	-0.03511	0.102802	-47.5226	0.08572	2.184089
	0	0.002364	0.003581	12.79465	0.002129	0
	0.918374	0.048783	#N/A	#N/A	#N/A	#N/A
	1626.901	723	#N/A	#N/A	#N/A	#N/A
	19.35799	1.720551	#N/A	#N/A	#N/A	#N/A
	#N/A	#N/A	#N/A	#N/A	#N/A	#N/A
t - test	α	-14.8535	28.70896	-3.71425	40.26524	α

(j) 10 /90 blended from experiment (j-1) and from equation (j-2), r^2 = 0.9183

Pure LLDPE (gain6, area1)

(k –1)

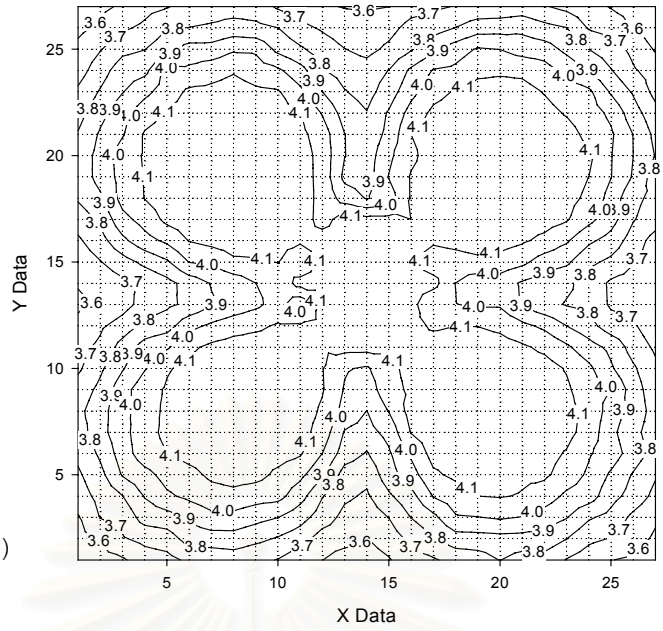

(k –2)

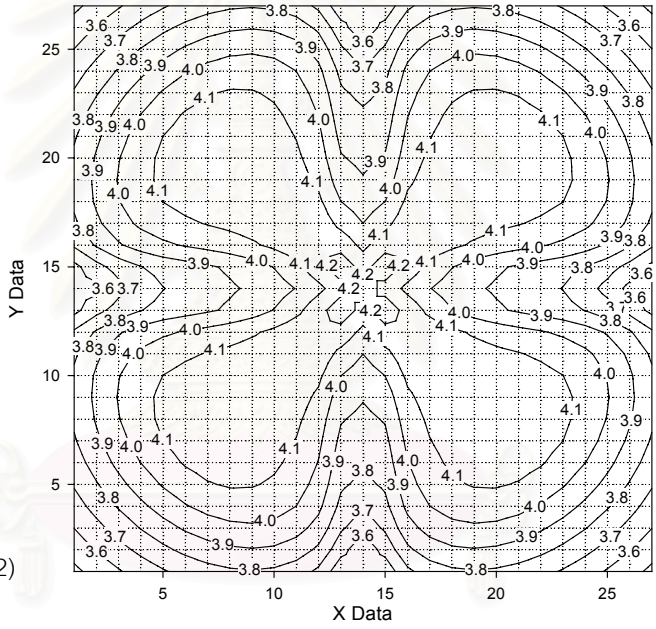

Regression Statistic Values

LLDPE	TERM5	TERM4	TERM3	TERM2	TERM1	B
	0.064805	-0.1664	0.229472	-61.4018	-0.01846	2.60777
	0	0.002728	0.003625	12.92035	0.002099	0
	0.929834	0.049262	#N/A	#N/A	#N/A	#N/A
	1916.226	723	#N/A	#N/A	#N/A	#N/A
	23.25077	1.754522	#N/A	#N/A	#N/A	#N/A
	#N/A	#N/A	#N/A	#N/A	#N/A	#N/A
t - test	α	-60.9924	63.3089	-4.75233	-8.79201	α

(k) pure LLDPE from experiment (k-1) and from equation (k-2), r^2 = 0.9298

Figure 5-9 : Comparison of light scattering contour graphs between experiment and equation of HDPE / LLDPE blends at gain no.6, area1 and their r^2 values

5.2.1 Example of intensity calculation from equation

From equation (5-10), input coefficients of each term come from fitting curve by LINEST function. For example, the equation for pure LLDPE is

$$\frac{\ln I_{HV}}{2} = (-0.0185)\text{Term1} - (61.4018)\text{Term2} + (0.2295)\text{Term3} + (22.8236)\text{Term4} + (0.0648)\text{Term5} - 2.6078$$

at $\theta = 2.8418^{\circ}$, $\phi = 45^{\circ}$ and Rs of LLDPE (from SEM) = 21.60 μm so

$$\frac{\ln I_{HV}}{2} = 0.1106 + 1.1623E\text{-}05 - 0.1591 - 1.1149 + 2.0332 - 2.6078$$

$$\frac{\ln I_{HV}}{2} = 3.4776$$

$$I_{HV} = 1048.686$$

Calculated intensity value is obtained by the sum of all terms. From the values of Term1 to Term5, these values can be shown as a pie chart;

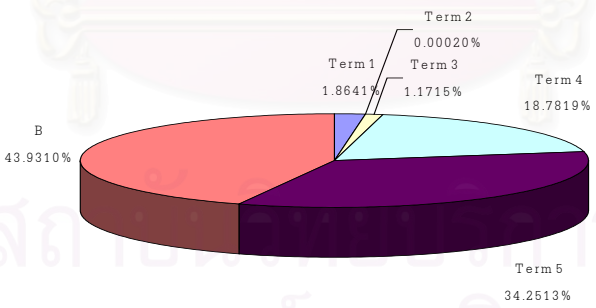

Figure 5-10 : A pie chart of each term of LLDPE 's equation.

This chart implies that Term1 and Term4 are the significant terms of the equation more than Term2 and Term3. These may be because they are the functions of Rs and θ which are the important parameters for the light scattering behavior. For Term5 which is the volume of spherulite, its value is constant and it is a significant term as same as Term B which is a constant value obtained from fitting curve.

From the results, most of the t test values fall in the rejection region therefore it can be concluded that all terms have particular practical significance for the model. And not only r^2 value, the least square method also provide coefficients of each term in the equation as shown in Table 5.1. The systematic methods of curve fitting can be performed within 7 minutes after obtain the values of ln(I) / 2 from the light scattering photograph and Rs from SEM photographs by using the new development of computer program. These coefficients can be used to indicate the composition of unknown and test the consistency of sample thickness.

Table 5-1 : Coefficients of each term at the light illumination no.6 (gain 6), area 1

%HDPE	0	10	20	30	40	50	60	70	80	90	100
Term1	-0.0185	0.0857	0.0657	0.0469	0.0516	0.0232	0.0113	-0.0175	-0.0296	-0.0220	0.0177
Term2	-61.4018	-47.5226	-53.1778	-63.0184	-55.9552	-35.6346	-65.6009	-62.8430	-55.4498	-69.4042	-74.4123
Term3	0.2295	0.1028	0.1113	0.0824	0.0709	0.1099	0.0830	0.0908	0.0980	0.0826	0.1174
Term4	-0.1664	-0.0351	-0.0599	-0.0743	-0.0613	-0.0704	-0.0737	-0.0834	-0.0850	-0.0988	-0.1247
Term5	0.0648	0.0676	0.0936	0.0694	0.0696	0.0001	0.0843	0.0412	0.0393	0.0882	0.0336
Term B(constant)	2.6078	2.1841	1.4575	2.2269	2.1584	4.4222	1.6564	3.0359	3.0894	1.5596	3.4828

Table 5-2 : Coefficients of each term at the light illumination no.6 (gain 6), area 2

%HDPE	0	10	20	30	40	50	60	70	80	90	100
Term1	-0.0170	0.0964	0.0686	0.0518	0.0578	0.0582	0.0285	0.0119	-0.0061	-0.0168	0.0383
Term2	-47.3939	-33.0349	-61.1844	-50.4292	-52.7747	-67.9935	-63.0118	-59.8887	-57.5774	-54.1441	-38.0462
Term3	0.2547	0.0882	0.1109	0.0770	0.0683	0.0984	0.0808	0.0987	0.1149	0.0878	0.1226
Term4	-0.1721	-0.0190	-0.0580	-0.0695	-0.0570	-0.0481	-0.0658	-0.0739	-0.0840	-0.1000	-0.1184
Term5	0.0596	0.0673	0.0829	0.0601	0.0655	0.0096	0.0872	0.0444	0.0497	0.0898	0.0367
Term B (constant)	2.7889	2.1134	1.7945	2.5034	2.2782	4.0686	1.5632	2.9680	2.8109	1.5276	3.4045

Table 5-3 : Coefficients of each term at the light illumination no.3 (gain 3), area 1

%HDPE	0	10	20	30	40	50	60	70	80	90	100
Term1	-0.0072	0.1188	0.1026	0.0900	0.0930	0.0716	0.0602	0.0311	0.0105	0.0265	0.0737
Term2	-68.7751	-46.7897	-52.7598	-66.3623	-56.9434	-38.1822	-70.2586	-72.0981	-69.0108	-85.2244	-83.2505
Term3	0.3070	0.0999	0.1121	0.0845	0.0703	0.1160	0.0886	0.1104	0.1376	0.1133	0.1409
Term4	-0.2020	-0.0153	-0.0416	-0.0573	-0.0440	-0.0558	-0.0611	-0.0820	-0.0989	-0.1102	-0.1159
Term5	0.0769	0.0476	0.0858	0.0687	0.0657	-0.0104	0.0848	0.0439	0.0363	0.0849	0.0329
Term B(constant)	2.1767	2.5430	1.4673	2.0529	2.0696	4.6146	1.5111	2.9110	3.2244	1.7079	3.4481

Table 5-4 : Coefficients of each term at the light illumination no.3 (gain 3), area 2

%HDPE	0	10	20	30	40	50	60	70	80	90	100
Term1	-0.0037	0.1279	0.1046	0.0929	0.0978	0.1016	0.0771	0.0619	0.0448	0.0350	0.0934
Term2	-51.9414	-32.3842	-61.9324	-52.4066	-52.8044	-67.5033	-65.8014	-64.4532	-63.7563	-67.2367	-44.1719
Term3	0.3186	0.0860	0.1115	0.0770	0.0669	0.0966	0.0813	0.1042	0.1344	0.1133	0.1370
Term4	-0.1985	-0.0009	-0.0403	-0.0518	-0.0397	-0.0308	-0.0498	-0.0605	-0.0774	-0.1050	-0.1020
Term5	0.0909	0.0520	0.0846	0.0692	0.0649	-0.0084	0.0766	0.0473	0.0353	0.0803	0.0341
Term B(constant)	1.7137	2.3296	1.5002	2.0007	2.0774	4.4468	1.7455	2.7437	3.2127	1.8476	3.3751

All steps of the analysis described previously can be summarized as follows:

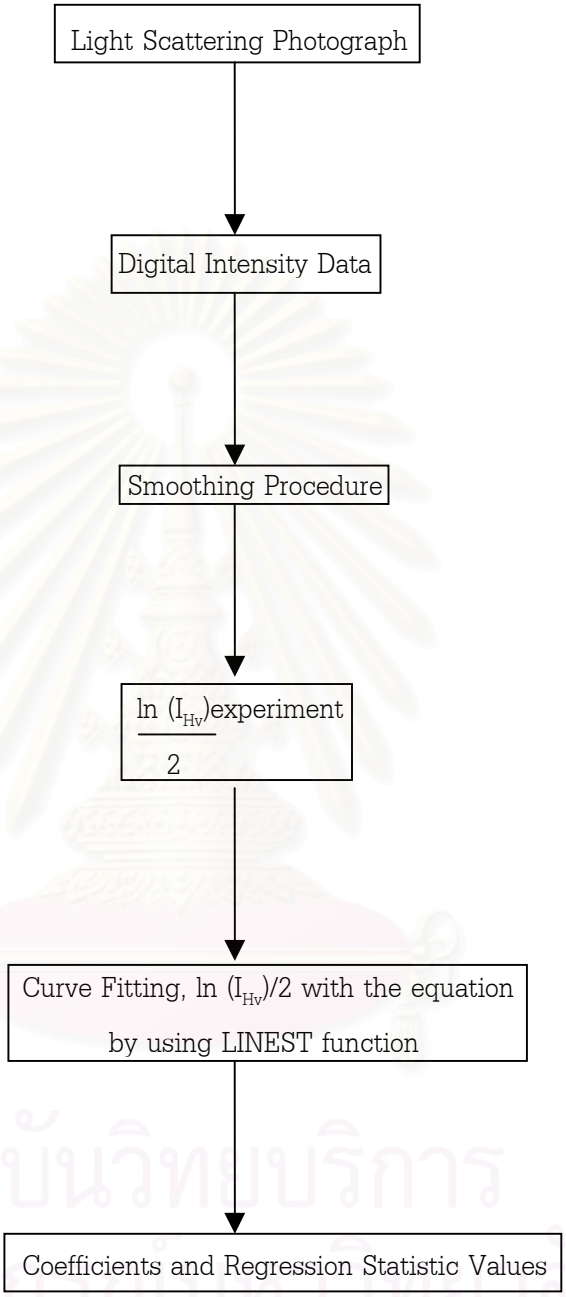

This procedure is auto – running by using sub – programming which can be run within 10 minutes.

5.3 Consistency testing of sample thickness and efficiency of the laser light source

Considering two different areas in gain 3 and gain 6 of the scattered light of the samples, Figure 5-11 shows the plot of the coefficients of each term vs %HDPE compositions.

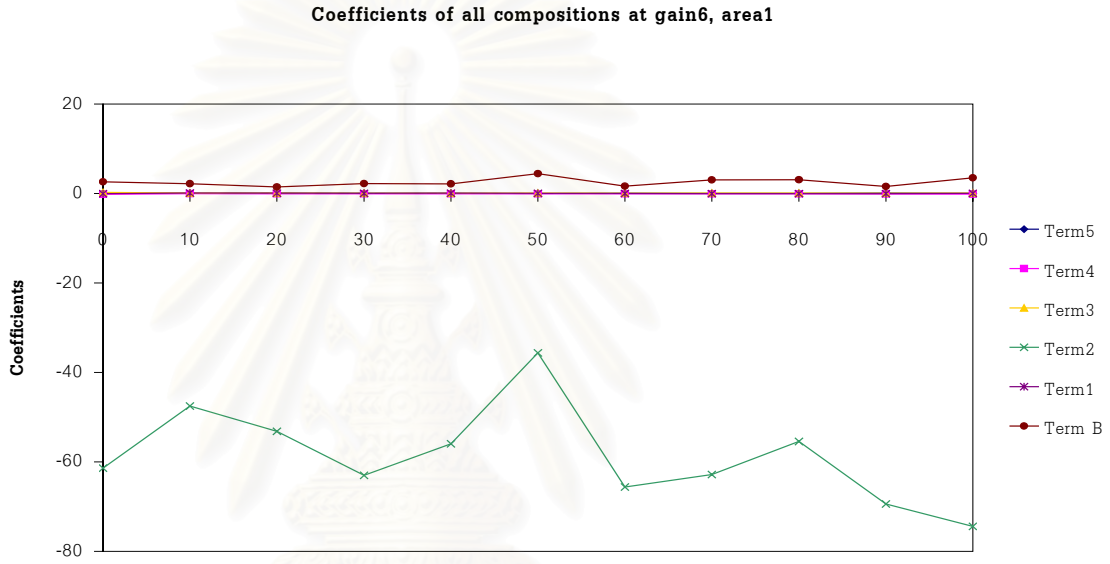

(a)

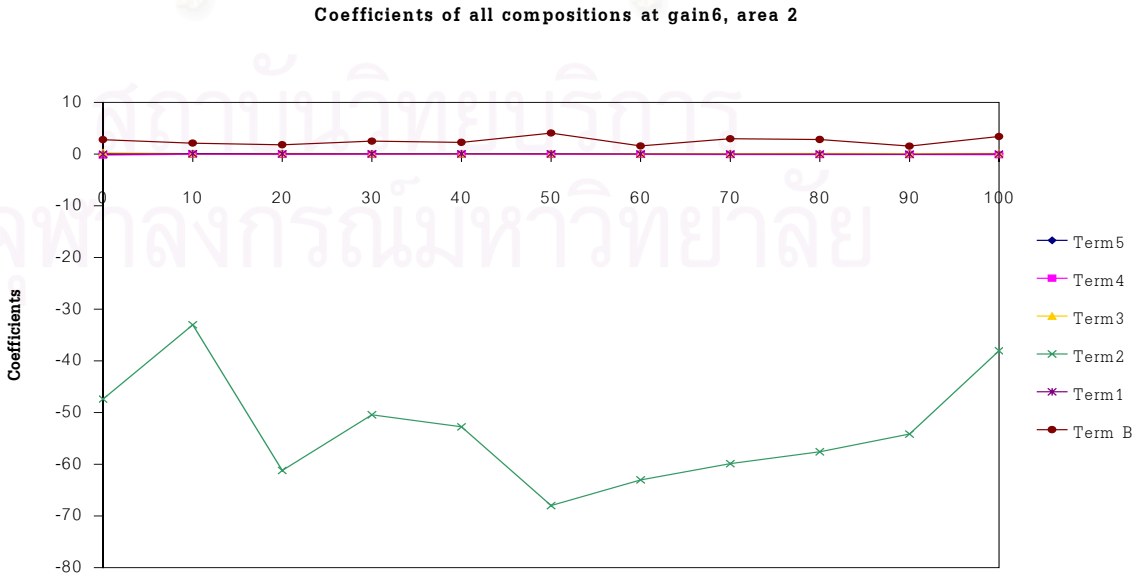

(b)

(c)

(d)

Figure 5-11 : Coefficient graphs of each term for all blends at (a) gain6, area1 , (b) gain6, area2 , (c) gain3, area1 and (d) gain3, area2

To test the consistency of sample thickness and the efficiency of the laser light source, coefficients of each term are considered by plotting them in the same scale as shown in Figure 5-12 . There are four curves in each term.

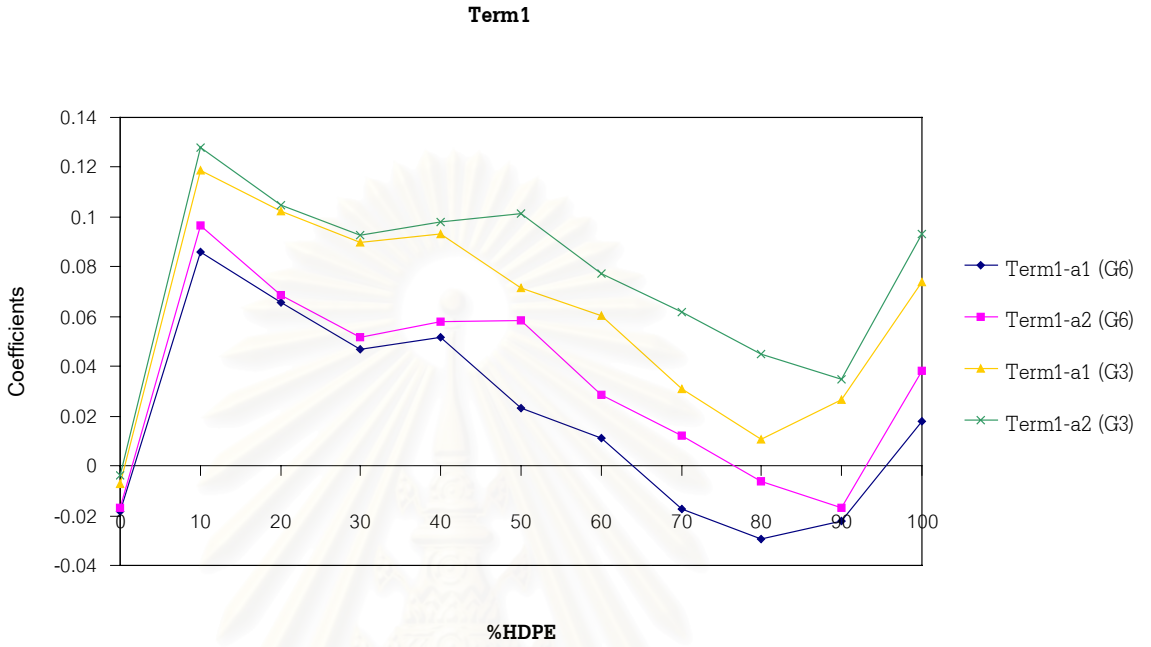

(a)

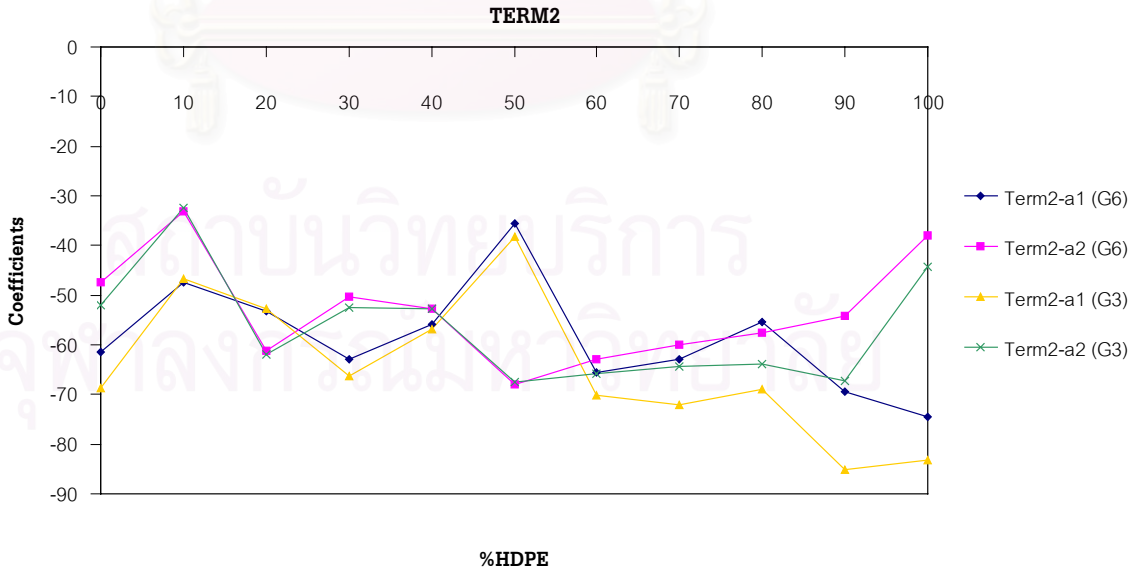

(b)

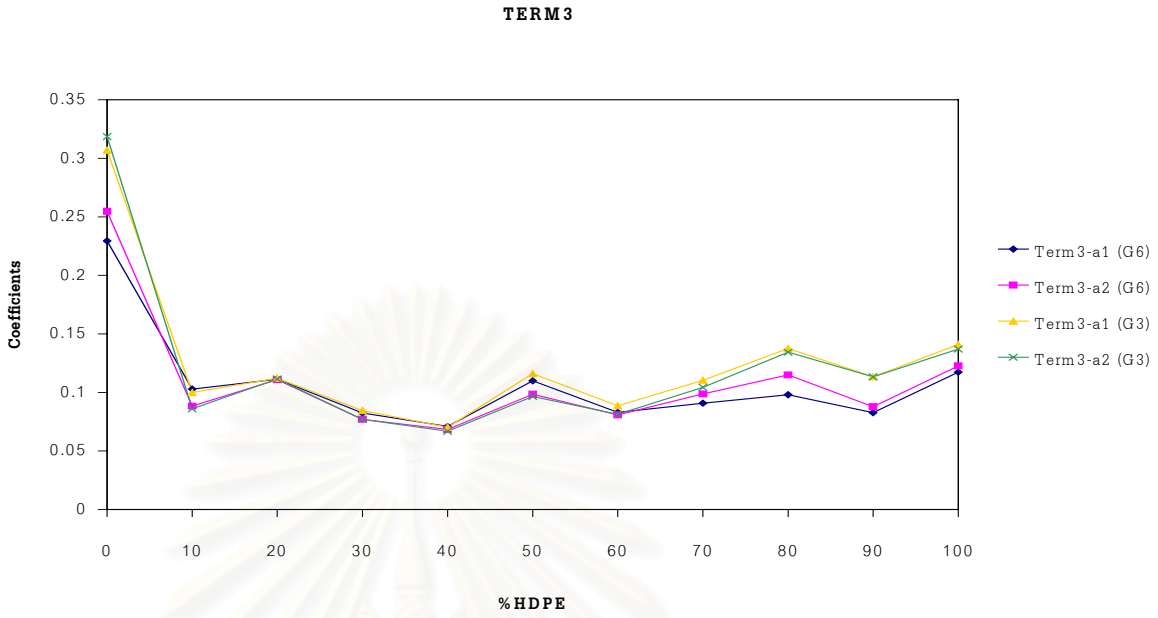

(c)

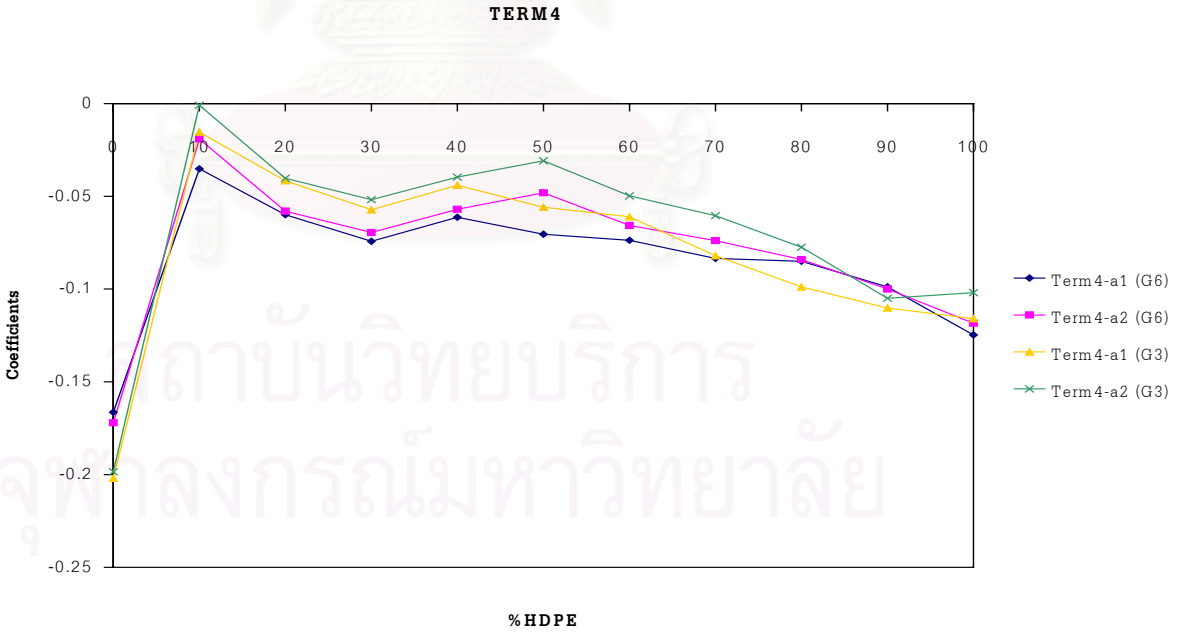

(d)

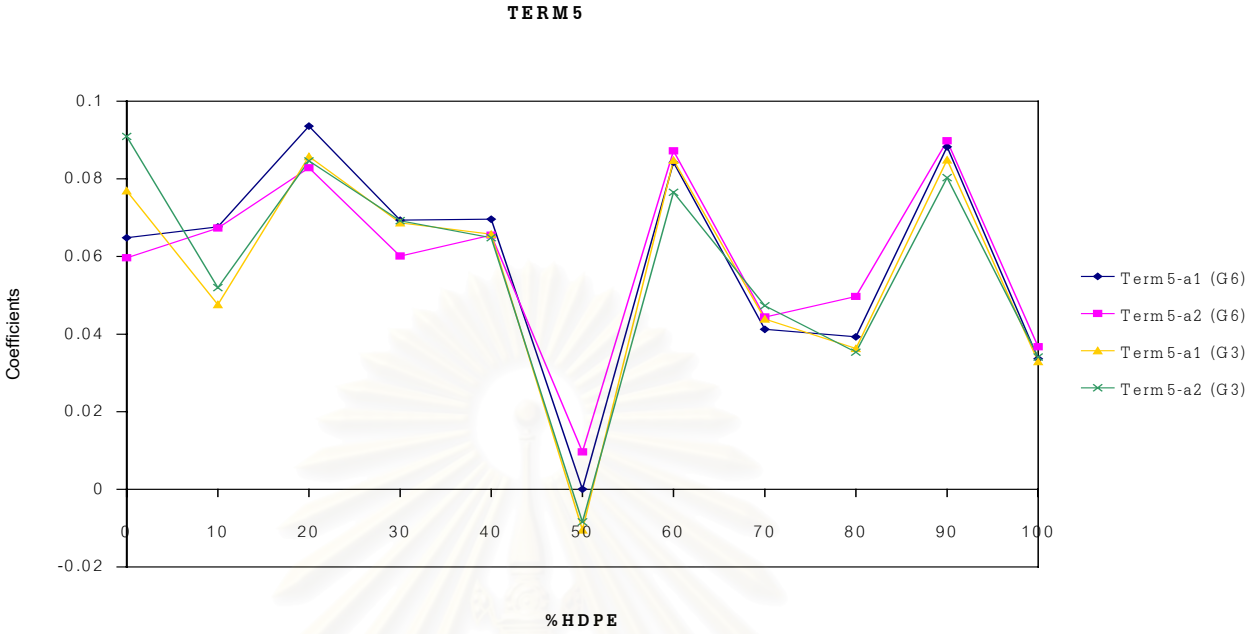

(e)

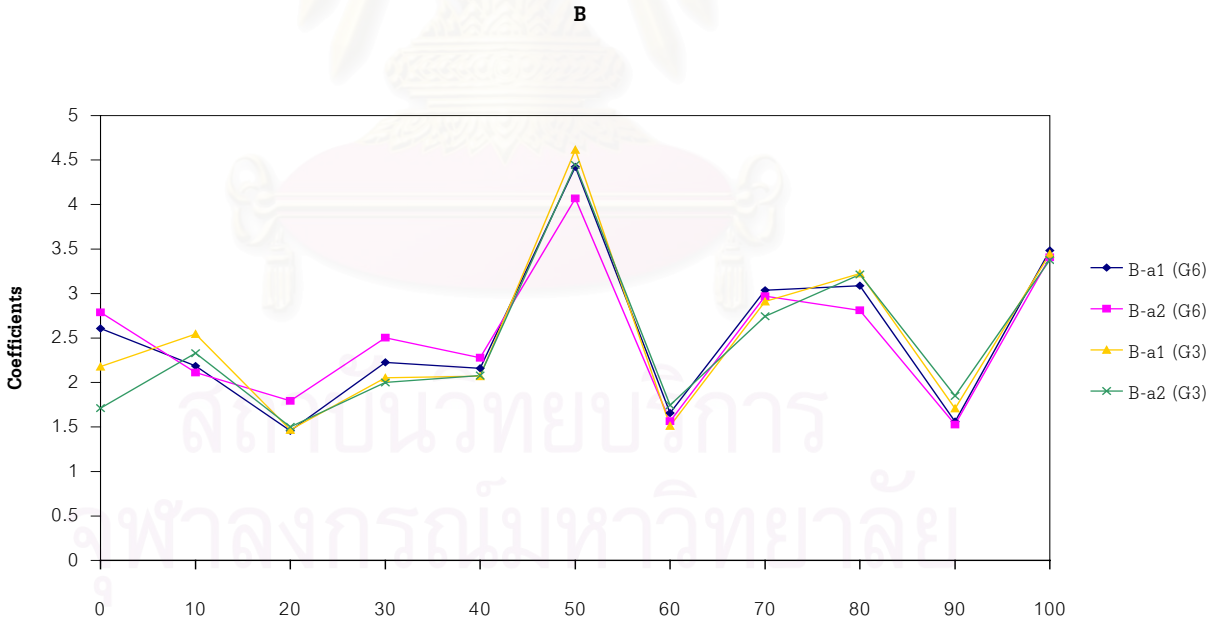

(f)

Figure 5-12 : Coefficient graphs of each term

Then the coefficient curve of each term was shifted to the reference curve of the illumination of light from gain no.6, area 1 because it showed the best light scattering pattern.

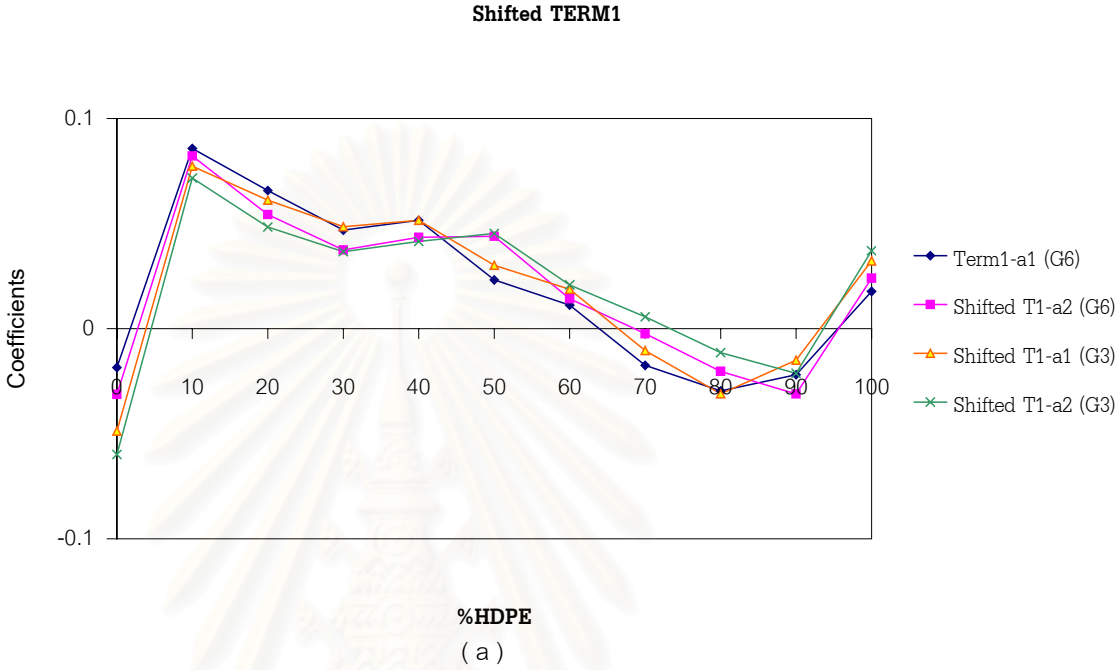

(a)

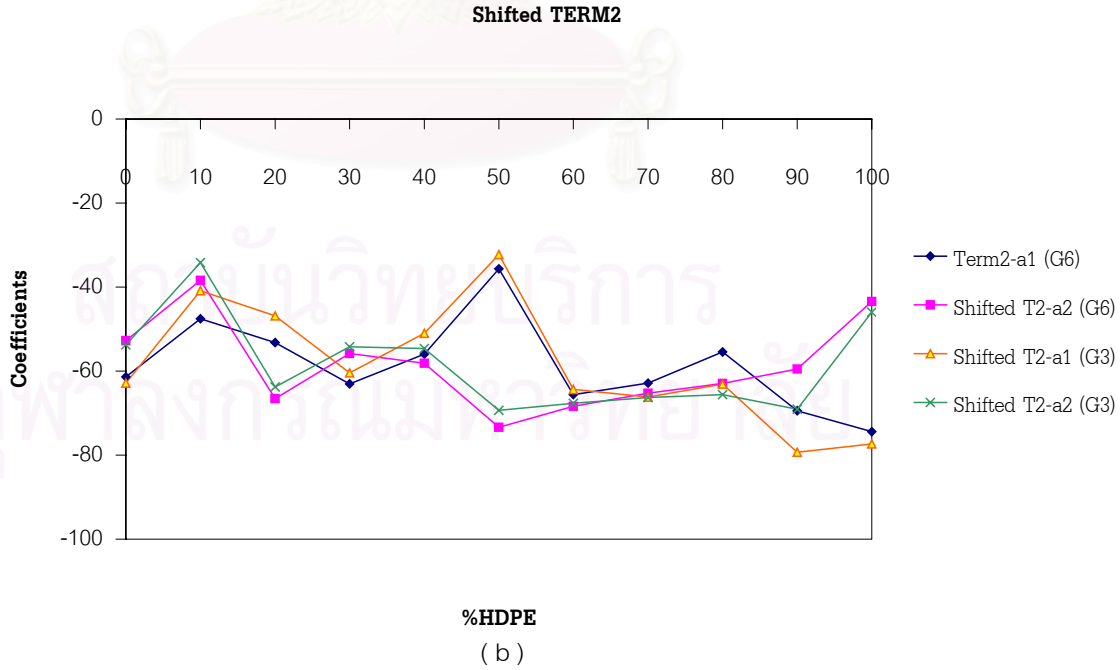

(b)

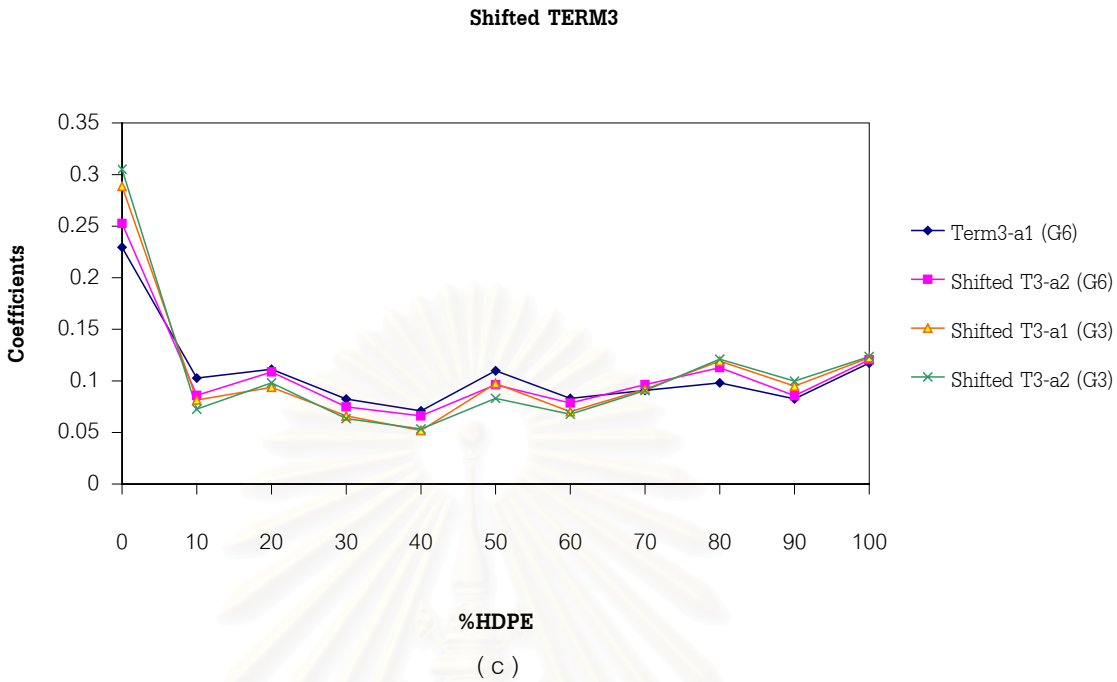
Shifted TERM3
Coefficients
0.35
0.3
0.25
0.2
0.15
0.1
0.05
0
0
10
20
30
40
50
60
70
80
90
100
%HDPE
Term3-a1 (G6)
Shifted T3-a2 (G6)
Shifted T3-a1 (G3)
Shifted T3-a2 (G3)

(c)

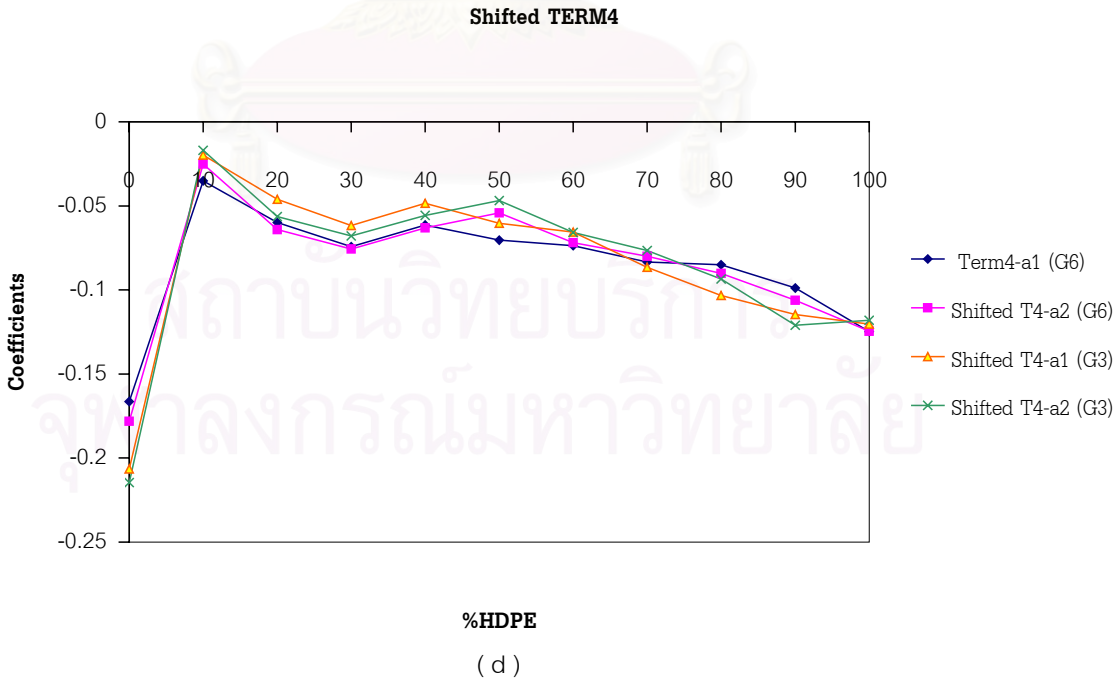
Shifted TERM4
Coefficients
0
-0.05
-0.1
-0.15
-0.2
-0.25
0
10
20
30
40
50
60
70
80
90
100
%HDPE
Term4-a1 (G6)
Shifted T4-a2 (G6)
Shifted T4-a1 (G3)
Shifted T4-a2 (G3)

(d)

(e)

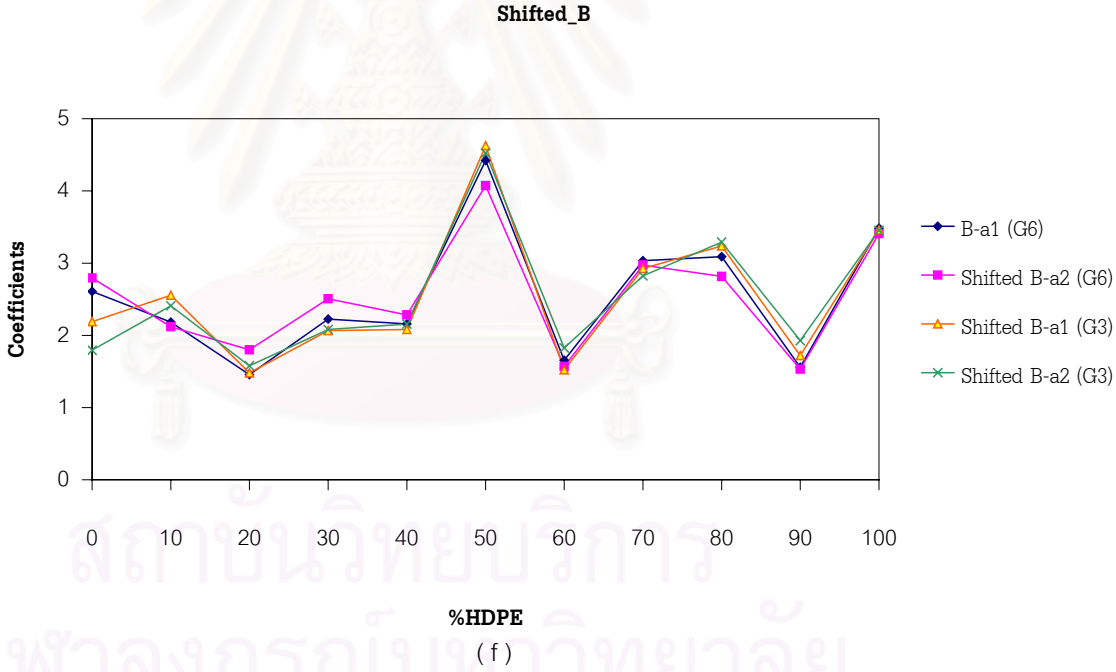

(f)

Figure 5-13 : Shifted coefficient curves of (a) Term1, (b) Term2, (c) Term3, (d) Term4, (e) Term5 and (f) Term B (constant)

From Figure 5-13, all shifted curves have the same characteristics. So they imply that samples have the same thickness all over the piece and there is no effect of the illumination of laser light source on the intensity calculations.

In addition, coefficient can be used to indicate the unknown composition of the blends by using the linear trend-line of the mean value of coefficient for each term which is valid in the blends, excluding pure HDPE and LLDPE because of the co – crystallization phenomena in the blends. The coefficients of two pure components can be negligible for the analysis of the unknown blends as shown in Figure 5-14

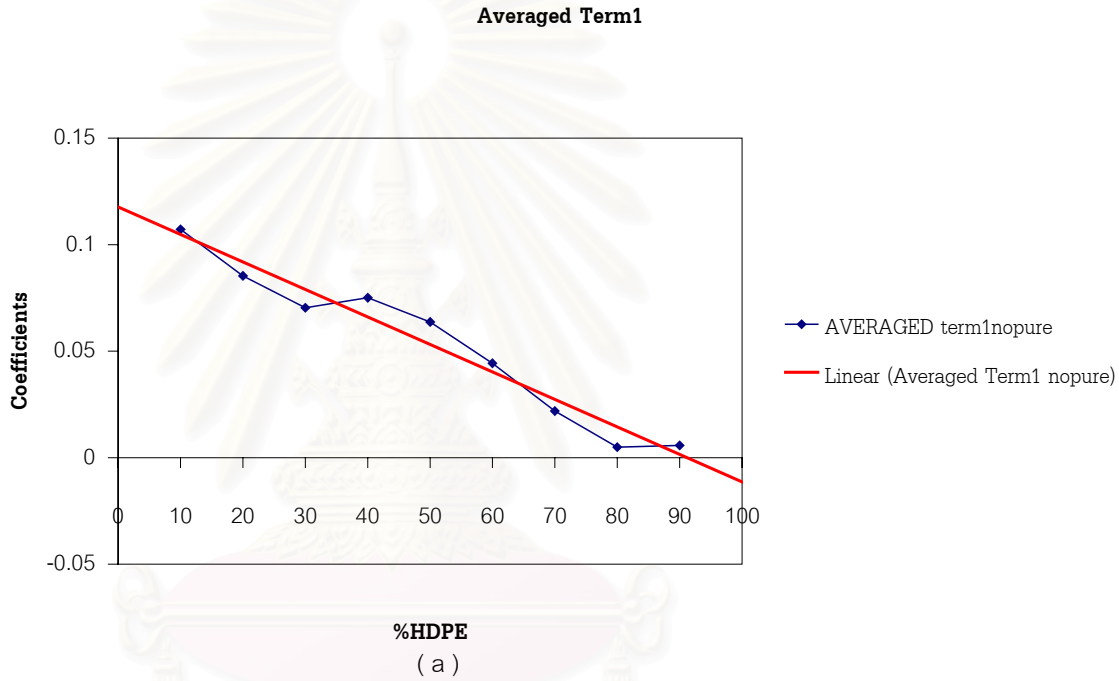

(a)

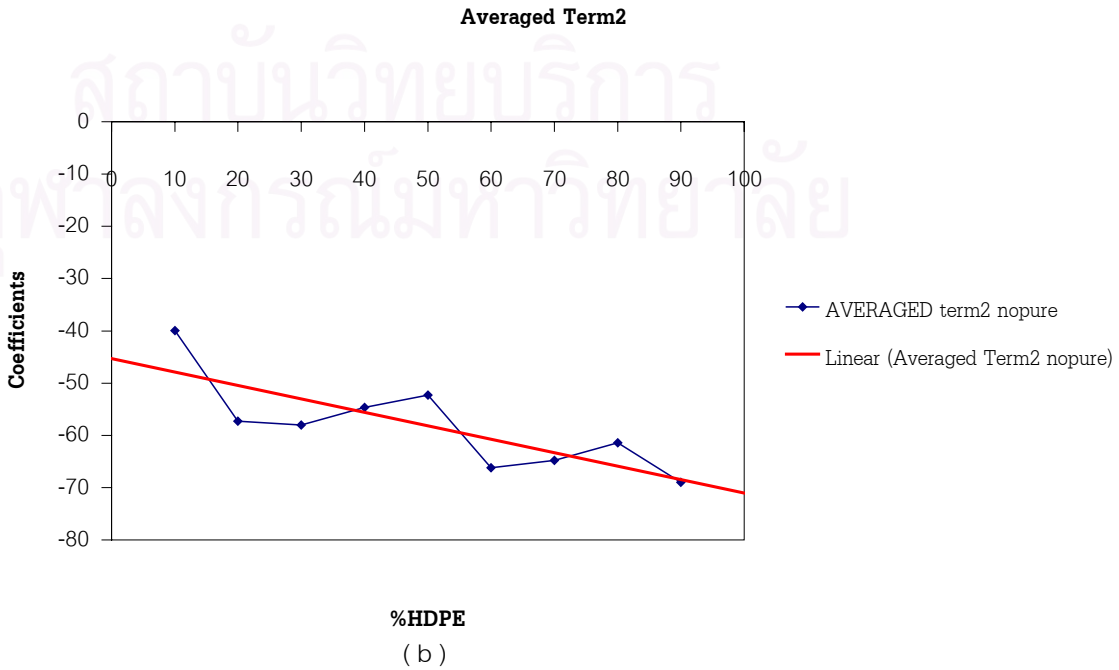

(b)

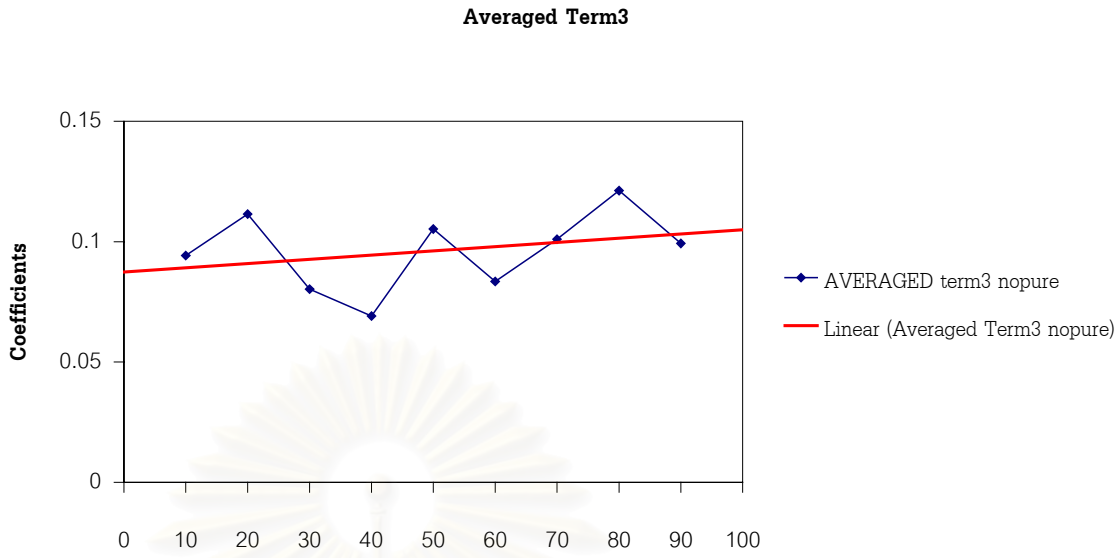

(c)

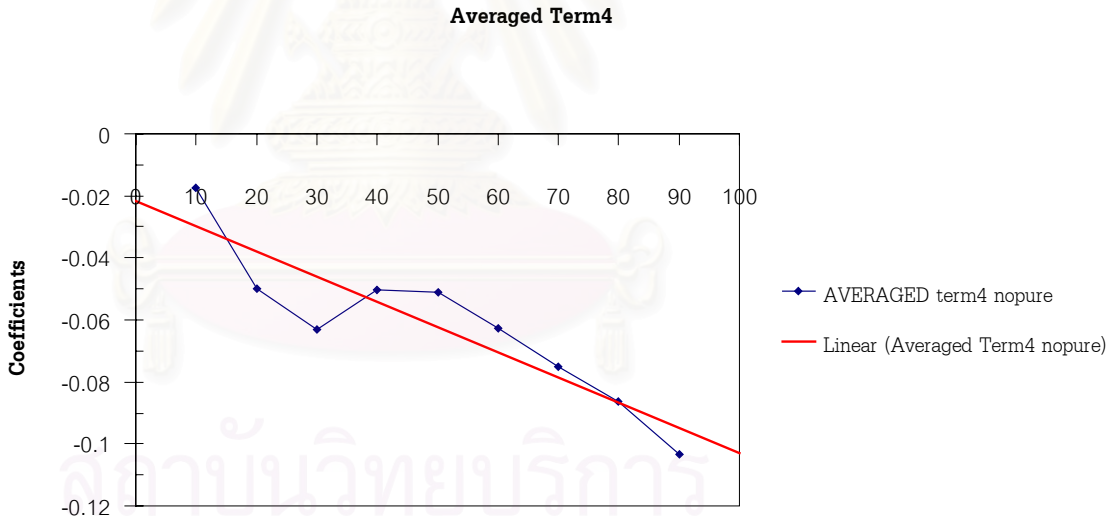

(d)

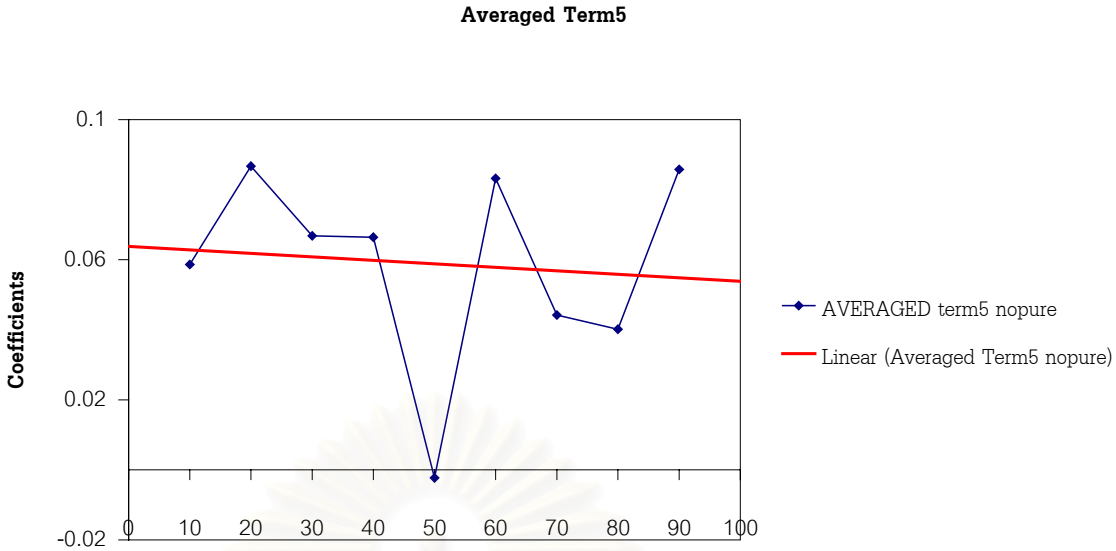

(e)

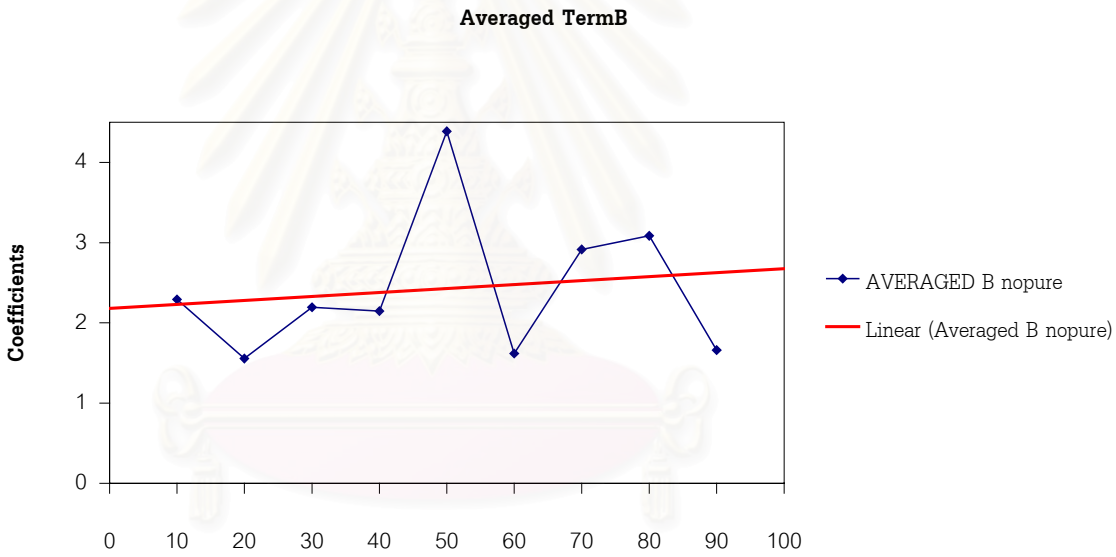

(f)

Figure 5-14 : Averaged coefficient curve and linear trend-line of (a) Term1, (b) Term2, (c) Term3, (d) Term4, (e) Term5, (f) TermB (constant)

Figure 5-14 shows the curves of mean value of coefficients of each term for all compositions without two pure components because this system has co-crystallization [Heon Sang Lee 2000] therefore there are differences of spherulite size between two pure components and their blends.

5.4 Etching and Scanning Electron Microscope (SEM)

In this section, the radius of spherulite, Rs, which is one input parameter in the equation (5-1), is determined using SEM photograph.

Before investigating the morphology of this system by SEM, sample surface is etched in order to reveal spherulite morphologies of crystalline polymer by using permanganic etching technique.

Permanganic etching technique is the best method for polyethylene etching. In this study, the solution of potassium permanganate in concentrated sulfuric acid 3.5% weight by volume at 60 $^{\circ}$C was used as etchant. There are two steps of etching method [Marsha, S. 1998]. To search the optimum etching time by vary etching time 5, 10, 15, 30, 45, 60, 75, 90, 105 and 120 minutes for each step. From that trial and error, the optimum etching time of each step is 10 minutes because the etched surface of sample can clearly show spherulite morphologies in order to measure the radius of spherulites easily. Results of spherulite morphologies of the blends at all compositions from SEM are shown in Figure 5-15

(a) pure HDPE

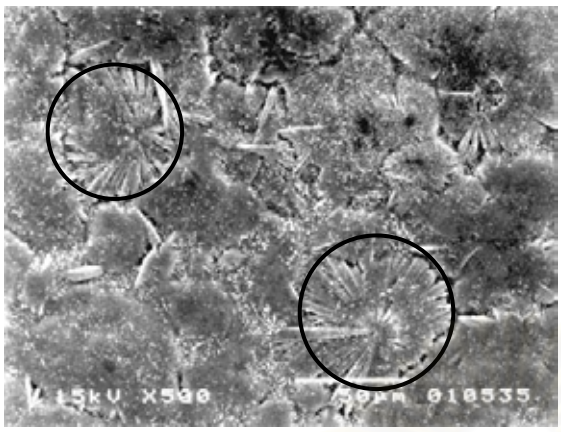

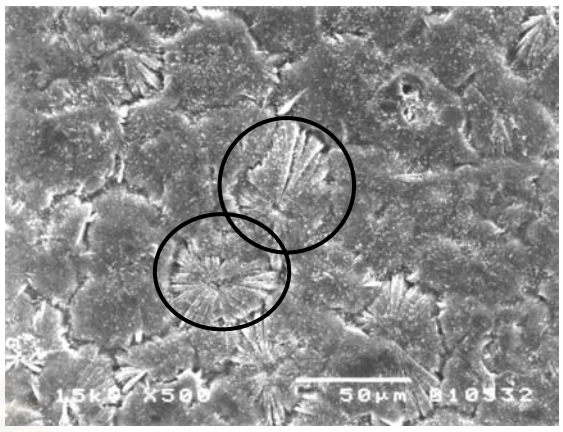

(b) 90 / 10

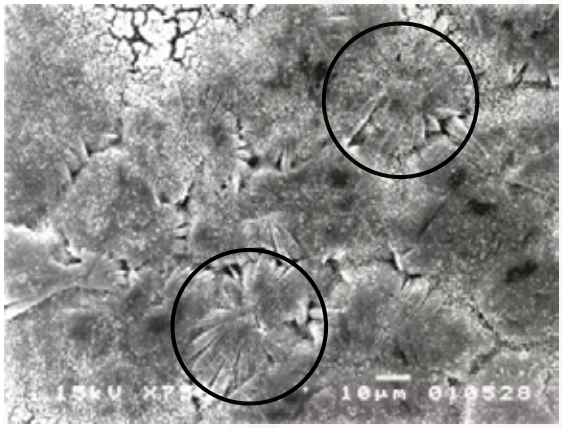

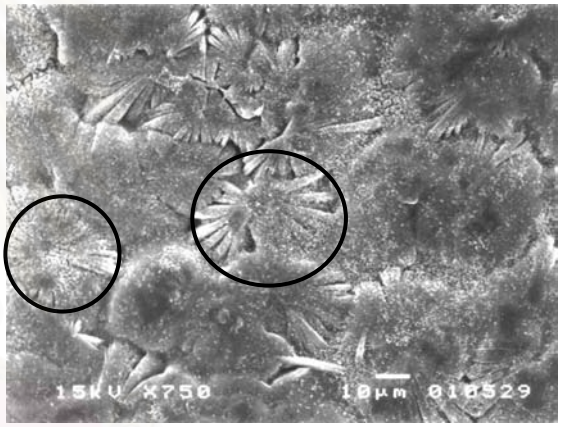

(c) 80 / 20

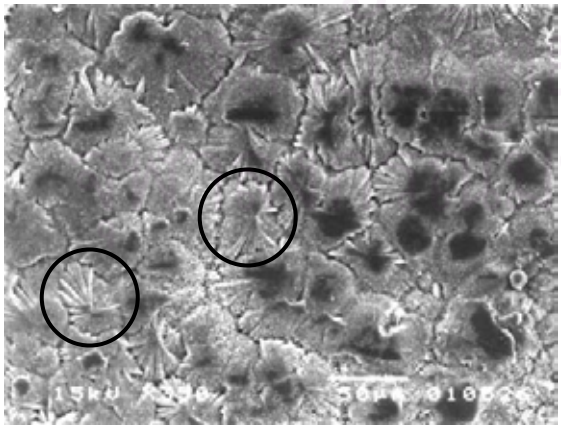

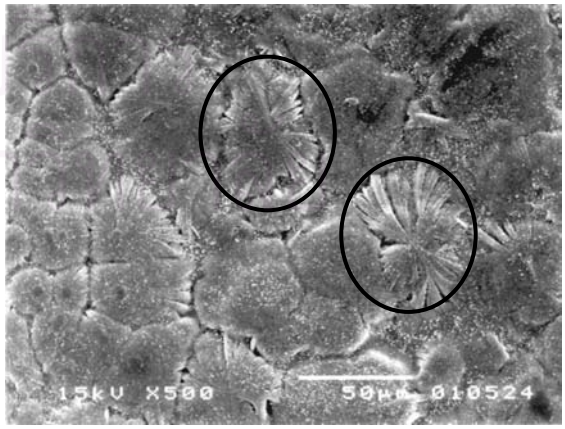

(d) 70 / 30

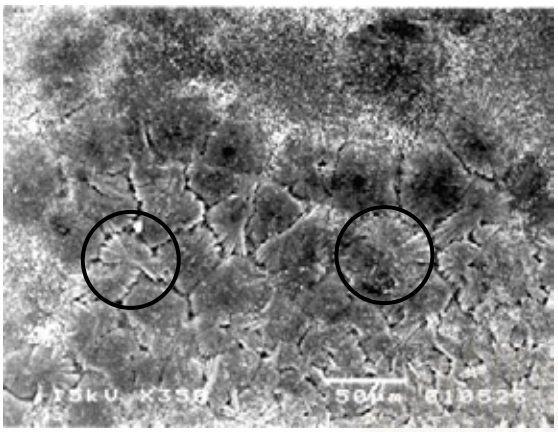

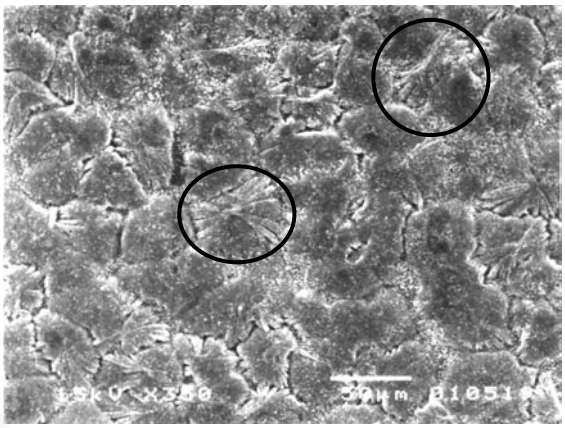

(e) 60 / 40

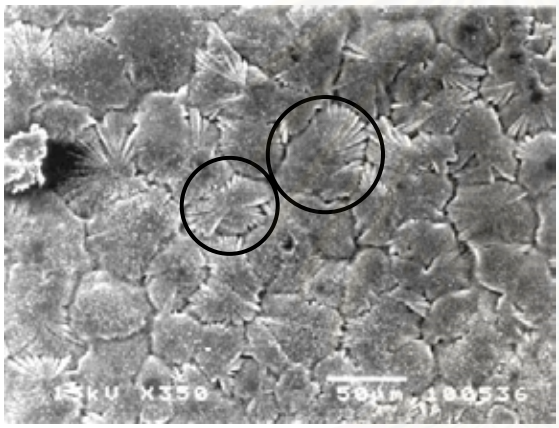

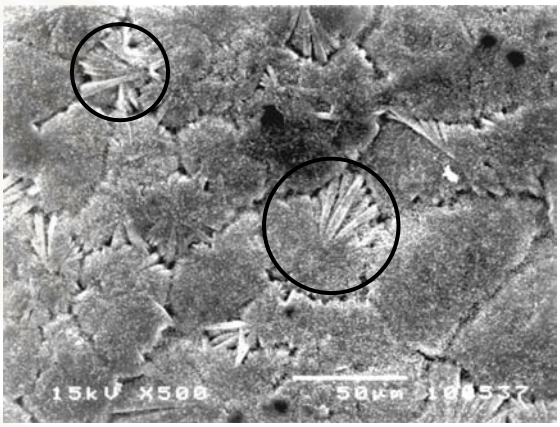

(f) 50 / 50

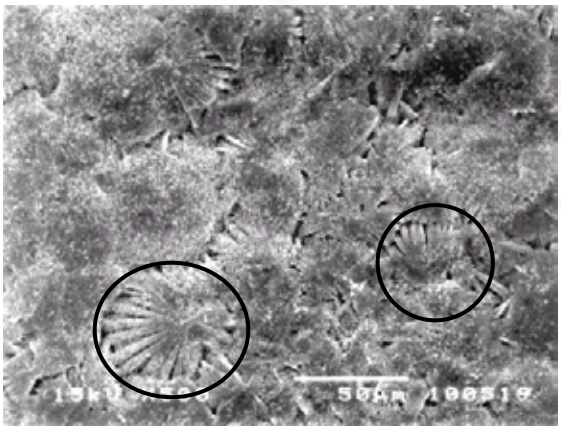

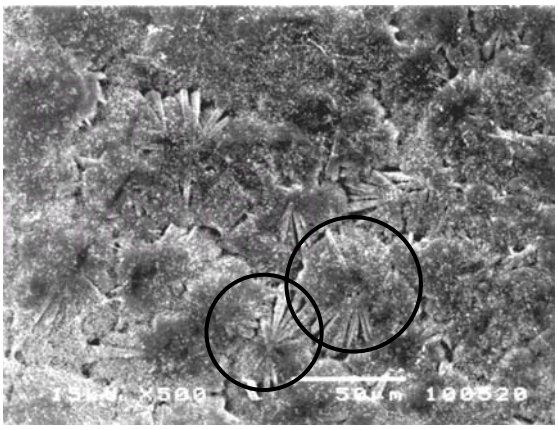

(g) 40 / 60

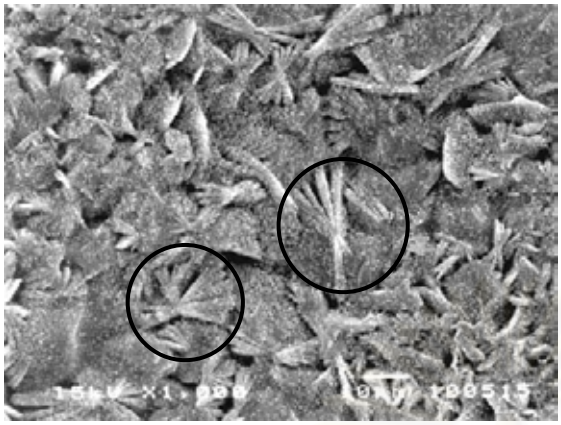

(h) 30 / 70

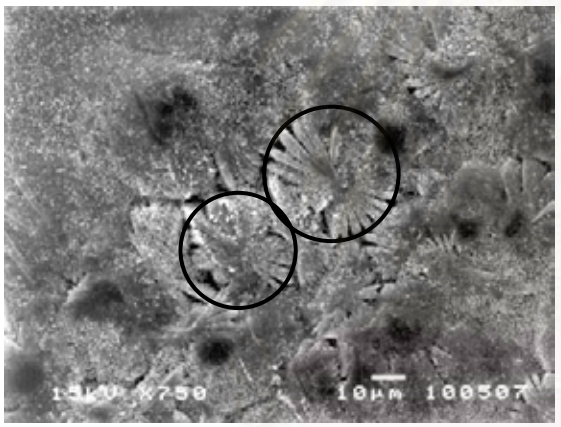

(i) 20 / 80

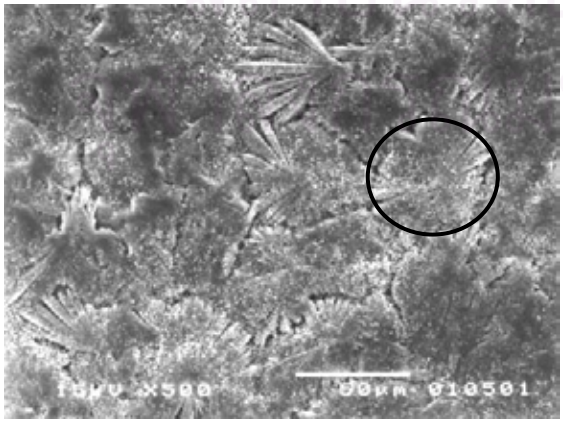

(j) 10 / 90

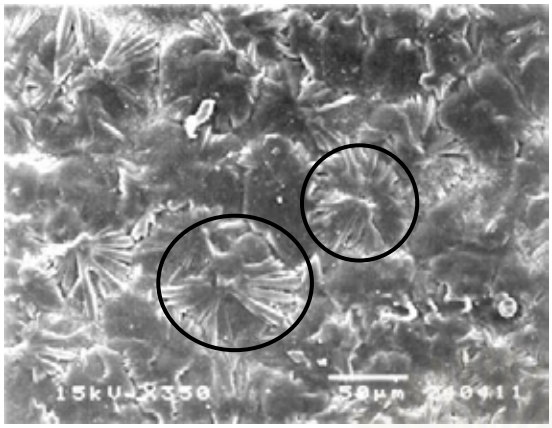

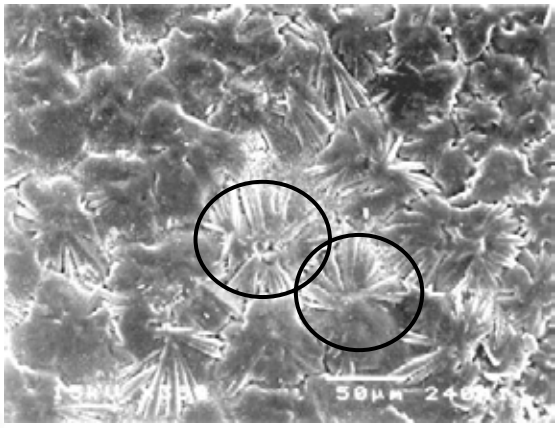

(k) pure LLDPE

Figure 5-15 : Spherulite morphologies of pure HDPE, pure LLDPE and their blends

Rs of each composition is obtained by taking the average radius of 15 – 20 spherulites of the sample as shown in Table 5-5

Table 5-5 : The radius of spherulite of each composition of blend

Composition of Blends (HDPE/LLDPE), (%wt/wt)	Radius of Spherulite (μm)	Standard Deviation (SD)
100 / 0 (pure HDPE)	23.15	2.8591
90 / 10	27.43	2.2254
80 / 20	29.72	2.8606
70 / 30	30.13	4.3620
60 / 40	30.53	2.3454
50 / 50	29.63	3.6345
40 / 60	26.47	2.9605
30 / 70	24.84	5.1483
20 / 80	23.67	5.5814
10 / 90	22.84	3.2247
0 / 100 (pure LLDPE)	21.60	4.3284

This polymer blend system occurs co-crystallization which makes the new crystalline structure [Heon Sang Lee 2000] so spherulites characteristics of blends are different from those of two pure components. From this reason, two pure components (HDPE, LLDPE) can be negligible for unknown analysis.

5.5 Analysis of unknown composition

For this system, the analysis procedure of the blends with unknown composition can be concluded as follows:

1. Investigate light scattering behavior of unknown. This step can identify the range of the composition of unknown.

2. Average Rs values from step one as Rs of unknown.

3. Substitute Rs in the equation (5-10) to find the coefficient of each term. And then compare with the linear trend-line in the average curve without two pure components of each term.

In this work (Appendix B), the result from term1 and term4 show about 27 and 26 %weight of HDPE, respectively which closed to the real composition of unknown, 29.92 %weight of HDPE. This may be arisen from term1 and term4 are the function of U which consists of two significant parameters for light scattering behavior. One of the parameters is the radius of spherulite, Rs, and another is the scattering angle, θ. For term2 and term3 , they have only the scattering angle.

CHAPTER VI

CONCLUSIONS AND RECOMMENDATIONS

For the preliminary study of light scattering behaviors and morphology of the system of HDPE/LLDPE blends. In this chapter, the conclusions and recommendations for further studies will be focused.

6.1 Conclusions

The following conclusions of this study were drawn.

1. New modification of SALS technique and new numerical analysis of the 2D image can relate the microstructure with the image of SALS.

2. New method for numerical analysis of the laser light scattering data from the blends of HDPE and LLDPE was developed.

3. From modification the equation at x, y axis by using the average intensity value follow the tangent of circle. r^2 of the fitting curve with ln(I) /2 ,I is intensity data, is in range of 0.90-0.94 for this system. This modification can be used as the new method for calculation of intensity value.

4. Two steps etching by using the solution of potassium-permanganate in conc. sulfuric acid 3.5% weight by volume as a etchant can be used as the new method of etching for this system. The optimum time for etching is 10 minutes per step.

5. In this study, we can analyze the intensity data of light scattering with in 10 minutes to get the best contour graph and the coefficients of the equation by using sub-program for auto-running.

6. The limitation of the systematic methods of analysis is the co – crystallization phenomena in the blended polymer which is confirmed by SEM and the differences in laser intensity on the scene were eliminated by shifting the data.

7. For examination of the HDPE/LLDPE blends, set the conditions of SALS technique are

7.1. The intensity data (I) should be used in form of (ln I /2) for curve fitting.

7.2 The optimum distance between the sample to the screne is 250 mm.

8. For the prediction the composition of unknown, the light scattering photograph together with the coefficient of term1 and term4 from the equation can be used to preliminary predict the composition of the unknown sample.

9. The value of Rs of HDPE/LLDPE blends observed by SEM technique is in the range of 31-21 μm.

6.2 Recommendations for Further Studies

The recommendations for further studies are as follows:

1. The systematic methods of measurement and the methods of analysis can be extended to study the light scattering behavior of new pair of crystalline polymer blends with some minor modifications, depend on their properties.

2. It should be interesting to study the kinetic of crystallization of crystalline polymers by using the light scattering technique.

3. The applications of this method to predict the concentration of HDPE/LLDPE blends from unknown concentration samples should be verified.

4. From the tilt sample holder of this static light scattering equipment, it leads to the interesting research to study light scattering of crystalline polymer blends with tilting the sample.

References

Akpalu, Y.; Kielhour, L.; Hsiao, B.S.; Stein, R.S.; Russell, T.P.; Egmond, J. van; and Muthukumar, M. Structure development during crystallization of homogeneous copolymer of ethene and 1-octene: Time-resolved synchrotron X-ray and SALS measurements. Macromolecules. 32 (1999): 765-770.

Billmeyer, Fred W. Textbook of Polymer Science. 3rd ed. New York: John Wiley & Sons, 1984.

Bischel, M.S.; Schultz, J.M.; and Kit, K.M. Two – step etching procedures for binary polymer blends. Polymer. 39, No. 11 (1998): 2123 – 2127.

Brydson, J. A. Plastics of Materials. 5th ed.: Butterworth Scientific, 1989.

Charrier, Jean – Michel. Polymeric Materials and Processing: plastics, elastomers and composites. New York: Hanser Publishers, 1990.

Freedman, A. M.; Bassett, D. C.; Vaughan A.S.; and Olley, R.H. On quantitation permanganic etching. Polymer. 27 (August 1986): 1163 – 1169.

Galante, M. J.; Mandelkern, L.; and Alamo R. G. The crystallization of blends of different types of polyethylene: The role of crystallization conditions. Polymer. 39, No.21 (1988), 5105 – 5119.

Gupta, A.K.; Rana, S.K.; and Deopura, B.L. Mechanical properties morphology of high – density polyethylene / linear low – density polyethylene blend. Journal of Applied Polymer Science. 46 (1992): 99 – 108.

Harper, C.H. Handbook of plastics, elastomers and composites. 2nd ed. New York: McGraw – Hill, Inc.,1992.

Hashimoto, M.; Toda, A.; and Miyaji, H. Isotropic scattering in *Hv* light scattering from spherulites of polymers. Polymer. 33, No.5 (1992): 909 – 913.

Heon Sang Lee; and Denn, M.M. Blends of linear and branched polyethylenes. Polymer Engineering and Science. 40, No.5 (May 2000): 1132 – 1142.

Lindenmeyer, P.H.; and Holland, V.F. Relationship between molecular weight, radial-growth rate, and the width of the extinction bands in polyethylene spherulites. Journal of Applied Physics 35, No.1 (1964): 55-2242.

Meeten, G.H.; and Navard, P. Small – angle scattering of polarized light. I. Comparison of theoretical predictions for isotropic and anisotropic spheres. Journal of Polymer Science: Part B: Polymer Physics. 27 (1989): 2023 – 2035.

Mendenhall, W.; and Sincich, T. A second course in statistics: Regression analysis. 5th ed.: Prentice – Hall, Inc.,1996.

Naylor, K.L.; and Phillips, P.J. Optimization of permanganic etching of polyethylenes for scanning electron microscopy. Journal of Polymer Science: Polymer Physics Edition. 21 (1983): 2011 – 2026.

Olley, R.H.; Hodge, A.M.; and Bassett, D.C. A permanganic etchant for polyolefins. Journal of Polymer Science: Polymer Physics Edition. 17 (1979): 627-643.

Point, J.J. Morphological features and mechanisms of crystallization. Polymer. 33, No.12 (1992): 2469 – 2474.

Ree, M.; Kyu, T.; and Stein, R.S. Quantitative small – angle light – scattering studies of the melting and crystallization of LLDPE/LDPE blends. Journal of Polymer Science: Part B: Polymer Physics. 25 (1987): 105-126.

Rodriguez, F. Principles of Polymer Systems. 2nd ed. New York: McGraw – Hill, 1982.

Shi-Ru Hu; Kyu, T.; and Stein, R.S. Characterization and properties of polyethylene blends I. linear low-density polyethylene with high-density polyethylene. Journal of Polymer Science: Part B: Polymer Physics. 25 (1987): 71-87.

Sperling, L. H. Introduction to Physical Polymer Science 3nd ed.: John Wiley & Sons, INC., 2001.

Stein. R.S.; and Hotta, T. Light scattering from oriented polymer films. Journal of Applied Physics. 35, No.7 (1964): 2237-2242.

Stein, R.S.; and Rhodes, M.B. Photographic light scattering by polyethylene films. Journal of Applied Physics. 31, No.11 (1960): 1873-1184.

Stein, R.S.; and Srinivasarao, M. Fifty years of light scattering: A perspective. Journal of Polymer Science: Part B: Polymer Physics. 31 (1993): 2003 – 2010.

Stein, R.S.; Cronauer, J.; and Zachmann, H.G. Real time scattering measurements of the crystallization of polymers and their blends. Journal of Molecular Structure. 383 (1996): 19-22.

Stein, R.S.; Misra, A.; Yuasa, T.; and Khambatta, F. Recent studies of light scattering from polymer films. Pure & Appl. Chem. 49 (1977): 915 – 928.

Stevens, M.P. Polymer Chemistry, An Introduction. 3rd ed. New York: Oxford University Press, 1999.

Tabar, R.J.; HU, S.R.; and Stein, R.S. Light scattering studies of high – impact polystyrene. Journal of Applied Polymer Science. 28 (1983): 1409-1420.

Tabar, R.J. Quantitative small – angle light scattering studies of semi – crystalline polymers. Doctorial dissertation Department of Polymer Science and Engineering, University of Massachusetts, 1983.

Woodward, A.E. Understanding Polymer Morphology. New York: Hanser Publishers, 1995.

Young, R. J.; and Lovell, P. A. Introduction to polymers. 2nd ed: Chapman & Hall, 1991.

Appendices

APPENDICES

Appendix A

The standard methods of the light scattering measurement and etching are as follows:

1. The investigation light scattering behavior ;

1.1 The laser beam passed through the sample which was mounted between two polarizers. Using the illumination of light from gain 6 and 3, collect 59049 digital intensity data from light scattering photographs.

1.2 To get the better contour graph of light scattering. From digital intensity data, we smoothed data by using average data. We averaged 81 data to be 1 data. Totally we got 729 averaged data.

1.3 Since we put a coin at the center of the screen, called beam stop, to protect the laser beam which has high intensity passed through the CCD camera directly, the contour graph at the center is very poor. So we modified averaged intensity data at the center of the contour graph of light scattering by adjusting data in the area of a coin to a new data which was closer to data around the outermost rim of a coin.

2. Etching ;

In this work, we made two steps of etching by using 20 ml of the solution of potassium-permanganate in conc. sulfuric acid 3.5% weight by volume, as the etchant. First etching, the sample was etched for 10 minutes, then washed by water for 5 minutes and then washed by acetone for 5 minutes. Second etching, the same sample was etched for 10 minutes in the new prepared etchant. Then the sample was washed by water for 10 minutes and then washed by acetone for 10 minutes. The thickness of the sample is 1 mm.

Appendix B. The prediction of the unknown composition

The light scattering photograph of unknown showed that it consisted of LLDPE about 70-90% by weight. And then we related the coefficient of term1 and term4 of unknown to the linear curve of the averaged coefficient curve of each term by using the average radius of spherulite (Rs) of 30, 20 and 10% by weight of HDPE. From this, we found that the composition of unknown was about 27% by weight of HDPE from Term1 and 26% HDPE from Term4 while the truly composition of unknown was 29.92% by weight of HDPE. So we can use the light scattering photograph couple with the coefficient of term1 and term4 from the equation to preliminary predict the composition of unknown.

Coefficients of unknown sample from curve fitting

Term1	Term2	Term3	Term4	Term5	Term B
0.0806	-53.4784	0.0769	-0.0430	0.4658	-10.4404

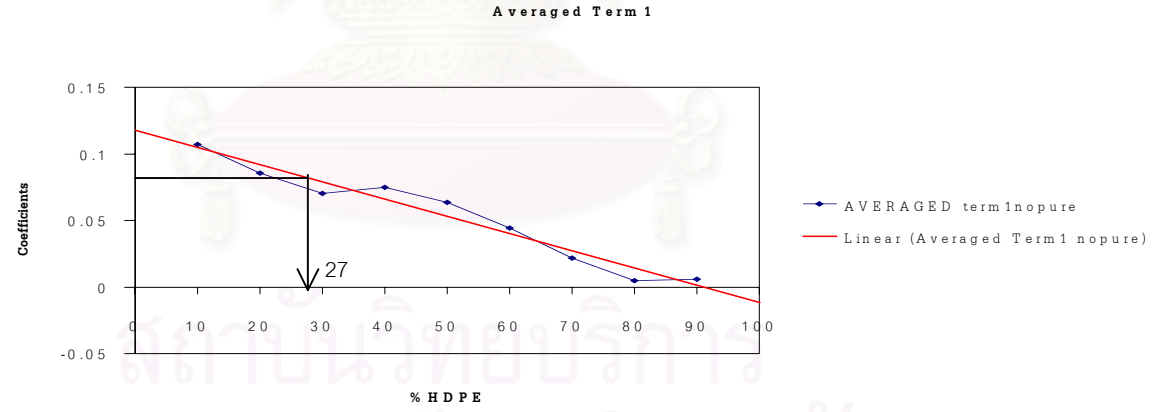

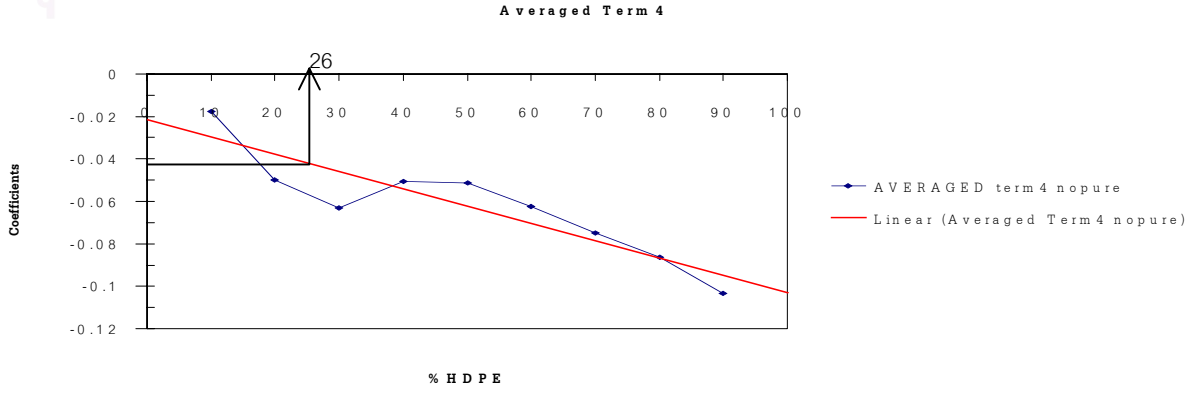

Appendix C.

Table C-1: Standard Normal Value at various degree of freedom of n-1

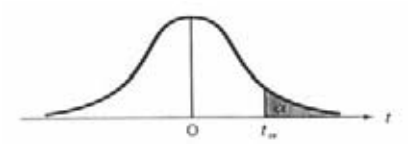

ν	$t_{.100}$	$t_{.050}$	$t_{.025}$	$t_{.010}$	$t_{.005}$	$t_{.001}$	$t_{.0005}$
1	3.078	6.314	12.706	31.821	63.657	318.31	636.62
2	1.886	2.92	4.303	6.965	9.925	22.326	31.598
3	1.638	2.353	3.182	4.541	5.841	10.213	12.924
4	1.533	2.132	2.776	3.747	4.604	7.173	8.61
5	1.476	2.015	2.571	3.365	4.032	5.893	6.869
6	1.44	1.943	2.447	3.143	3.707	5.208	5.959
7	1.415	1.895	2.365	2.998	3.499	4.785	5.408
8	1.397	1.86	2.306	2.896	3.355	4.501	5.041
9	1.383	1.833	2.262	2.821	3.25	4.297	4.781
10	1.372	1.812	2.228	2.764	3.169	4.144	4.587
11	1.363	1.796	2.201	2.718	3.106	4.025	4.437
12	1.356	1.782	2.179	2.681	3.055	3.93	4.318
13	1.35	1.771	2.16	2.65	3.012	3.852	4.221
14	1.345	1.761	2.145	2.624	2.977	3.787	4.14
15	1.341	1.753	2.131	2.602	2.947	3.733	4.073
16	1.337	1.746	2.12	2.583	2.921	3.686	4.015
17	1.333	1.74	2.11	2.567	2.898	3.646	3.965
18	1.33	1.734	2.101	2.552	2.878	3.61	3.922
19	1.328	1.729	2.093	2.539	2.861	3.579	3.883
20	1.325	1.725	2.086	2.528	2.845	3.552	3.85
21	1.323	1.721	2.08	2.518	2.831	3.527	3.819
22	1.321	1.717	2.074	2.508	2.819	3.505	3.792
23	1.319	1.714	2.069	2.5	2.807	3.485	3.767
24	1.318	1.711	2.064	2.492	2.797	3.467	3.745
25	1.316	1.708	2.06	2.485	2.787	3.45	3.725
26	1.315	1.706	2.056	2.479	2.779	3.435	3.707
27	1.314	1.703	2.052	2.473	2.771	3.421	3.69
28	1.313	1.701	2.048	2.467	2.763	3.408	3.674
29	1.311	1.699	2.045	2.462	2.756	3.396	3.659
30	1.31	1.697	2.042	2.457	2.75	3.385	3.646
40	1.303	1.684	2.021	2.423	2.704	3.307	3.551
60	1.296	1.671	2	2.39	2.66	3.232	3.46
120	1.289	1.658	1.98	2.358	2.617	3.16	3.373
α	1.282	1.645	1.96	2.326	2.576	3.09	3.291

Source: E.S. Pearson and H.O. Hartley (eds.), The Biometrika Tables for Statisticians,Vol.1,3rd ed.,Biometrika,1966.

Table C-2: Critical Values for the F Statistic: $F_{.05}$

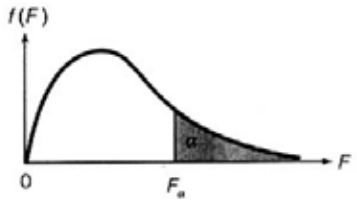

DENOMINATOR DEGREES OF FREEDOM (ν_2) \ NUMERATOR DEGREES OF FREEDOM (ν_1)	1	2	3	4	5	6	7	8	9
1	161.4	199.5	215.7	224.6	230.2	234.0	236.8	238.9	240.5
2	18.51	19.00	19.16	19.25	19.30	19.33	19.35	19.37	19.38
3	10.13	9.55	9.28	9.12	9.01	8.94	8.89	8.85	8.81
4	7.71	6.94	6.59	6.39	6.26	6.16	6.09	6.04	6.00
5	6.61	5.79	5.41	5.19	5.05	4.95	4.88	4.82	4.77
6	5.99	5.14	4.76	4.53	4.39	4.28	4.21	4.15	4.10
7	5.59	4.74	4.35	4.12	3.97	3.87	3.79	3.73	3.68
8	5.32	4.46	4.07	3.84	3.69	3.58	3.50	3.44	3.39
9	5.12	4.26	3.86	3.63	3.48	3.37	3.29	3.23	3.18
10	4.96	4.10	3.71	3.48	3.33	3.22	3.14	3.07	3.02
11	4.84	3.98	3.59	3.36	3.20	3.09	3.01	2.95	2.90
12	4.75	3.89	3.49	3.26	3.11	3.00	2.91	2.85	2.80
13	4.67	3.81	3.41	3.18	3.03	2.92	2.83	2.77	2.71
14	4.60	3.74	3.34	3.11	2.96	2.85	2.76	2.70	2.65
15	4.54	3.68	3.29	3.06	2.90	2.79	2.71	2.64	2.59
16	4.49	3.63	3.24	3.01	2.85	2.74	2.66	2.59	2.54
17	4.45	3.59	3.20	2.96	2.81	2.70	2.61	2.55	2.49
18	4.41	3.55	3.16	2.93	2.77	2.66	2.58	2.51	2.46
19	4.38	3.52	3.13	2.90	2.74	2.63	2.54	2.48	2.42
20	4.35	3.49	3.10	2.87	2.71	2.60	2.51	2.45	2.39
21	4.32	3.47	3.07	2.84	2.68	2.57	2.49	2.42	2.37
22	4.30	3.44	3.05	2.82	2.66	2.55	2.46	2.40	2.34
23	4.28	3.42	3.03	2.80	2.64	2.53	2.44	2.37	2.32
24	4.26	3.40	3.01	2.78	2.62	2.51	2.42	2.36	2.30
25	4.24	3.39	2.99	2.76	2.60	2.49	2.40	2.34	2.28
26	4.23	3.37	2.98	2.74	2.59	2.47	2.39	2.32	2.27
27	4.21	3.35	2.96	2.73	2.57	2.46	2.37	2.31	2.25
28	4.20	3.34	2.95	2.71	2.56	2.45	2.36	2.29	2.24
29	4.18	3.33	2.93	2.70	2.55	2.43	2.35	2.28	2.22
30	4.17	3.32	2.92	2.69	2.53	2.42	2.33	2.27	2.21
40	4.08	3.23	2.84	2.61	2.45	2.34	2.25	2.18	2.12
60	4.00	3.15	2.76	2.53	2.37	2.25	2.17	2.10	2.04

Source: From M. Merrington and C. M. Thompson, "Tables of percentage points of the inverted beta (F) – distribution," Biometrika, 1943, 33, 73 – 88. Reproduced by permission of the Biometrika Trustees.

APPENDIX D. Comparison of light scattering contour graphs between experiment and equation of HDPE/LLDPE blends and their regression statistic values.

D.1 At gain no.6, area 2

D.2 At gain no.3, area 1

D.3 At gain no.3, area 2

pure HDPE (gain no.6, area2)

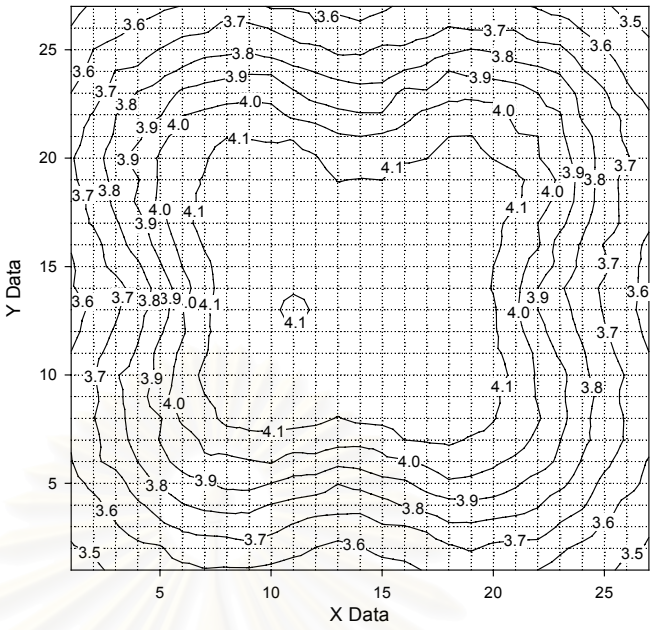

(a-

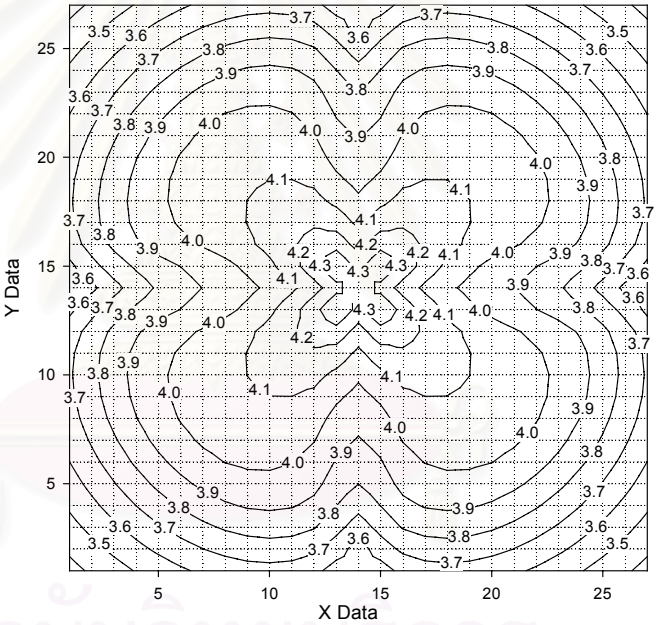

(a-

Regression Statistic Values

HDPE	TERM5	TERM4	TERM3	TERM2	TERM1	B
	0.03673	-0.11837	0.122604	-38.0462	0.038271	3.404503
	488.7154	0.00312	0.00486	17.37911	0.002912	15434.45
	0.903817	0.066262	#N/A	#N/A	#N/A	#N/A
	1358.781	723	#N/A	#N/A	#N/A	#N/A
	29.82954	3.174428	#N/A	#N/A	#N/A	#N/A
	#N/A	#N/A	#N/A	#N/A	#N/A	#N/A
t - test	7.52E-05	-37.9403	25.22544	-2.18919	13.14469	0.000221

(a) pure HDPE from experiment (a-1) and from equation (a-2), r^2 = 0.9038

HDPE/LLDPE : 90/10 (gain no.6, area2)

(b-1)

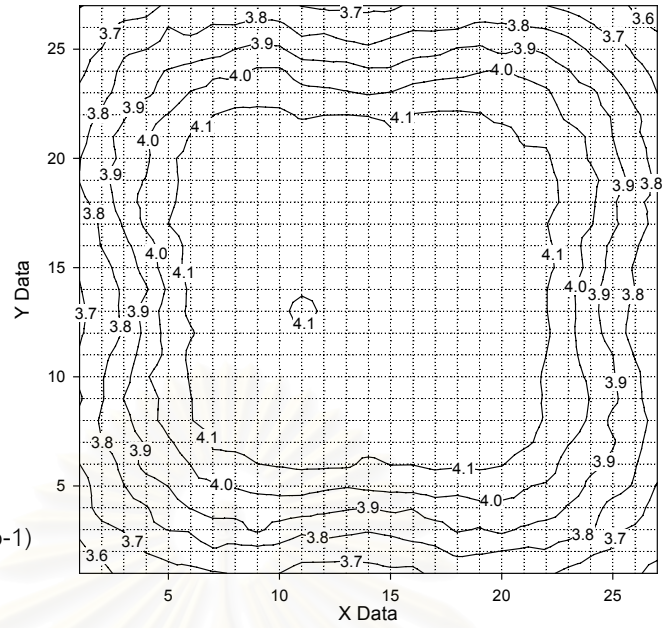

(b-2)

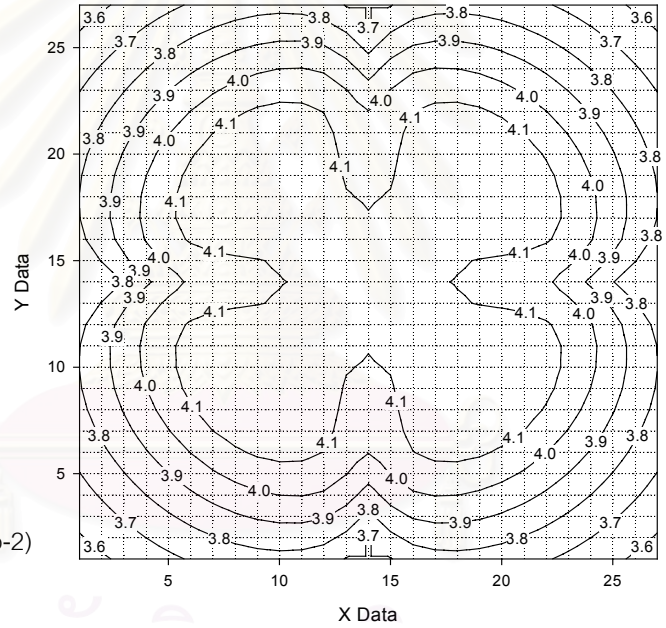

Regression Statistic Values

90-10	TERM5	TERM4	TERM3	TERM2	TERM1	B
	0.089787	-0.1	0.087832	-54.1441	-0.01678	1.52756
	0	0.001444	0.00289	10.45081	0.001956	0
	0.948929	0.039846	#N/A	#N/A	#N/A	#N/A
	2686.753	723	#N/A	#N/A	#N/A	#N/A
	21.32896	1.147916	#N/A	#N/A	#N/A	#N/A
	#N/A	#N/A	#N/A	#N/A	#N/A	#N/A
t - test	α	-69.2547	30.38893	-5.18085	-8.58239	α

(b) 90 / 10 blended from experiment (b-1) and from equation (b-2), r^2 = 0.9489

HDPE/LLDPE : 80/20 (gain no.6, area2)

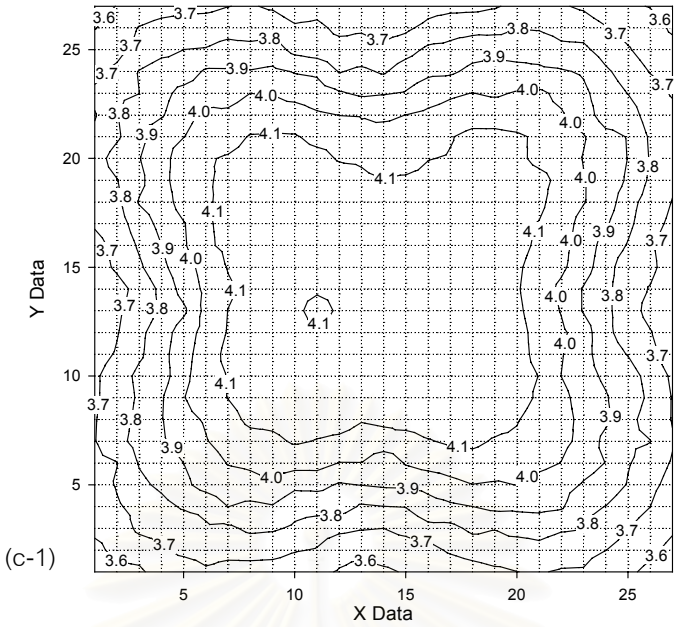

(c-1)

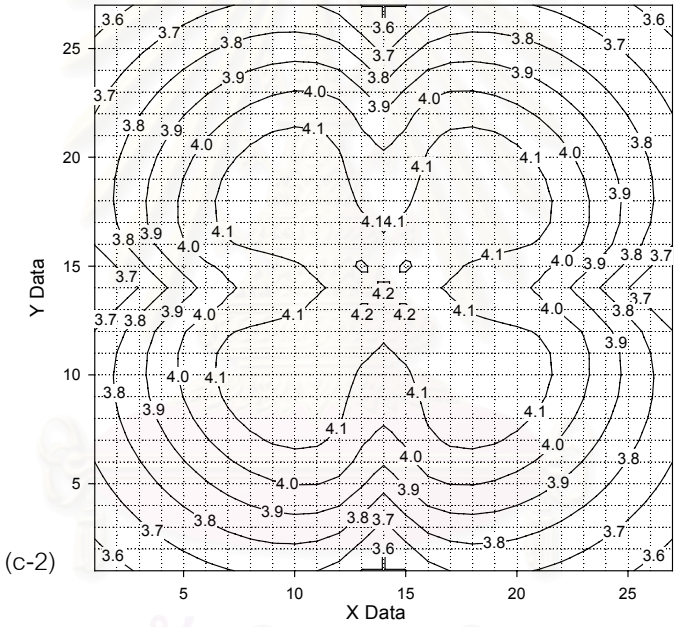

(c-2)

Regression Statistic Values

80-20	TERM5	TERM4	TERM3	TERM2	TERM1	B
	0.049708	-0.08404	0.114916	-57.5774	-0.00605	2.810864
	355.3411	0.001438	0.003071	11.16426	0.002227	11488.58
	0.946275	0.042566	#N/A	#N/A	#N/A	#N/A
	2546.871	723	#N/A	#N/A	#N/A	#N/A
	23.07325	1.309996	#N/A	#N/A	#N/A	#N/A
	#N/A	#N/A	#N/A	#N/A	#N/A	#N/A
t - test	0.00014	-58.4529	37.41359	-5.1573	-2.71605	0.000245

(c) 80 / 20 blended from experiment (c-1) and from equation (c-2), r^2 = 0.9462

HDPE/LLDPE : 70/30 (gain no.6, area2)

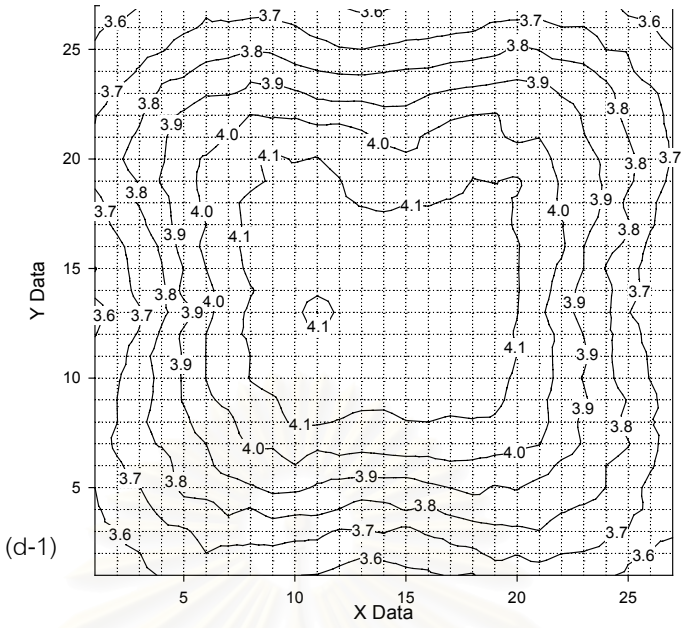

(d-1)

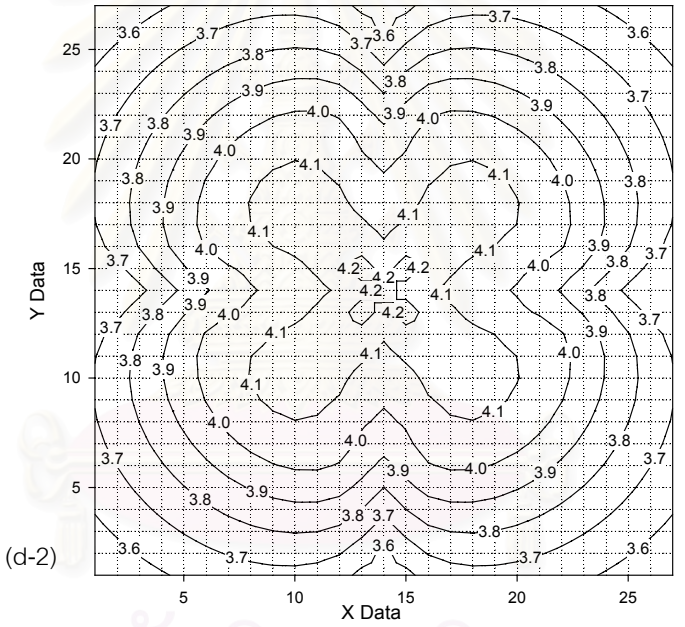

(d-2)

Regression Statistic Values

70-30	TERM5	TERM4	TERM3	TERM2	TERM1	B
	0.044399	-0.07389	0.098654	-59.8887	0.0119	2.967957
	0	0.001407	0.003032	11.02835	0.002226	0
	0.948796	0.042048	#N/A	#N/A	#N/A	#N/A
	2679.371	723	#N/A	#N/A	#N/A	#N/A
	23.68624	1.278296	#N/A	#N/A	#N/A	#N/A
	#N/A	#N/A	#N/A	#N/A	#N/A	#N/A
t - test	α	-52.5	32.54272	-5.43043	5.346863	α

(d) 70 / 30 blended from experiment (d-1) and from equation (d-2), r^2 = 0.9487

HDPE/LLDPE : 60/40 (gain no.6, area2)

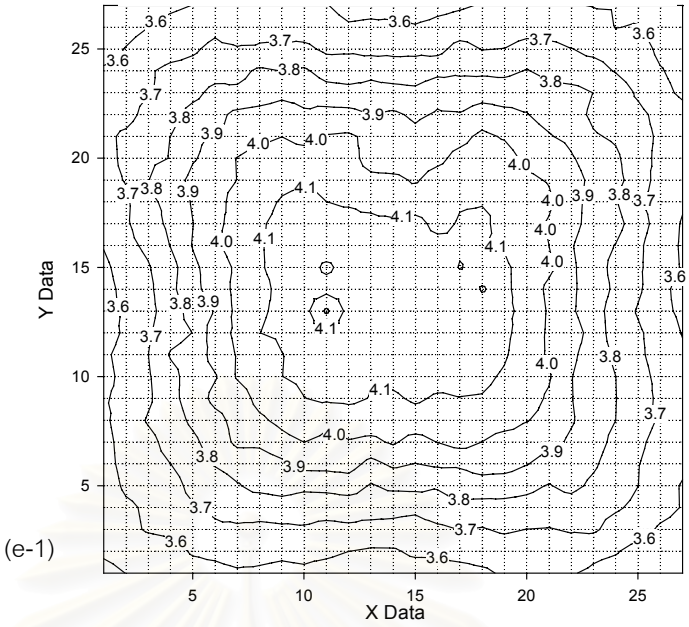

(e-1)

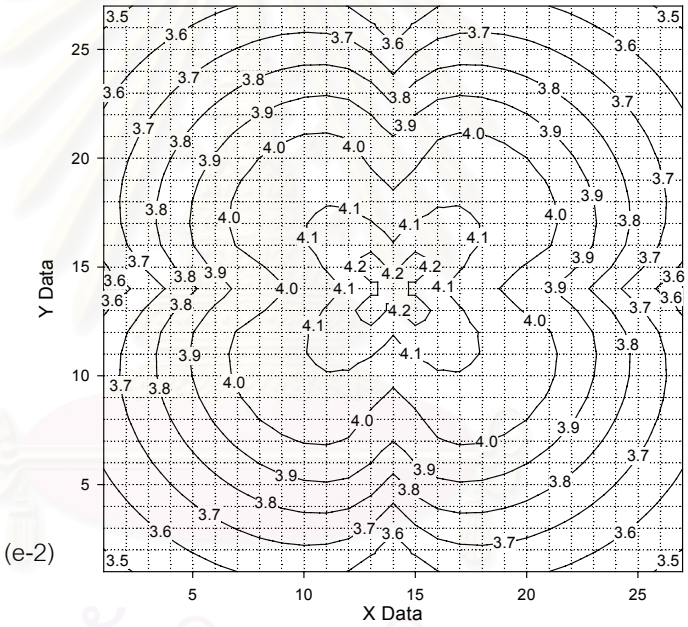

(e-2)

Regression Statistic Values

60-40	TERM5	TERM4	TERM3	TERM2	TERM1	B
	0.087217	-0.06576	0.080758	-63.0118	0.028543	1.563211
	0	0.001394	0.003025	11.01366	0.002248	0
	0.951633	0.041992	#N/A	#N/A	#N/A	#N/A
	2845.043	723	#N/A	#N/A	#N/A	#N/A
	25.08387	1.274894	#N/A	#N/A	#N/A	#N/A
	#N/A	#N/A	#N/A	#N/A	#N/A	#N/A
t - test	α	-47.1712	26.69628	-5.72124	12.69852	α

(e) 60 / 40 blended from experiment (e-1) and from equation (e-2), r^2 = 0.9516

HDPE/LLDPE : 50/50 (gain no.6, area2)

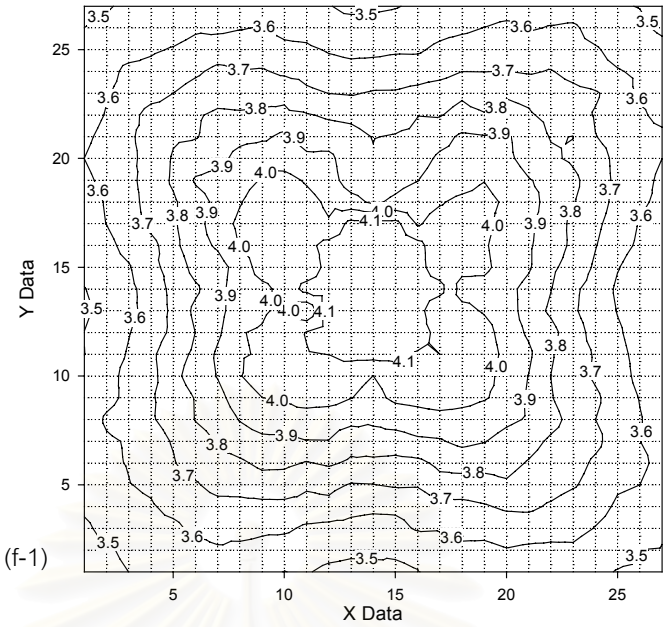

(f-1)

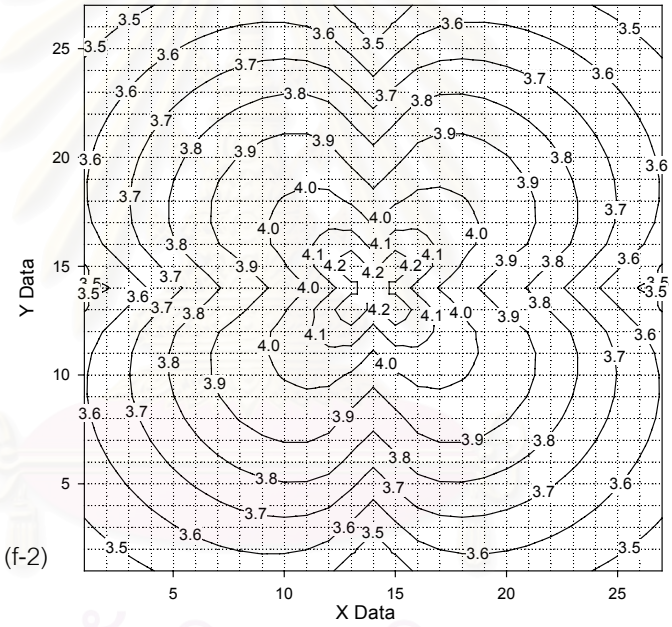

(f-2)

Regression Statistic Values

50-50	TERM5	TERM4	TERM3	TERM2	TERM1	B
	0.009642	-0.04808	0.098381	-67.9935	0.058234	4.068609
	432.0073	0.001436	0.003062	11.12606	0.002214	13963.36
	0.94896	0.042421	#N/A	#N/A	#N/A	#N/A
	2688.459	723	#N/A	#N/A	#N/A	#N/A
	24.18958	1.301048	#N/A	#N/A	#N/A	#N/A
	#N/A	#N/A	#N/A	#N/A	#N/A	#N/A
t - test	2.23E-05	-33.4817	32.13427	-6.11119	26.30418	0.000291

(f) 50 / 50 blended from experiment (f-1) and from equation (f-2), r^2 = 0.9489

HDPE/LLDPE : 40/60 (gain no.6, area2)

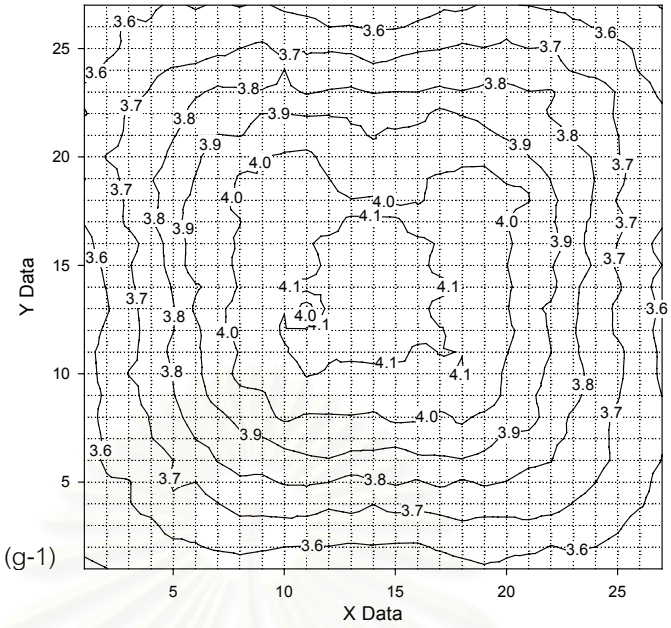

(g-1)

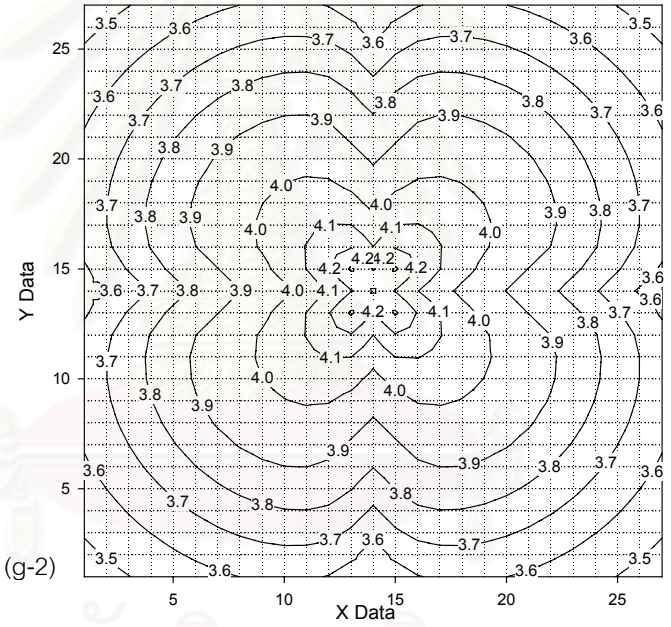

(g-2)

Regression Statistic Values

40-60	TERM5	TERM4	TERM3	TERM2	TERM1	B
	0.065496	-0.05698	0.068299	-52.7747	0.057782	2.278165
	0	0.001745	0.00336	12.12034	0.002209	0
	0.935433	0.046212	#N/A	#N/A	#N/A	#N/A
	2094.947	723	#N/A	#N/A	#N/A	#N/A
	22.3689	1.543973	#N/A	#N/A	#N/A	#N/A
	#N/A	#N/A	#N/A	#N/A	#N/A	#N/A
t - test	α	-32.6524	20.32617	-4.35423	26.15727	α

(g) 40 / 60 blended from experiment (g-1) and from equation (g-2), r^2 = 0.9354

HDPE/LLDPE : 30/70 (gain no.6, area2)

(h-1)

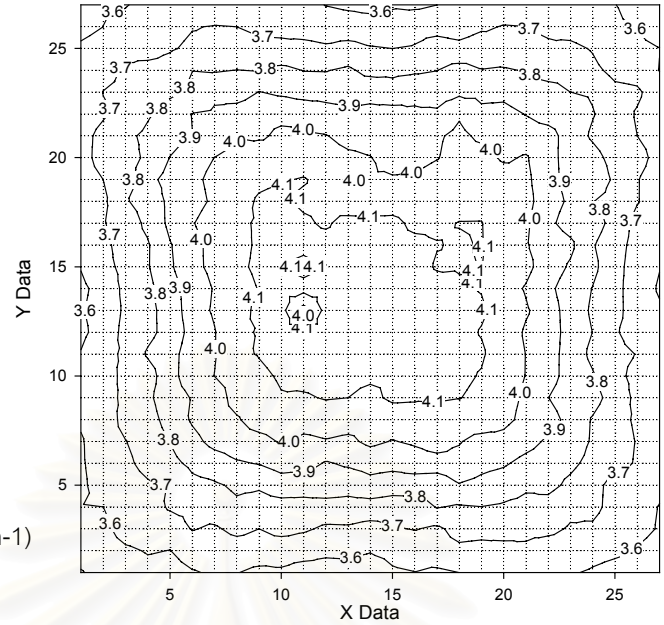

(h-2)

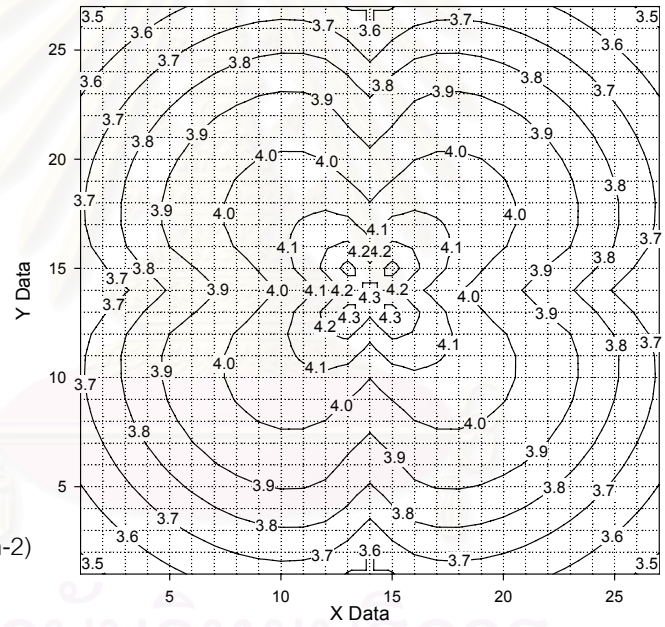

Regression Statistic Values

30-70	TERM5	TERM4	TERM3	TERM2	TERM1	B
	0.060104	-0.06949	0.077037	-50.4292	0.05175	2.503426
	405.8499	0.002211	0.003904	14.02075	0.002447	12903.2
	0.913597	0.053457	#N/A	#N/A	#N/A	#N/A
	1528.96	723	#N/A	#N/A	#N/A	#N/A
	21.84643	2.066107	#N/A	#N/A	#N/A	#N/A
	#N/A	#N/A	#N/A	#N/A	#N/A	#N/A
t - test	0.000148	-31.4363	19.73351	-3.59675	21.14595	0.000194

(h) 30 / 70 blended from experiment (h-1) and from equation (h-2), r^2 = 0.9135

HDPE/LLDPE : 20/80 (gain no.6, area2)

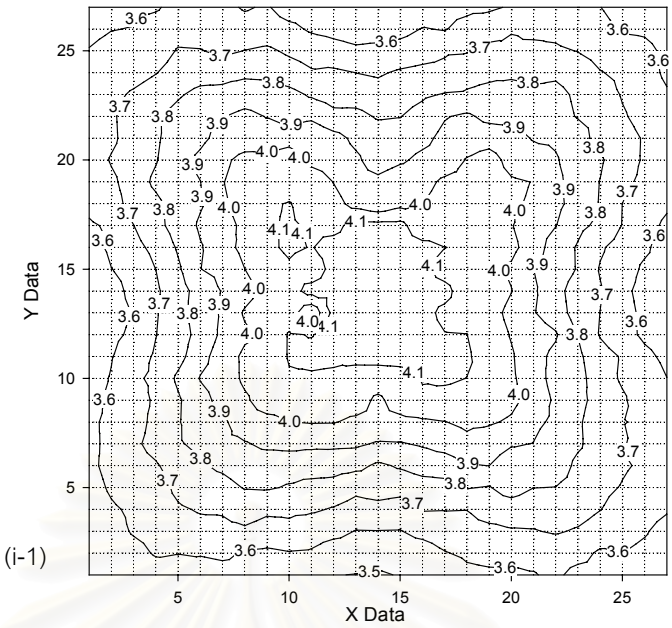

(i-1)

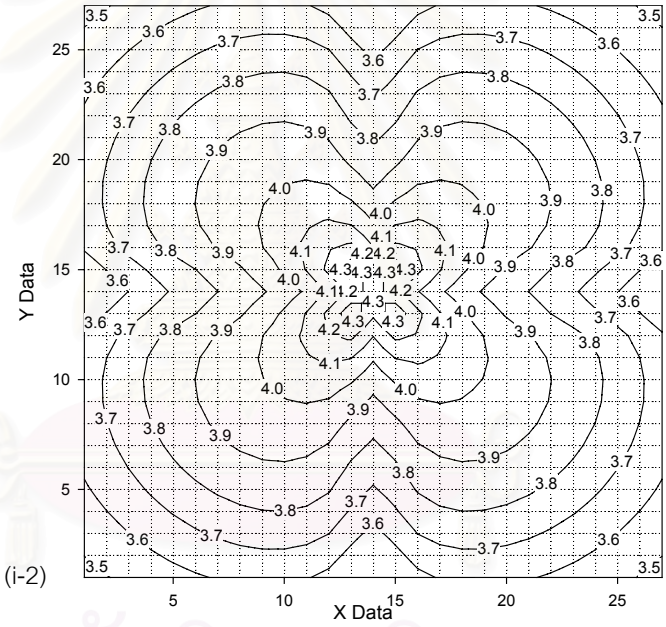

(i-2)

Regression Statistic Values

20-80	TERM5	TERM4	TERM3	TERM2	TERM1	B
	0.082852	-0.05795	0.110873	-61.1844	0.068567	1.79445
	507.2589	0.0025	0.004066	14.55846	0.002468	16053.88
	0.906319	0.055507	#N/A	#N/A	#N/A	#N/A
	1398.93	723	#N/A	#N/A	#N/A	#N/A
	21.5511	2.227623	#N/A	#N/A	#N/A	#N/A
	#N/A	#N/A	#N/A	#N/A	#N/A	#N/A
t - test	0.000163	-23.1831	27.26693	-4.20267	27.77675	0.000112

(i) 20 / 80 blended from experiment (i-1) and from equation (i-2), r^2 = 0.9063

HDPE/LLDPE : 10/90 (gain no.6, area2)

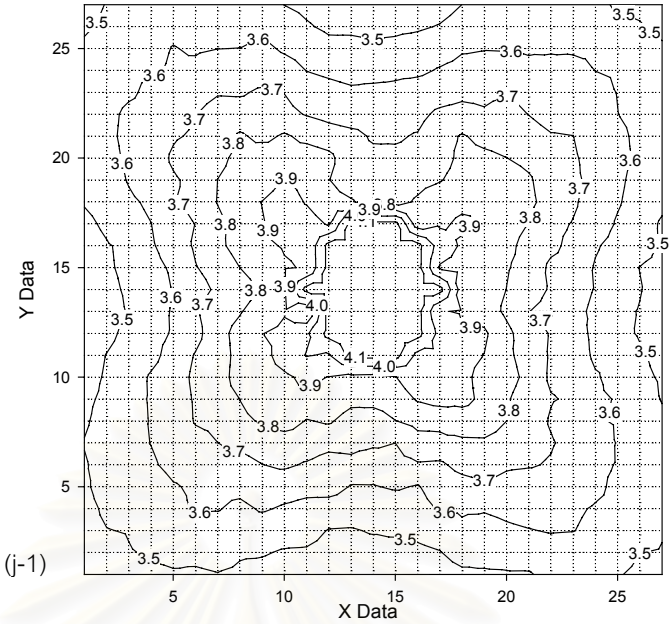

(j-1)

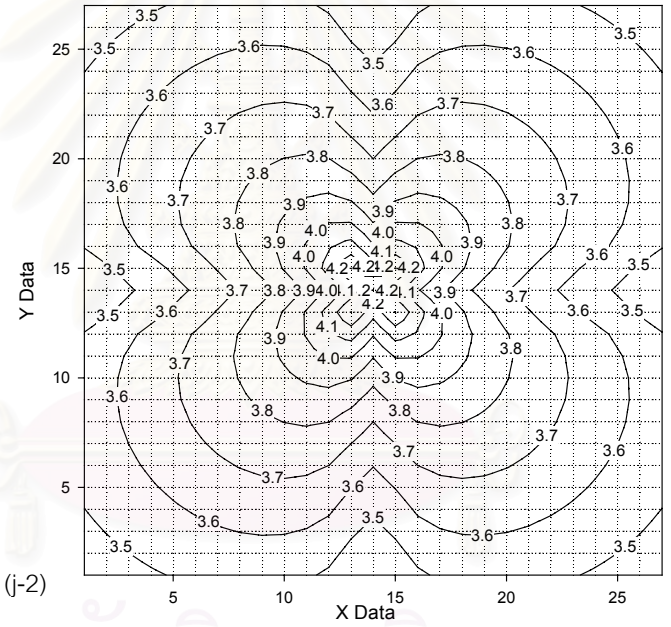

(j-2)

Regression Statistic Values

10.0-90.0	TERM5	TERM4	TERM3	TERM2	TERM1	B
	0.067325	-0.01903	0.088236	-33.0349	0.096423	2.113351
	0	0.002201	0.003334	11.91359	0.001982	0
	0.925438	0.045423	#N/A	#N/A	#N/A	#N/A
	1794.716	723	#N/A	#N/A	#N/A	#N/A
	18.51498	1.491749	#N/A	#N/A	#N/A	#N/A
	#N/A	#N/A	#N/A	#N/A	#N/A	#N/A
t - test	α	-8.64347	26.46337	-2.77288	48.64218	α

(j) 10 / 90 blended from experiment (j-1) and from equation (j-2), r^2 = 0.9254

pure LLDPE (gain no.6, area2)

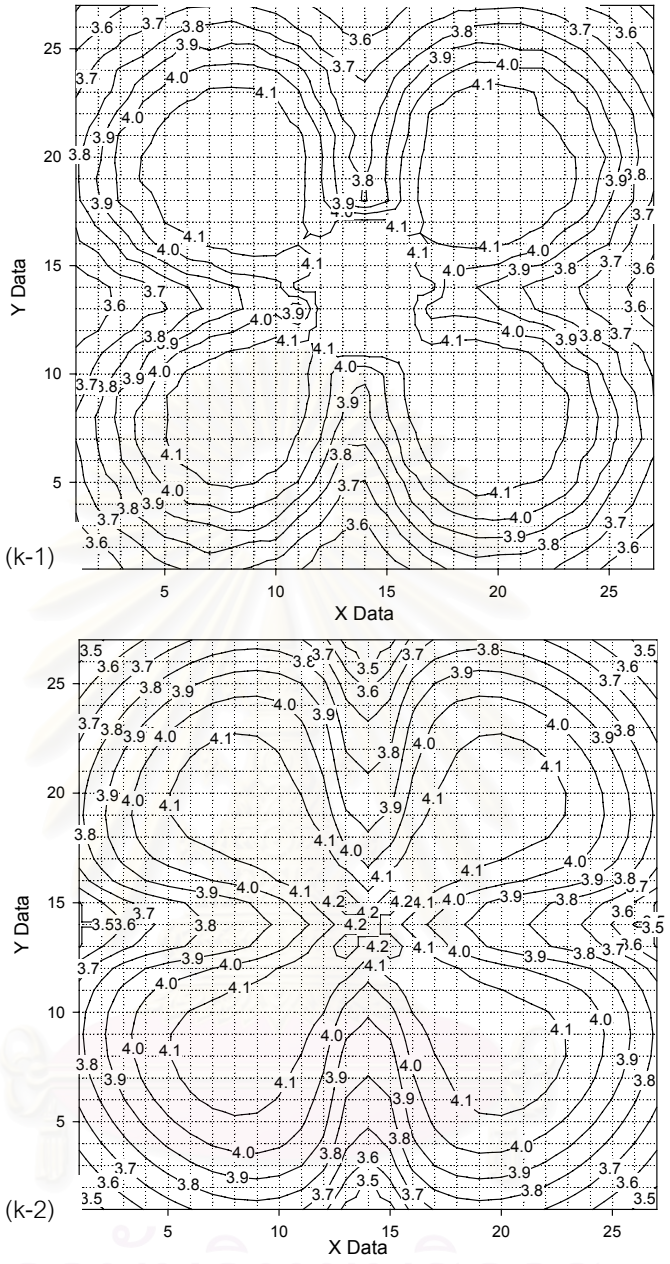

Regression Statistic Values

LLDPE	TERM5	TERM4	TERM3	TERM2	TERM1	B
	0.059643	-0.17206	0.25471	-47.3939	-0.01703	2.788859
	0	0.003016	0.004007	14.28275	0.00232	0
	0.925139	0.054456	#N/A	#N/A	#N/A	#N/A
	1786.974	723	#N/A	#N/A	#N/A	#N/A
	26.49623	2.144046	#N/A	#N/A	#N/A	#N/A
	#N/A	#N/A	#N/A	#N/A	#N/A	#N/A
t - test	α	-57.0506	63.56878	-3.31826	-7.33848	α

(k) pure LLDPE from experiment (k-1) and from equation (k-2), r^2 = 0.9251

Figure D-1 : Comparison of light scattering contour graphs between experiment and equation of HDPE / LLDPE blends at gain no.6, area2 and their r^2 values

pure HDPE (gain3, area1)

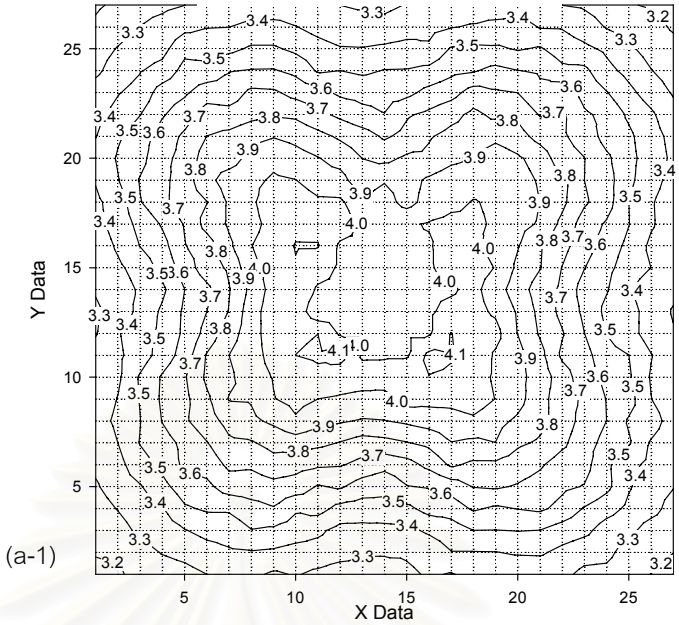

(a-1)

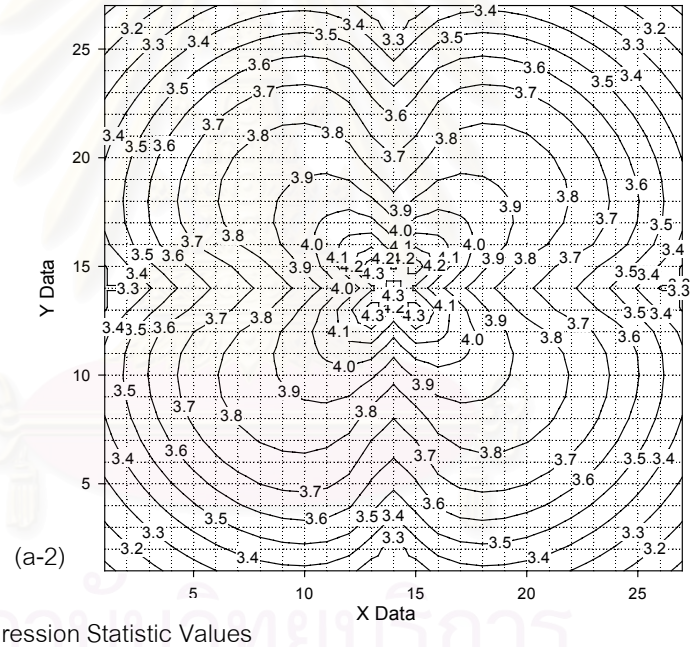

(a-2)

Regression Statistic Values

HDPE	TERM5	TERM4	TERM3	TERM2	TERM1	B
	0.032906	-0.11592	0.140923	-83.2505	0.073704	3.448102
	596.2479	0.003806	0.00593	21.20305	0.003552	18830.5
	0.902751	0.080842	#N/A	#N/A	#N/A	#N/A
	1342.301	723	#N/A	#N/A	#N/A	#N/A
	43.86202	4.725058	#N/A	#N/A	#N/A	#N/A
	#N/A	#N/A	#N/A	#N/A	#N/A	#N/A
t - test	5.52E-05	-30.4523	23.76531	-3.92635	20.74914	0.000183

(a) Pure HDPE from experiment (a-1) and from equation (a-2), r^2 =

HDPE/LLDPE: 90/10 (gain3, area1)

(b-1)

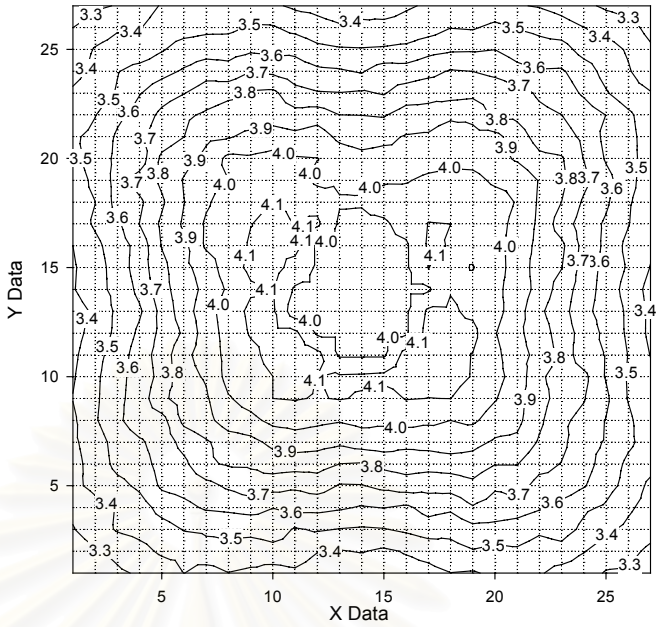

(b-2)

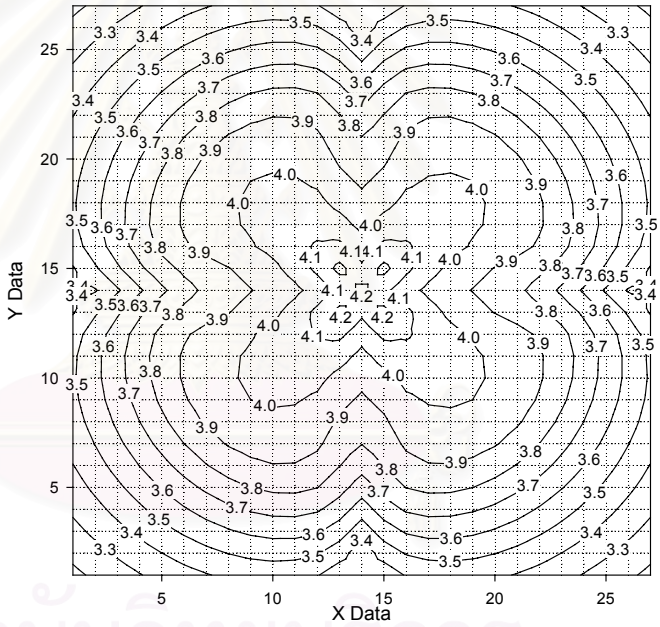

Regression Statistic Values

90-10	TERM5	TERM4	TERM3	TERM2	TERM1	B
	0.084895	-0.11017	0.113296	-85.2244	0.02653	1.707863
	0	0.002481	0.004966	17.95778	0.00336	0
	0.926678	0.068468	#N/A	#N/A	#N/A	#N/A
	1827.536	723	#N/A	#N/A	#N/A	#N/A
	42.83645	3.389346	#N/A	#N/A	#N/A	#N/A
	#N/A	#N/A	#N/A	#N/A	#N/A	#N/A
t - test	α	-44.4019	22.81251	-4.74582	7.895249	α

(b) 90 / 10 blended from experiment (b-1) and from equation (b-2), r^2 = 0.9266

HDPE/LLDPE: 80/20 (gain3,

(c-1)

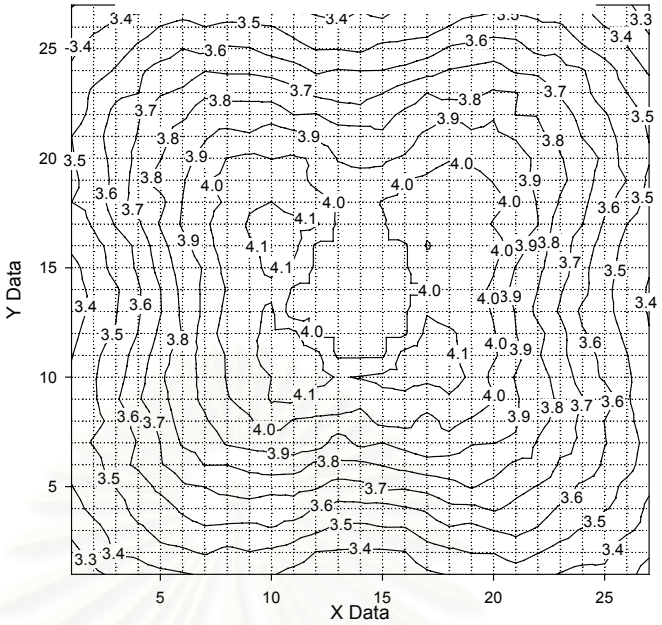

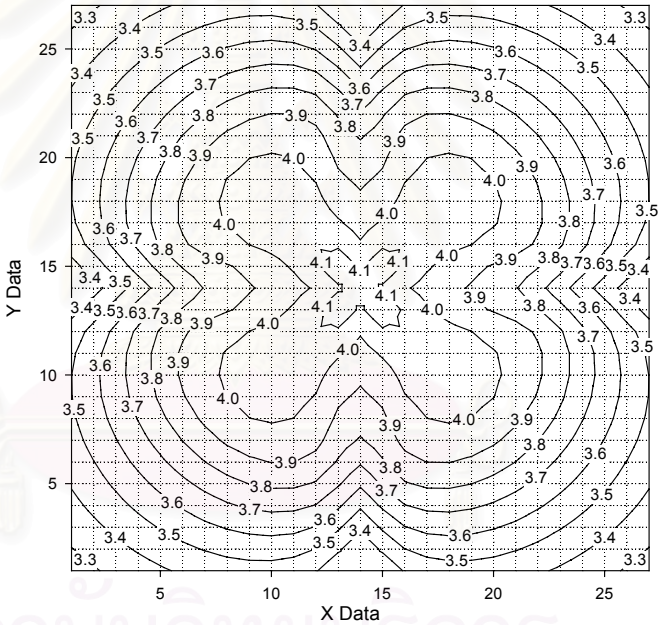

(c-2)

Regression Statistic Values

80-20	TERM5	TERM4	TERM3	TERM2	TERM1	B
	0.036291	-0.09886	0.137584	-69.0108	0.010467	3.224439
	496.2991	0.002008	0.00429	15.59293	0.003111	16045.91
	0.938052	0.059452	#N/A	#N/A	#N/A	#N/A
	2189.597	723	#N/A	#N/A	#N/A	#N/A
	38.69566	2.555443	#N/A	#N/A	#N/A	#N/A
	#N/A	#N/A	#N/A	#N/A	#N/A	#N/A
t - test	7.31E-05	-49.2273	32.07147	-4.42577	3.365031	0.000201

(c) 80 / 20 blended from experiment (c-1) and from equation (c-2), r^2 = 0.9380

HDPE/LLDPE: 70/30 (gain3,

(d-1)

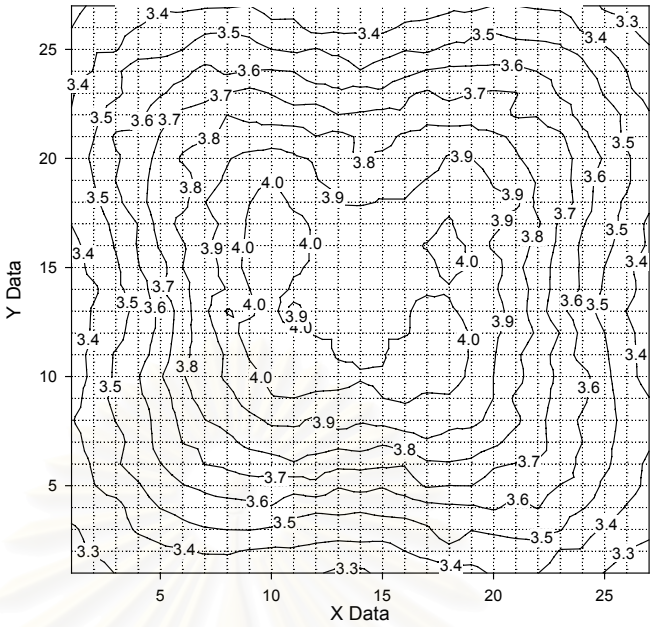

(d-2)

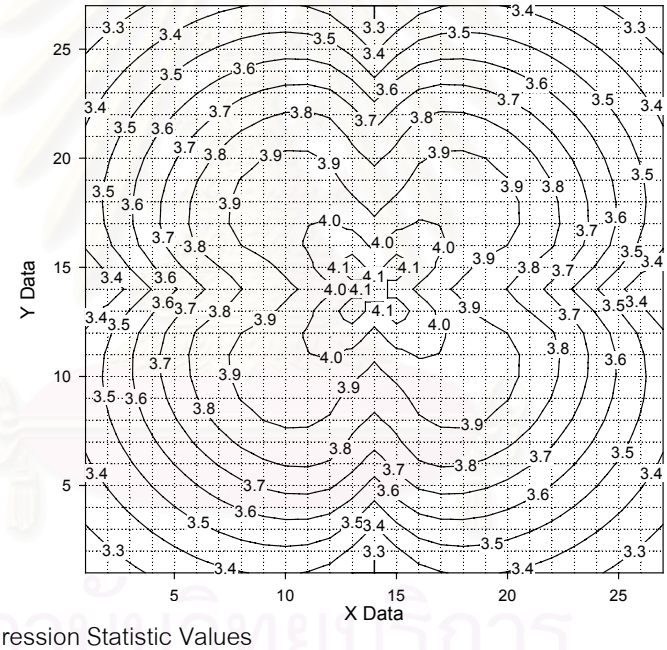

Regression Statistic Values

70-30	TERM5	TERM4	TERM3	TERM2	TERM1	B
	0.0439	-0.08202	0.110408	-72.0981	0.031087	2.911007
	0	0.001821	0.003923	14.27054	0.00288	0
	0.944003	0.05441	#N/A	#N/A	#N/A	#N/A
	2437.667	723	#N/A	#N/A	#N/A	#N/A
	36.08255	2.140382	#N/A	#N/A	#N/A	#N/A
	#N/A	#N/A	#N/A	#N/A	#N/A	#N/A
t - test	α	-45.0392	28.14543	-5.05224	10.79506	α

(d) 70 / 30 blended from experiment (d-1) and from equation (d-2), r^2 = 0.9440

HDPE/LLDPE: 60/40 (gain3,

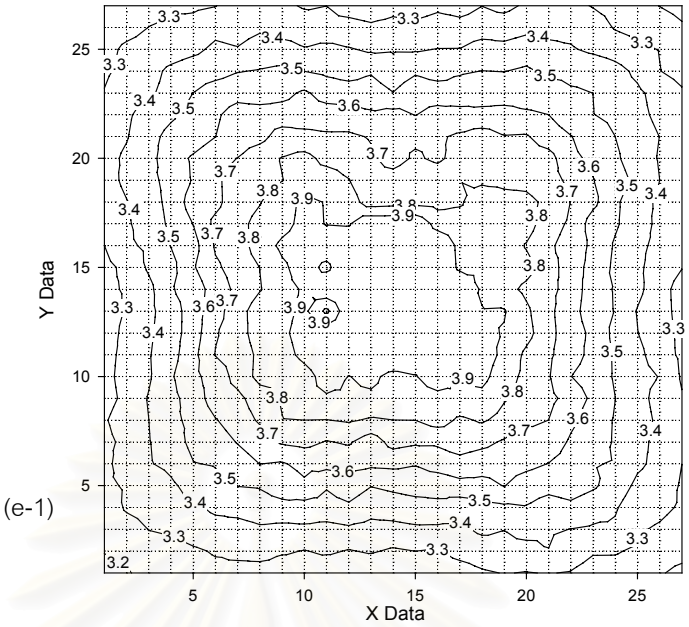

(e-1)

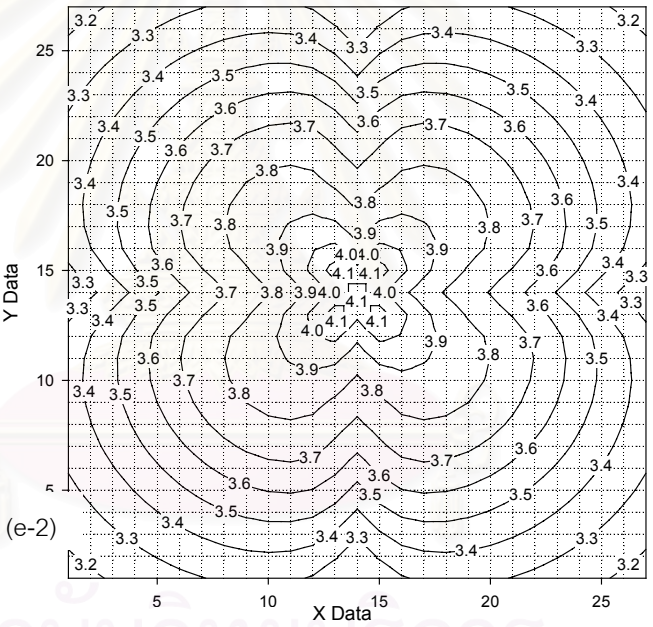

(e-2)

Regression Statistic Values

60-40	TERM5	TERM4	TERM3	TERM2	TERM1	B
	0.084821	-0.06108	0.088607	-70.2586	0.060223	1.511126
	0	0.001577	0.003422	12.4593	0.002543	0
	0.954567	0.047504	#N/A	#N/A	#N/A	#N/A
	3038.113	723	#N/A	#N/A	#N/A	#N/A
	34.27943	1.631541	#N/A	#N/A	#N/A	#N/A
	#N/A	#N/A	#N/A	#N/A	#N/A	#N/A
t - test	α	-38.7287	25.89238	-5.63905	23.68436	α

(e) 60 / 40 blended from experiment (e-1) and from equation (e-2), r^2 = 0.9545

HDPE/LLDPE: 50/50 (gain3,

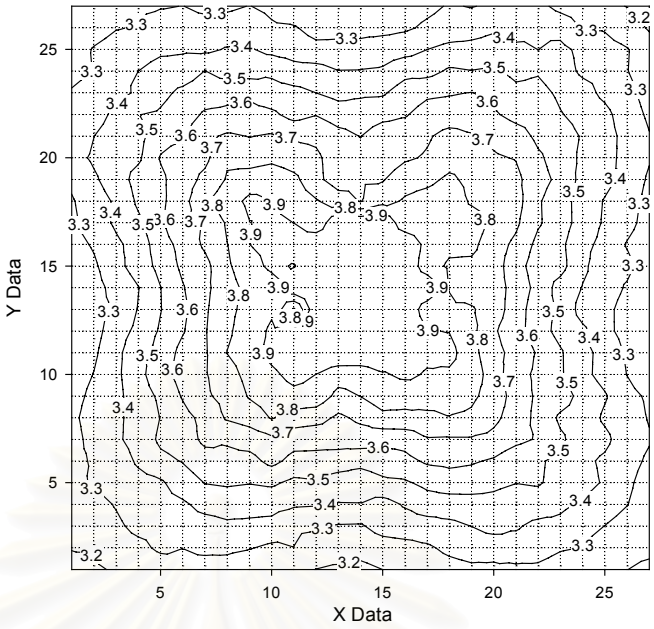

(f-1)

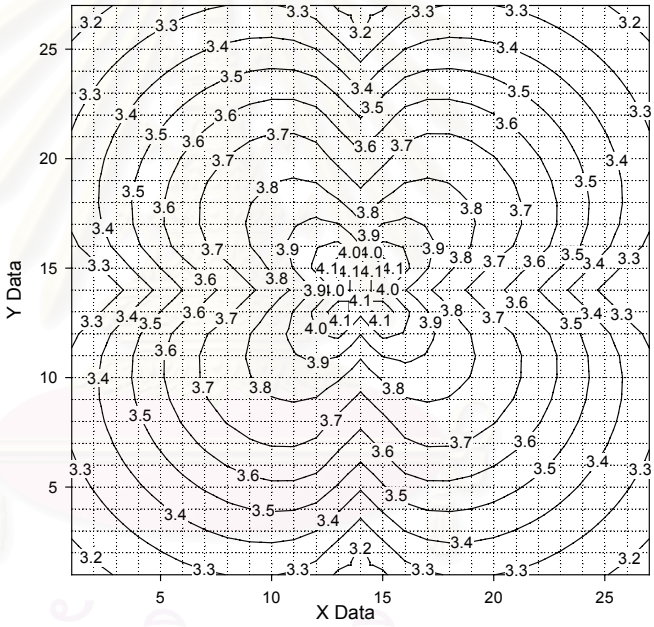

(f-2)

Regression Statistic Values

50-50	TERM5	TERM4	TERM3	TERM2	TERM1	B
	-0.01044	-0.05584	0.115963	-38.1822	0.071642	4.61459
	519.7521	0.001728	0.003683	13.38587	0.002664	16799.45
	0.947889	0.051037	#N/A	#N/A	#N/A	#N/A
	2630.22	723	#N/A	#N/A	#N/A	#N/A
	34.25527	1.883231	#N/A	#N/A	#N/A	#N/A
	#N/A	#N/A	#N/A	#N/A	#N/A	#N/A
t - test	-2E-05	-32.325	31.48253	-2.85243	26.89746	0.000275

(f) 50 / 50 blended from experiment (f-1) and from equation (f-2), r^2 = 0.9478

HDPE/LLDPE: 40/60 (gain3,

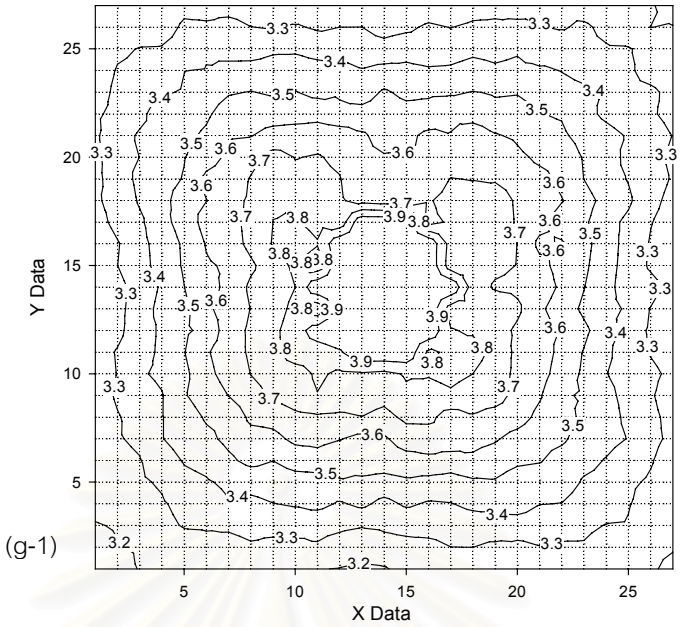

(g-1)

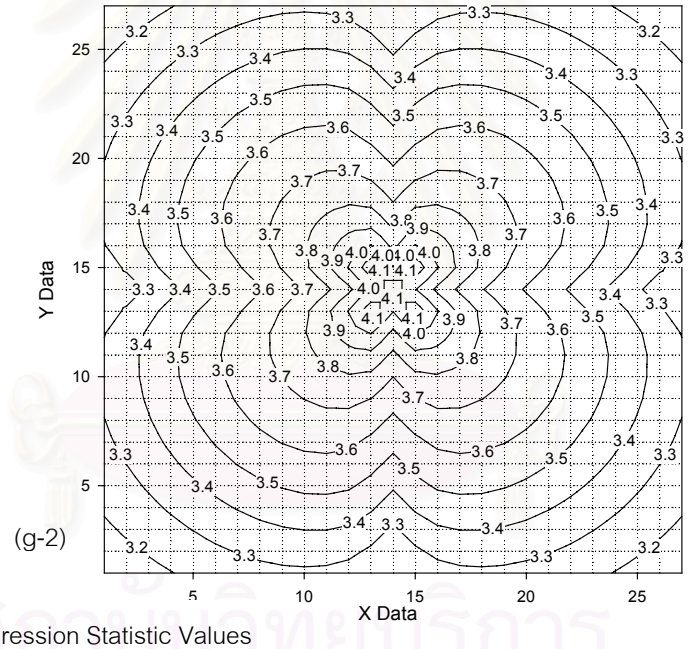

(g-2)

Regression Statistic Values

40-60	TERM5	TERM4	TERM3	TERM2	TERM1	B
	0.065723	-0.04403	0.070253	-56.9434	0.093037	2.069614
	0	0.001846	0.003554	12.82085	0.002337	0
	0.944703	0.048882	#N/A	#N/A	#N/A	#N/A
	2470.393	723	#N/A	#N/A	#N/A	#N/A
	29.51493	1.727604	#N/A	#N/A	#N/A	#N/A
	#N/A	#N/A	#N/A	#N/A	#N/A	#N/A
t - test	α	-23.8545	19.76552	-4.44147	39.81566	α

(g) 40 / 60 blended from experiment (g-1) and from equation (g-2), r^2 = 0.9447

HDPE/LLDPE: 30/70 (gain3,

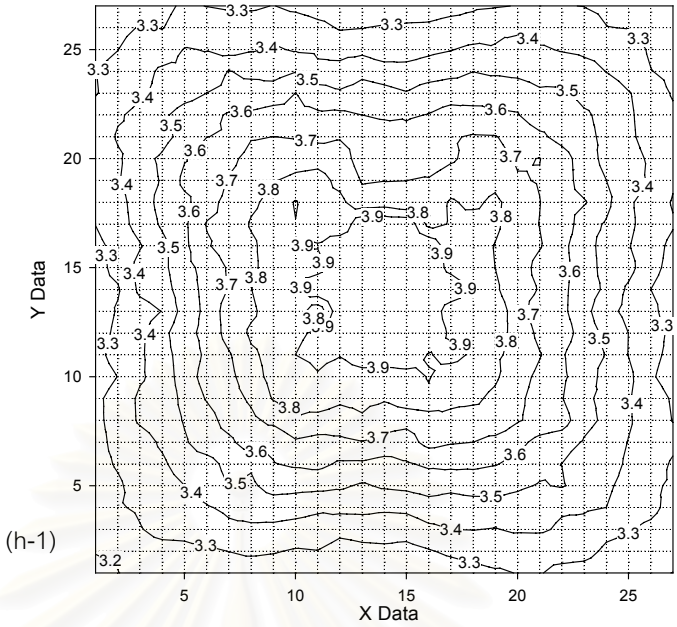

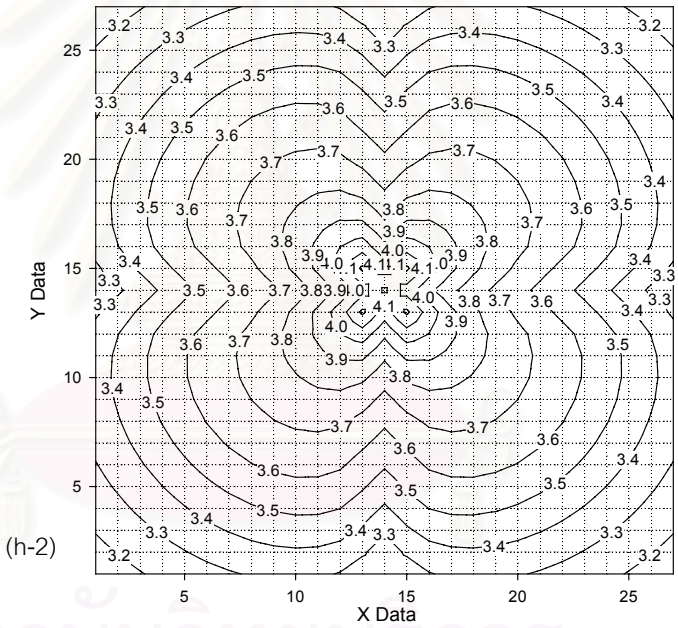

Regression Statistic Values

30-70	TERM5	TERM4	TERM3	TERM2	TERM1	B
	0.068672	-0.05726	0.08447	-66.3623	0.090038	2.052919
	427.2219	0.002327	0.004109	14.75907	0.002576	13582.68
	0.93151	0.056272	#N/A	#N/A	#N/A	#N/A
	1966.652	723	#N/A	#N/A	#N/A	#N/A
	31.13781	2.289437	#N/A	#N/A	#N/A	#N/A
	#N/A	#N/A	#N/A	#N/A	#N/A	#N/A
t - test	0.000161	-24.6058	20.55488	-4.49637	34.95013	0.000151

(h) 30 / 70 blended from experiment (h-1) and from equation (h-2), r^2 = 0.9315

HDPE/LLDPE: 20/80 (gain3,

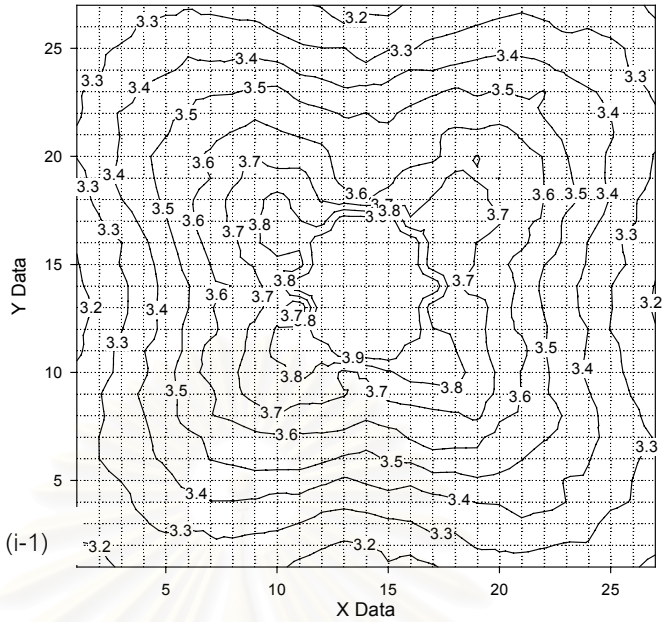

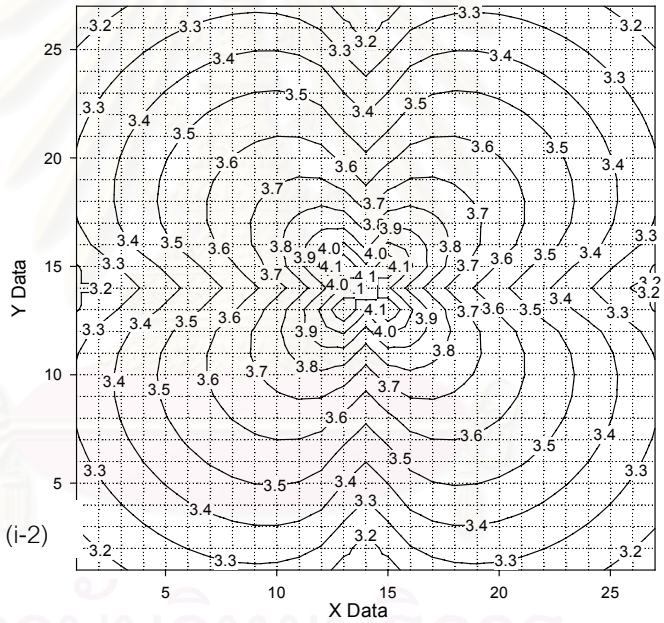

Regression Statistic Values

20-80	TERM5	TERM4	TERM3	TERM2	TERM1	B
	0.08577	-0.04158	0.112127	-52.7598	0.102586	1.467314
	499.6426	0.002462	0.004005	14.33987	0.002431	15812.84
	0.929551	0.054674	#N/A	#N/A	#N/A	#N/A
	1907.96	723	#N/A	#N/A	#N/A	#N/A
	28.51689	2.161231	#N/A	#N/A	#N/A	#N/A
	#N/A	#N/A	#N/A	#N/A	#N/A	#N/A
t - test	0.000172	-16.8884	27.99553	-3.67924	42.19145	9.28E-05

(i) 20 / 80 blended from experiment (i-1) and from equation (i-2), r^2 = 0.9295

HDPE/LLDPE: 10/90 (gain3,

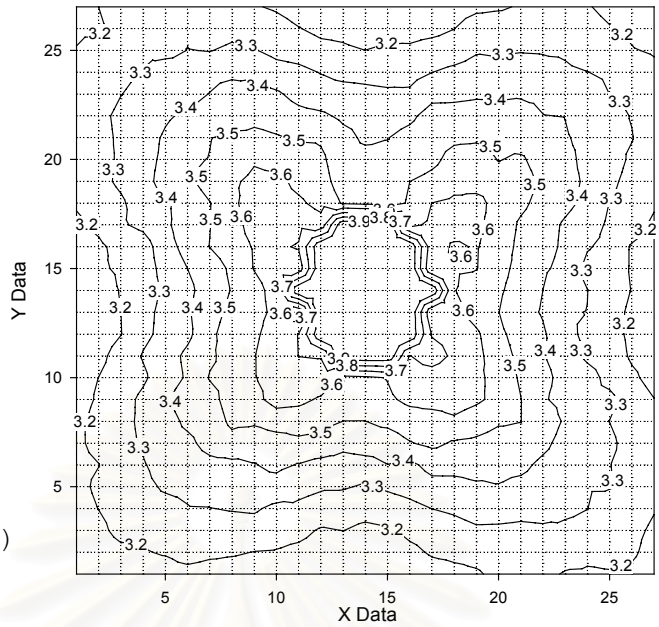

(j-1)

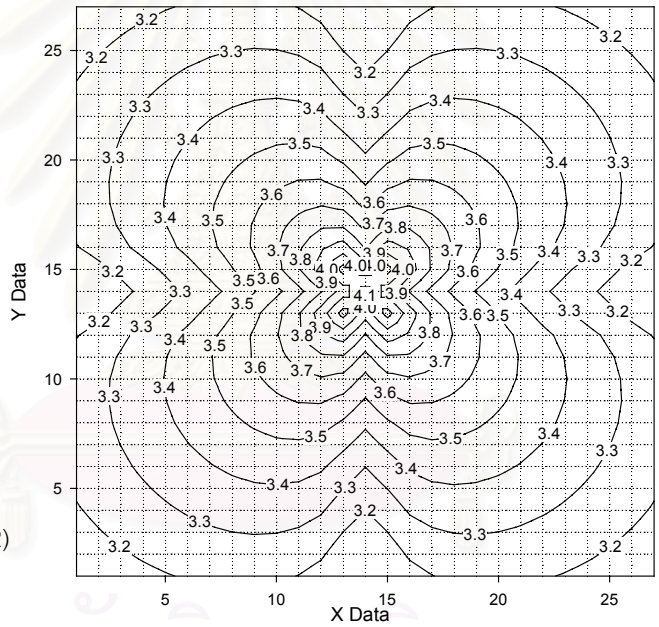

(j-2)

Regression Statistic Values

10.0-90.0	TERM5	TERM4	TERM3	TERM2	TERM1	B
	0.047613	-0.01532	0.099911	-46.7897	0.118764	2.543025
	0	0.002709	0.004104	14.66454	0.00244	0
	0.918896	0.055912	#N/A	#N/A	#N/A	#N/A
	1638.304	723	#N/A	#N/A	#N/A	#N/A
	25.60787	2.260202	#N/A	#N/A	#N/A	#N/A
	#N/A	#N/A	#N/A	#N/A	#N/A	#N/A
t - test	α	-5.65542	24.34369	-3.19067	48.67339	α

(j) 10 / 90 blended from experiment (j-1) and from equation (j-2), r^2 = 0.9188

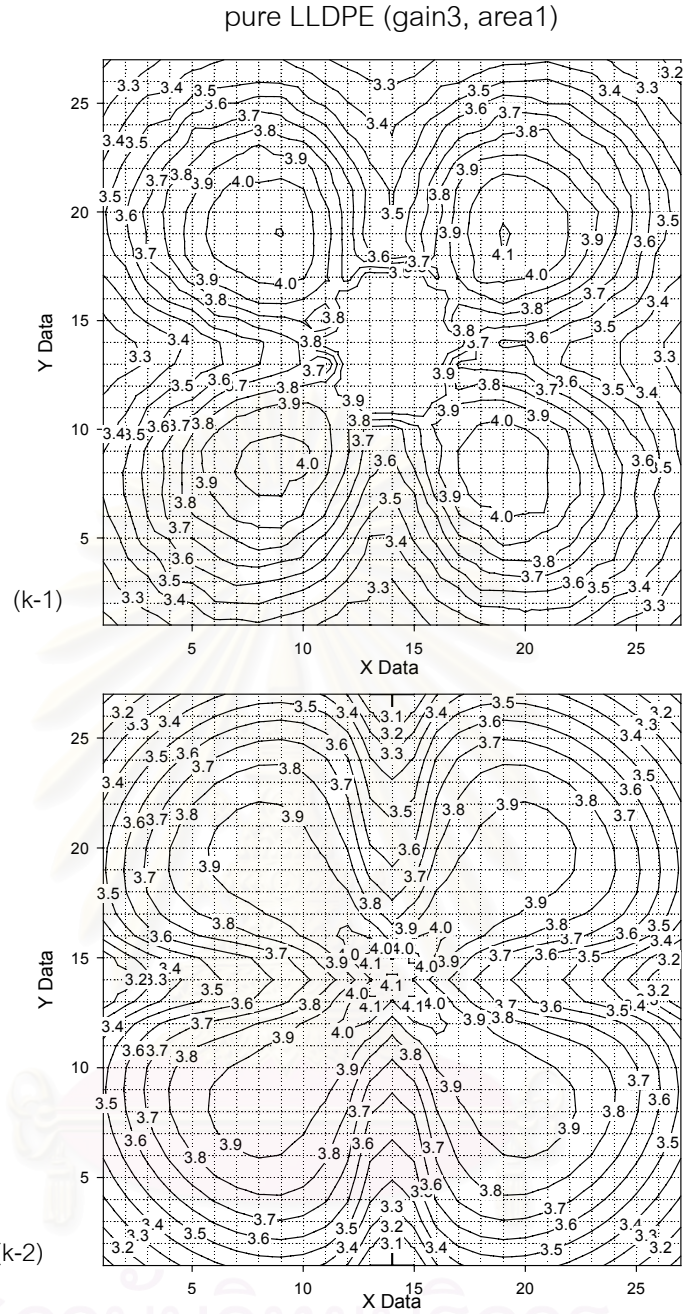

Regression Statistic Values

LLDPE	TERM5	TERM4	TERM3	TERM2	TERM1	B
	0.07692	-0.20202	0.306994	-68.7751	-0.00721	2.176741
	0	0.004366	0.005801	20.67863	0.00336	0
	0.901417	0.078842	#N/A	#N/A	#N/A	#N/A
	1322.177	723	#N/A	#N/A	#N/A	#N/A
	41.09371	4.494217	#N/A	#N/A	#N/A	#N/A
	#N/A	#N/A	#N/A	#N/A	#N/A	#N/A
t - test	α	-46.2675	52.91965	-3.3259	-2.14622	α

(k) pure LLDPE from experiment (k-1) and from equation (k-2), r^2 = 0.9014

Figure D-2 : Comparison of light scattering contour graphs between experiment and equation of HDPE / LLDPE blends at gain no.3, area1 and their r^2 values

pure HDPE (gain3,

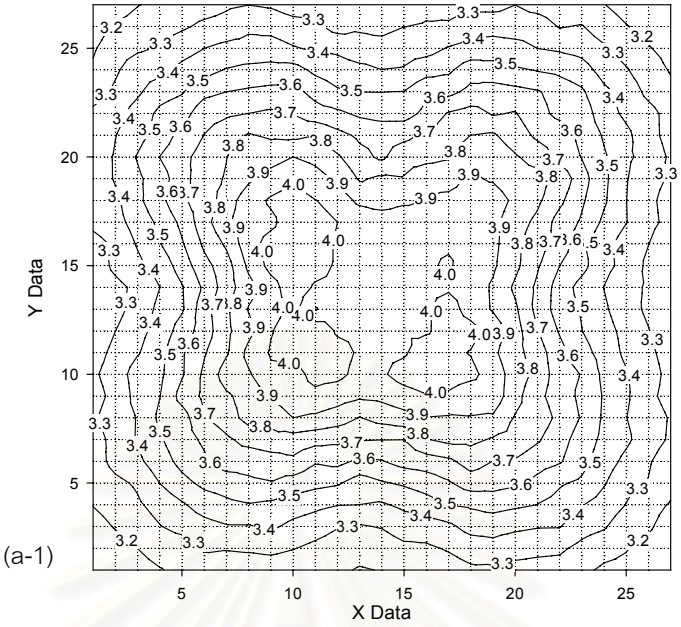

(a-1)

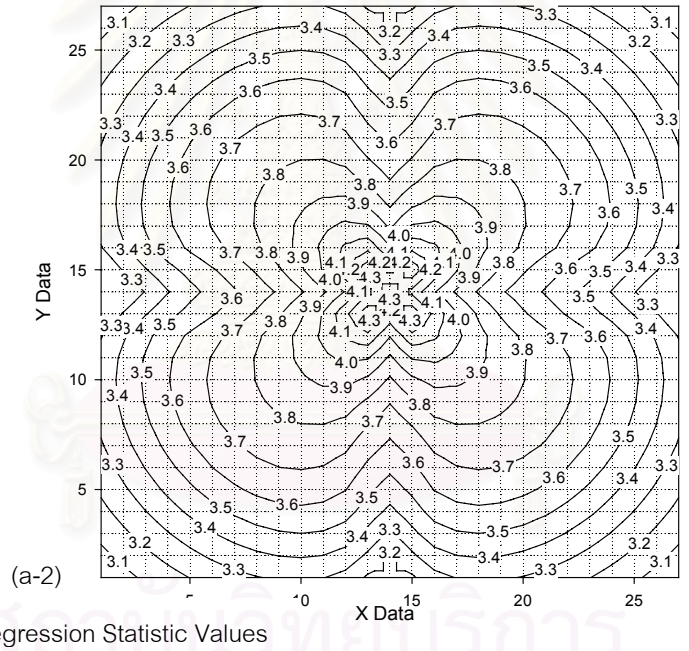

(a-2)

Regression Statistic Values

HDPE	TERM5	TERM4	TERM3	TERM2	TERM1	B
	0.034084	-0.10196	0.137048	-44.1719	0.093376	3.375138
	591.0103	0.003773	0.005878	21.0168	0.003521	18665.09
	0.909867	0.080131	#N/A	#N/A	#N/A	#N/A
	1459.688	723	#N/A	#N/A	#N/A	#N/A
	46.86357	4.64241	#N/A	#N/A	#N/A	#N/A
	#N/A	#N/A	#N/A	#N/A	#N/A	#N/A
t - test	5.77E-05	-27.0229	23.31664	-2.10174	26.52025	0.000181

(a) pure HDPE from experiment (a-1) and from equation (a-2), r^2 = 0.9098

HDPE/LLDPE: 90/10 (gain3,

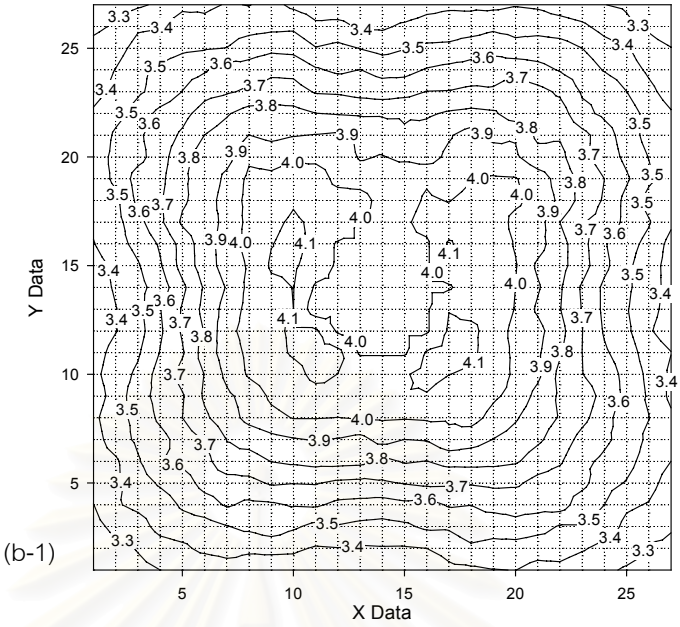

(b-1)

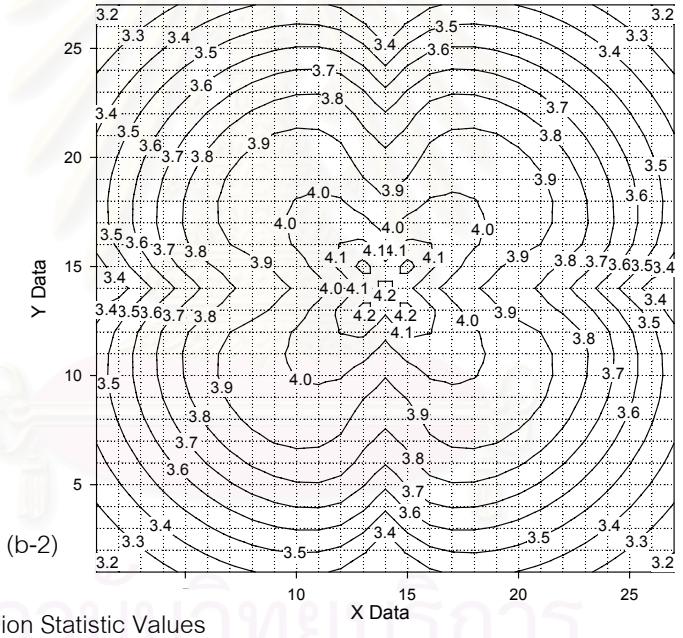

(b-2)

Regression Statistic Values

90-10	TERM5	TERM4	TERM3	TERM2	TERM1	B
	0.080283	-0.10497	0.113318	-67.2367	0.035024	1.847647
	0	0.002466	0.004936	17.84878	0.00334	0
	0.927933	0.068053	#N/A	#N/A	#N/A	#N/A
	1861.867	723	#N/A	#N/A	#N/A	#N/A
	43.11297	3.348325	#N/A	#N/A	#N/A	#N/A
	#N/A	#N/A	#N/A	#N/A	#N/A	#N/A
t - test	α	-42.5644	22.95638	-3.76702	10.48654	α

(b) 90 / 10 blended from experiment (b-1) and from equation (b-2), r^2 = 0.9279

HDPE/LLDPE: 80/20 (gain3,

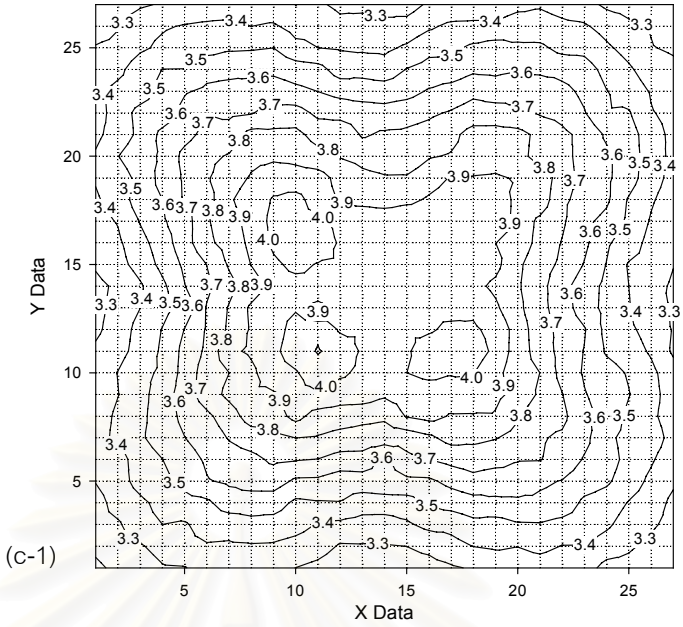

(c-1)

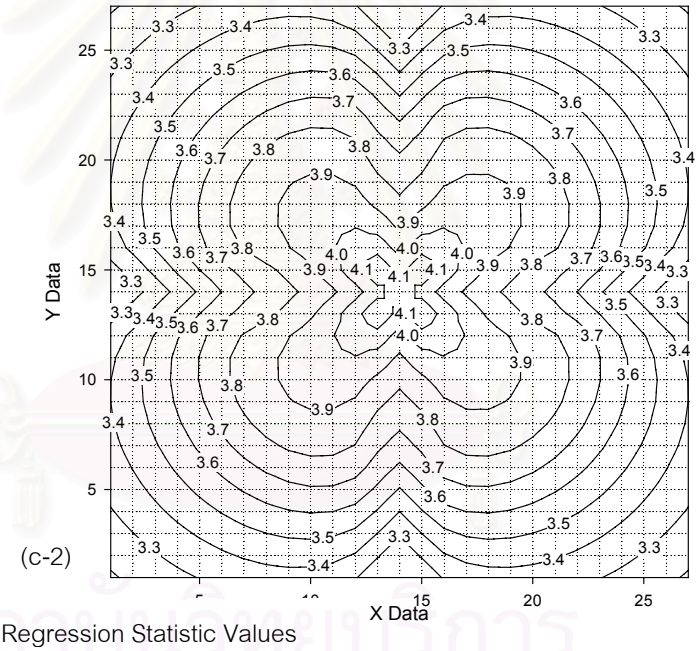

(c-2)

Regression Statistic Values

80-20	TERM5	TERM4	TERM3	TERM2	TERM1	B
	0.035343	-0.0774	0.13441	-63.7563	0.044842	3.212711
	463.2254	0.001874	0.004004	14.55381	0.002903	14976.6
	0.944668	0.05549	#N/A	#N/A	#N/A	#N/A
	2468.7	723	#N/A	#N/A	#N/A	#N/A
	38.00703	2.226199	#N/A	#N/A	#N/A	#N/A
	#N/A	#N/A	#N/A	#N/A	#N/A	#N/A
t - test	7.63E-05	-41.2939	33.56864	-4.38073	15.44529	0.000215

(c) 80 / 20 blended from experiment (c-1) and from equation (c-2), r^2 = 0.9446

HDPE/LLDPE: 70/30 (gain3,

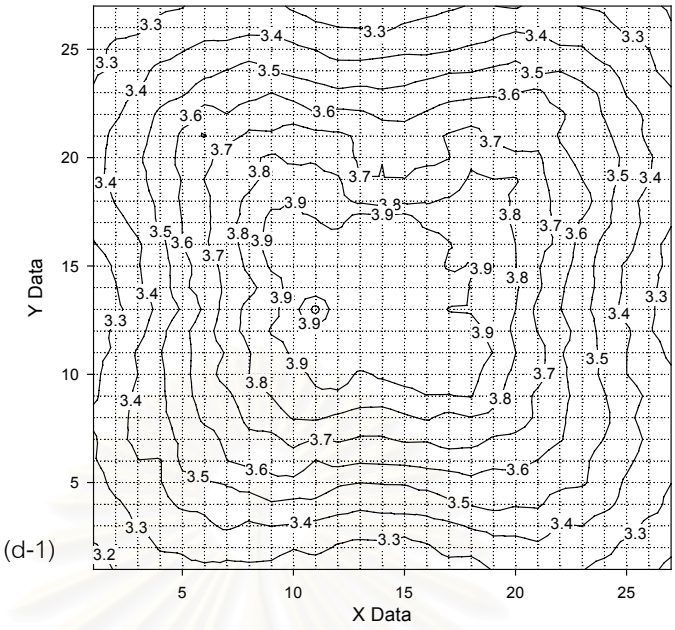

(d-1)

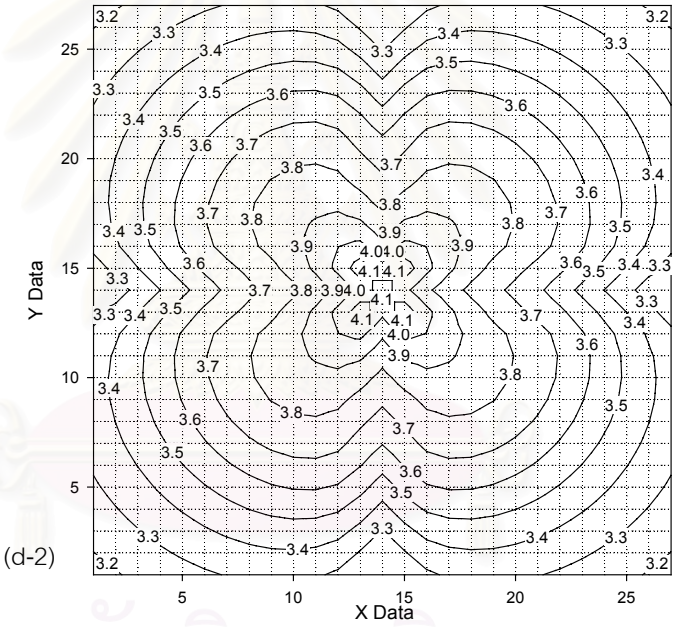

(d-2)

Regression Statistic Values

70-30	TERM5	TERM4	TERM3	TERM2	TERM1	B
	0.047292	-0.06045	0.104221	-64.4532	0.061873	2.743655
	0	0.001649	0.003553	12.92518	0.002608	0
	0.950855	0.04928	#N/A	#N/A	#N/A	#N/A
	2797.684	723	#N/A	#N/A	#N/A	#N/A
	33.97144	1.755834	#N/A	#N/A	#N/A	#N/A
	#N/A	#N/A	#N/A	#N/A	#N/A	#N/A
t - test	α	-36.65	29.33372	-4.98664	23.72156	α

(d) 70 / 30 blended from experiment (d-1) and from equation (d-2), r^2 = 0.9508

HDPE/LLDPE: 60/40 (gain3,

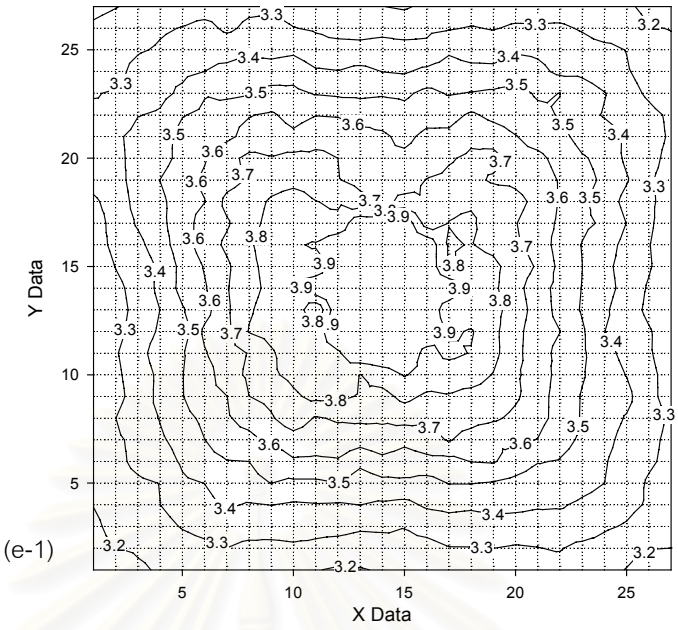

(e-1)

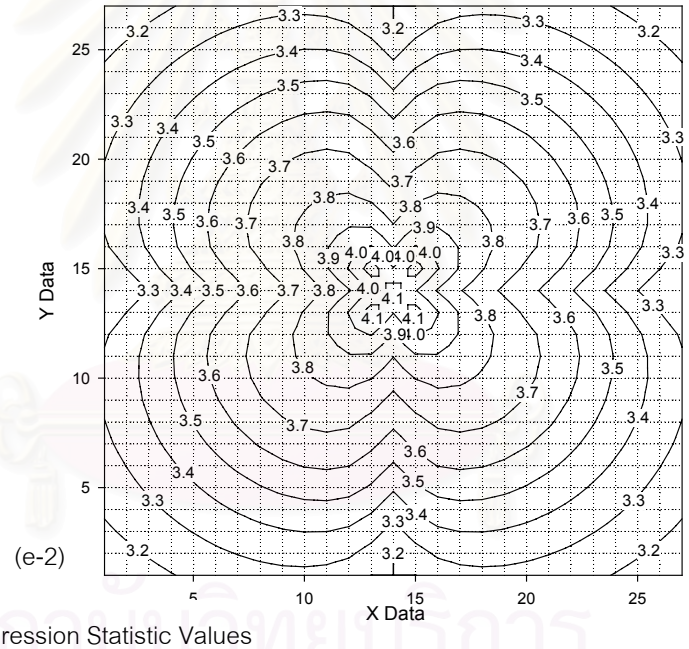

(e-2)

Regression Statistic Values

60-40	TERM5	TERM4	TERM3	TERM2	TERM1	B
	0.076552	-0.04978	0.081295	-65.8014	0.077106	1.745529
	0	0.001584	0.003436	12.51029	0.002553	0
	0.953275	0.047698	#N/A	#N/A	#N/A	#N/A
	2950.084	723	#N/A	#N/A	#N/A	#N/A
	33.5592	1.644923	#N/A	#N/A	#N/A	#N/A
	#N/A	#N/A	#N/A	#N/A	#N/A	#N/A
t - test	α	-31.4358	23.65885	-5.25978	30.2005	α

(e) 60 / 40 blended from experiment (e-1) and from equation (e-2), r^2 = 0.9532

HDPE/LLDPE: 50/50 (gain3,

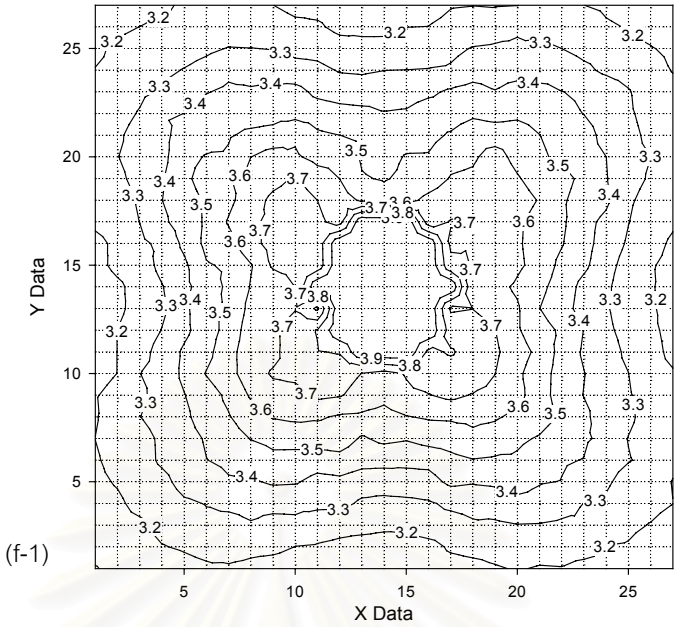

(f-1)

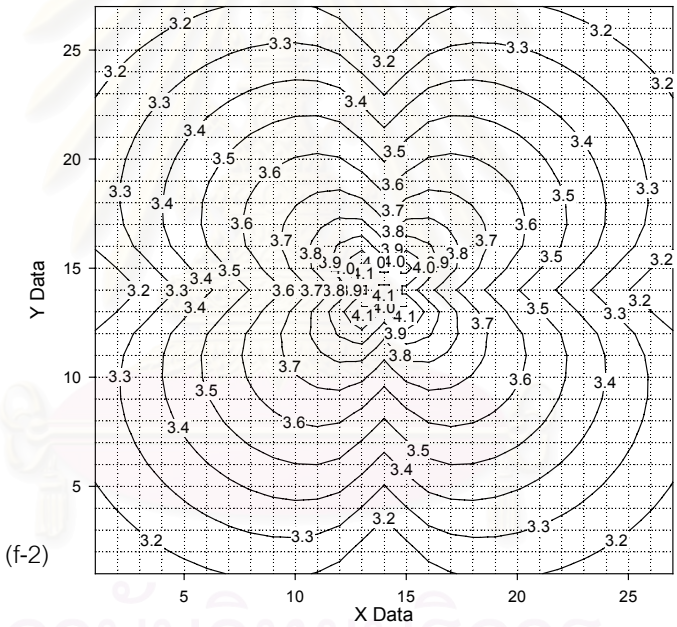

(f-2)

Regression Statistic Values

50-50	TERM5	TERM4	TERM3	TERM2	TERM1	B
	-0.00839	-0.03083	0.096599	-67.5033	0.101587	4.446763
	502.8837	0.001672	0.003564	12.95143	0.002577	16254.23
	0.946061	0.04938	#N/A	#N/A	#N/A	#N/A
	2536.187	723	#N/A	#N/A	#N/A	#N/A
	30.92141	1.762975	#N/A	#N/A	#N/A	#N/A
	#N/A	#N/A	#N/A	#N/A	#N/A	#N/A
t - test	-1.7E-05	-18.4442	27.1053	-5.21203	39.41933	0.000274

(f) 50 / 50 blended from experiment (f-1) and from equation (f-2), r^2 = 0.9460

HDPE/LLDPE: 40/60 (gain3, area2)

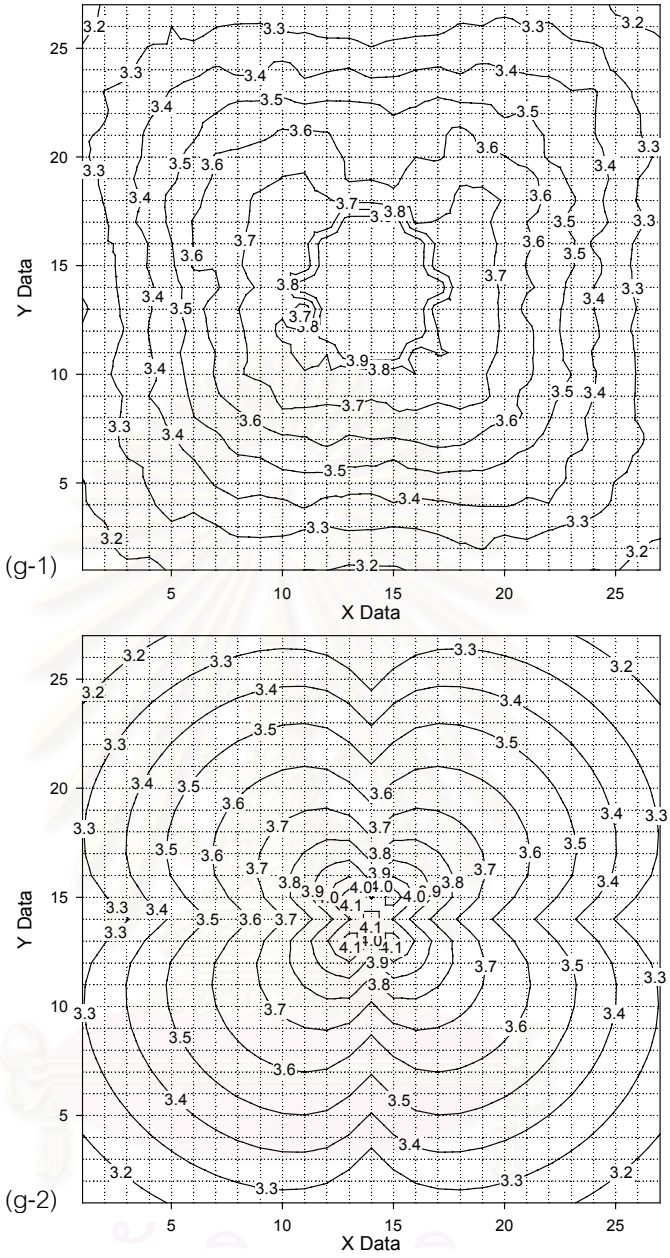

Regression Statistic Values

40-60	TERM5	TERM4	TERM3	TERM2	TERM1	B
	0.06485	-0.03965	0.066887	-52.8044	0.097784	2.07736
	0	0.001831	0.003525	12.71554	0.002318	0
	0.945162	0.048481	#N/A	#N/A	#N/A	#N/A
	2492.273	723	#N/A	#N/A	#N/A	#N/A
	29.28918	1.699339	#N/A	#N/A	#N/A	#N/A
	#N/A	#N/A	#N/A	#N/A	#N/A	#N/A
t - test	α	-21.6577	18.97419	-4.15275	42.19359	α

(g) 40 / 60 blended from experiment (g-1) and from equation (g-2), r^2 = 0.9451

HDPE/LLDPE: 30/70 (gain3,

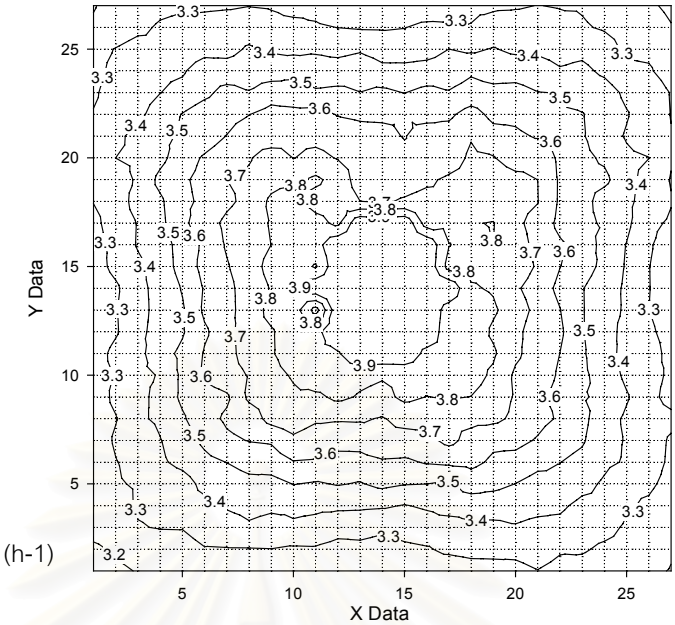

(h-1)

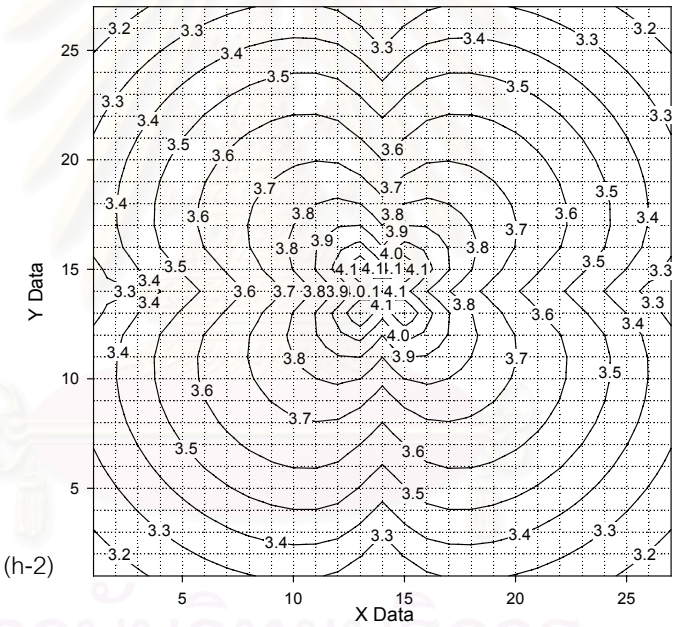

(h-2)

Regression Statistic Values

30-70	TERM5	TERM4	TERM3	TERM2	TERM1	B
	0.069207	-0.05183	0.076964	-52.4066	0.092896	2.000654
	407.206	0.002218	0.003917	14.0676	0.002455	12946.32
	0.934909	0.053636	#N/A	#N/A	#N/A	#N/A
	2076.907	723	#N/A	#N/A	#N/A	#N/A
	29.87438	2.079937	#N/A	#N/A	#N/A	#N/A
	#N/A	#N/A	#N/A	#N/A	#N/A	#N/A
t - test	0.00017	-23.3688	19.64906	-3.72534	37.83215	0.000155

(h) 30 / 70 blended from experiment (h-1) and from equation (h-2), r^2 = 0.9349

HDPE/LLDPE: 20/80 (gain3,

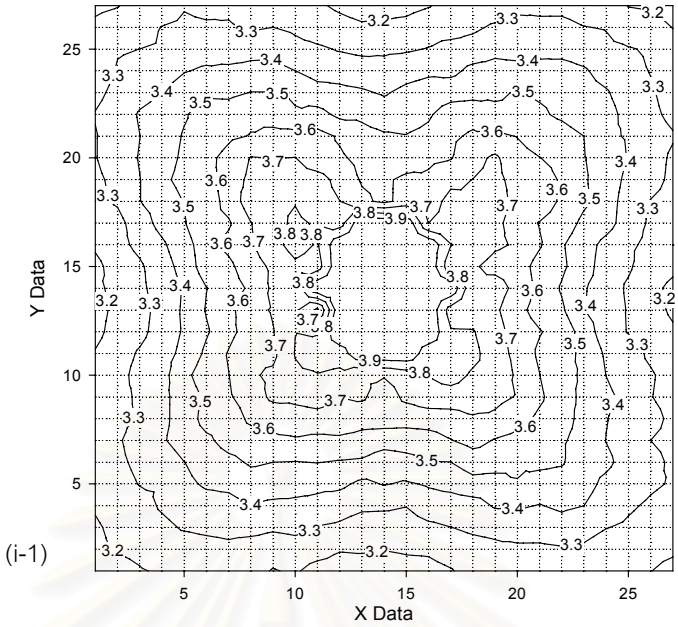

(i-1)

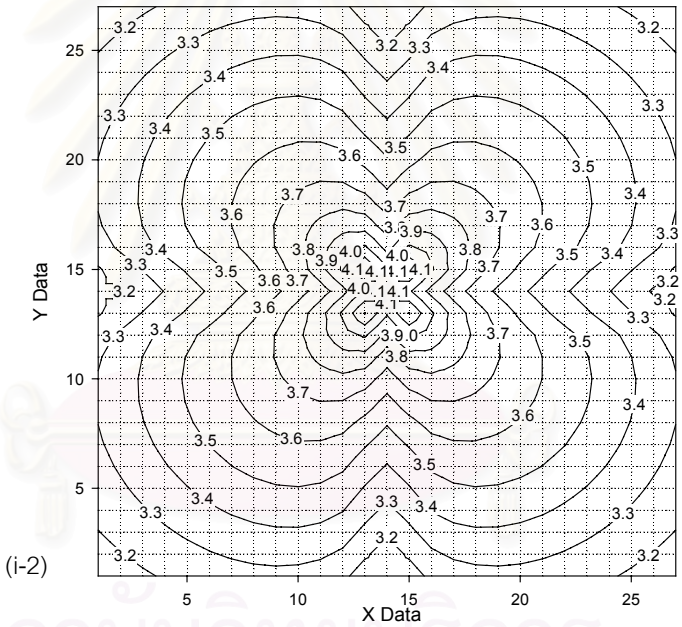

(i-2)

Regression Statistic Values

20-80	TERM5	TERM4	TERM3	TERM2	TERM1	B
	0.084626	-0.04025	0.111516	-61.9324	0.104629	1.500213
	503.1075	0.002479	0.004033	14.43932	0.002448	15922.5
	0.929432	0.055053	#N/A	#N/A	#N/A	#N/A
	1904.486	723	#N/A	#N/A	#N/A	#N/A
	28.86112	2.19131	#N/A	#N/A	#N/A	#N/A
	#N/A	#N/A	#N/A	#N/A	#N/A	#N/A
t - test	0.000168	-16.2325	27.65127	-4.28915	42.73553	9.42E-05

(i) 20 / 80 blended from experiment (i-1) and from equation (i-2), r^2 = 0.9294

HDPE/LLDPE: 10/90 (gain3,

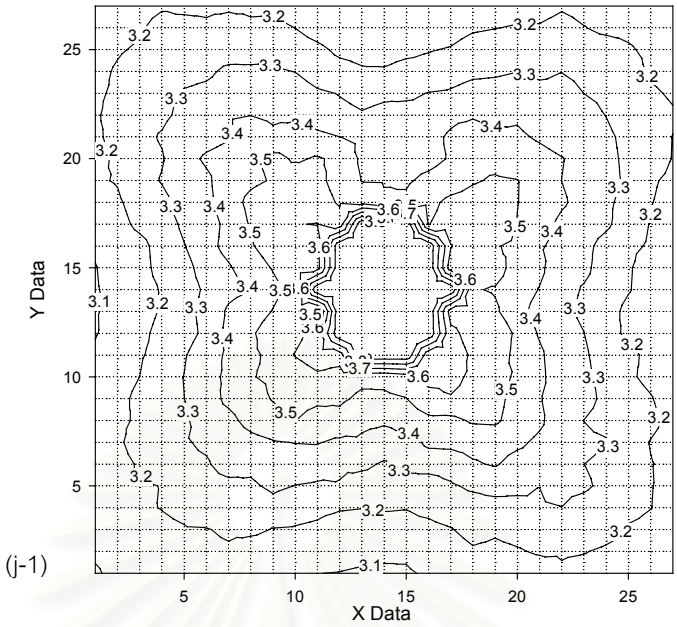

(j-1)

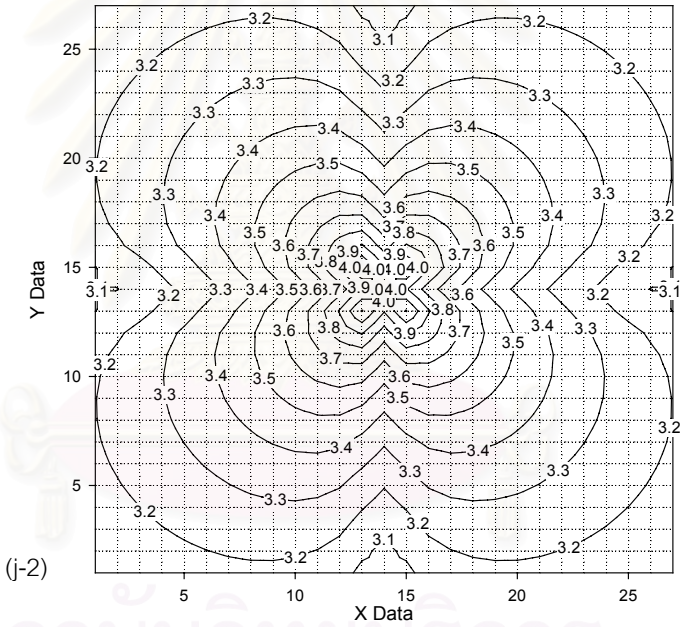

(j-2)

Regression Statistic Values

10.0-90.0	TERM5	TERM4	TERM3	TERM2	TERM1	B
	0.051991	-0.00087	0.085996	-32.3842	0.127908	2.329633
	0	0.002891	0.004379	15.64648	0.002603	0
	0.906104	0.059656	#N/A	#N/A	#N/A	#N/A
	1395.407	723	#N/A	#N/A	#N/A	#N/A
	24.82999	2.573025	#N/A	#N/A	#N/A	#N/A
	#N/A	#N/A	#N/A	#N/A	#N/A	#N/A
t - test	α	-0.29999	19.63829	-2.06974	49.1312	α

(j) 10 / 90 blended from experiment (j-1) and from equation (j-2), r^2 = 0.9061

Pure LLDPE (gain3, area2)

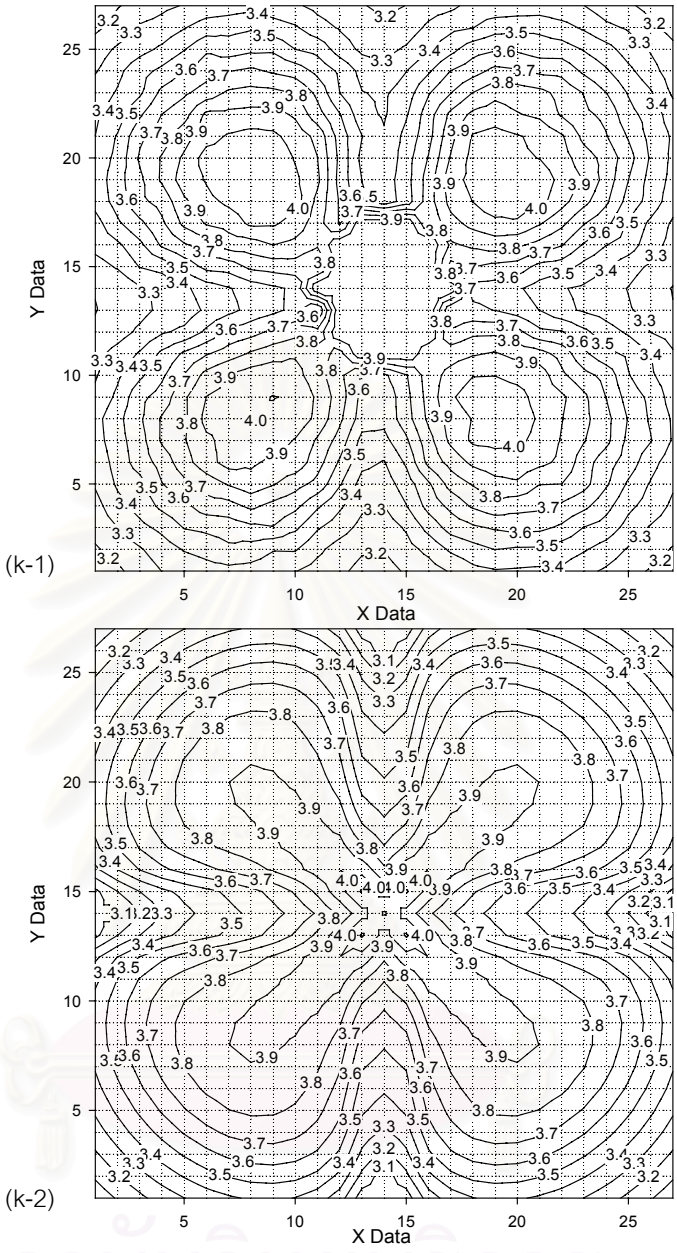

Regression Statistic Values

LLDPE	TERM5	TERM4	TERM3	TERM2	TERM1	B
	0.090909	-0.1985	0.318635	-51.9414	-0.00365	1.713652
	0	0.004708	0.006255	22.29546	0.003622	0
	0.889927	0.085007	#N/A	#N/A	#N/A	#N/A
	1169.069	723	#N/A	#N/A	#N/A	#N/A
	42.23915	5.224484	#N/A	#N/A	#N/A	#N/A
	#N/A	#N/A	#N/A	#N/A	#N/A	#N/A
t - test	α	-42.1637	50.94321	-2.32969	-1.00651	α

(k) pure LLDPE from experiment (k-1) and from equation (k-2), r^2 = 0.8899

Figure D-3 : Comparison of light scattering contour graphs between experiment and equation of HDPE / LLDPE blends at gain no.3, area2 and their r^2 values

Vita

Miss Paveena Meesap was born in Bangkok, Thailand in November 1, 1977. She received the Bachelor Degree of Science in Chemical Technology from the Department of Chemical Technology, Faculty of Science, Chulalongkorn University in 1998. She entered the Master of Engineering in Chemical Engineering Program at Chulalongkorn University in 1999.